

Summer 8-18-2010

Design and Synthesis of Novel Serotonin Receptor Ligands

Jeffrey D. Klenc
Georgia State University

Follow this and additional works at: https://scholarworks.gsu.edu/chemistry_diss

 Part of the [Chemistry Commons](#)

Recommended Citation

Klenc, Jeffrey D., "Design and Synthesis of Novel Serotonin Receptor Ligands." Dissertation, Georgia State University, 2010.
https://scholarworks.gsu.edu/chemistry_diss/50

This Dissertation is brought to you for free and open access by the Department of Chemistry at ScholarWorks @ Georgia State University. It has been accepted for inclusion in Chemistry Dissertations by an authorized administrator of ScholarWorks @ Georgia State University. For more information, please contact scholarworks@gsu.edu.

DESIGN AND SYNTHESIS OF NOVEL SEROTONIN RECEPTOR LIGANDS

by

JEFFREY D. KLENC

Under the Direction of Dr. Lucjan Strekowski

ABSTRACT

Novel and potent ligands to the serotonin₇ (5-HT₇) receptor have been synthesized. The synthesized compounds include a set of substituted pyrimidines which show high affinity to the 5-HT₇ receptor, synthesized by previously described methods [1,2] in high yield. Comparing the affinities of substituted pyrimidines to previously calculated models [3,4] yielded new hypotheses about the nature of interaction between the pyrimidine ligands and the 5-HT₇ binding site. Several new series of compounds were synthesized by various methods to validate these hypotheses, including a conjugate addition to vinylpyrimidines [5]. These compounds include benzofurans, oximes, hydrazones, as well as a group of substituted piperazines. All series of compounds show affinity to the 5-HT₇ receptor

comparable to previously synthesized 5-HT₇ ligands. Several of the synthesized ligands show affinity which exceeds that of currently available ligands.

The synthesized compounds were evaluated quantitatively by calculating a three-dimensional quantitative structure-affinity relationship (3D-QSAR) for the 5-HT₇ receptor. Evaluation of the calculated model validated qualitative assumptions about the data set as well as described regions of interaction in greater detail than previously available. These observations give further insight on the nature of ligand-binding site interactions with highly potent ligands such as 4-(3-furyl)-2-(*N*-methylpiperazino)pyrimidine which will lead to more potent 5-HT₇ receptor ligands. Additionally, a model was calculated for affinity to the 5-HT_{2a} receptor. Comparing this model to that calculated for affinity to the 5-HT₇ receptor identified two regions which may be exploited in future sets of ligands to increase selectivity to the 5HT₇ receptor.

INDEX WORDS: Serotonin, 5-HT, Depression, Schizophrenia, Pyrimidine, 1-4 Addition, 3D-QSAR,

Molecular modeling, 5-HT₇ receptor, 5-HT₇ ligands, 5-HT_{1a}, 5-HT_{2a}, Pharmacophore

DESIGN AND SYNTHESIS OF NOVEL SEROTONIN RECEPTOR LIGANDS

by

JEFFREY D. KLENC

A Dissertation Submitted in Partial Fulfillment of the Requirements for the Degree of

Doctor of Philosophy

in the College of Arts and Sciences

Georgia State University

2010

Copyright by
Jeffrey David Klenc
2010

DESIGN AND SYNTHESIS OF NOVEL SEROTONIN RECEPTOR LIGANDS

by

JEFFREY D. KLENC

Committee Chair: Dr. Lucjan Strekowski

Committee: Dr. Alfons Baumstark

Dr. Markus Germann

Electronic Version Approved:

Office of Graduate Studies

College of Arts and Sciences

Georgia State University

August 2010

DEDICATION

I dedicate this work to the memory of my late grandparents Bernard and Rose Hakenewerth.

ACKNOWLEDGEMENTS

I would like to sincerely thank Dr. Lucjan Strekowski for the opportunity to explore several different projects while working under his direction. The opportunity to work independently in his lab has led me to learn on my own. Straightforward criticism and succinct, accurate advice on the direction projects should take has shown me how to pursue scientific problems efficiently. This unique environment has provided an opportunity for me to develop into an efficient chemist and an effective project leader, for which I am sincerely grateful.

I would also like to thank my parents for their support in every endeavor for which I have expressed an interest in since I was old enough to remember. It is truly a testament to their patience and dedication that I have been able to complete this work. Without their encouragement at a very young age to learn math, music, and science, I would have undoubtedly lacked the skills to work in such a demanding and rewarding field. Without their patience and quiet guidance during my adolescence, I would have undoubtedly wasted those gifts they have given me.

I must also thank the efforts of those I have worked with under Dr. Strekowski. Particularly, I am thankful for Ava's efforts as an undergraduate and graduate student which have helped me become a better teacher and to understand my role as a leader more clearly. I thank Beth for providing invaluable insight into the industrial lab setting, bringing not only her experience from outside academia, but also her contagious work ethic and passion for synthesis. I also thank Adam, Reid, Nilmi, Jamie, and Shirish for their curiosity about chemistry which was essential to my education during this program.

At last, I must thank Amy for her love and friendship. Above all others she has been near day in and day out to comfort, console, encourage and empathize with me during all my hardships and successes throughout this program.

ACKNOWLEDGEMENTS.....	v
LIST OF TABLES.....	viii
LIST OF FIGURES.....	ix
1 INTRODUCTION.....	1
1.1 The characterization of serotonin.....	1
1.2 The serotonergic system.....	2
1.3 Therapeutic relevance	5
1.4 The need for more selective serotonin receptor ligands.....	7
2 LITERATURE REVIEW	9
2.1 Serotonin receptor subtypes and other related G-protein coupled receptors (GPCR)	9
2.2 The 5-HT ₇ receptor	10
2.2.1 Biological expression and functions of 5-HT ₇ receptors	12
2.2.2 Mechanism of signal transduction.....	13
2.2.3 Conformational changes upon binding.....	14
2.2.4 Pharmacophores of 5-HT _{1a} , 5-HT _{2a} , and 5-HT ₇ receptors	17
2.3 Current 5-HT ₇ receptor ligands	22
3 SYNTHESIS.....	27
3.1 Synthesis of substituted pyrimidines as a diverse set of 5-HT receptor ligands	27
3.2 Synthesis of substituted pyrimidines by 1,4 addition to vinyl-substituted pyrimidines.....	30
3.3 Synthesis and facile modification of 2-chloro-4-(acetyl)pyrimidine.....	32
3.4 Synthesis of 5-HT ₇ receptor ligands with piperazine extensions.....	34
3.5 Synthesis of fused ring 5-HT ₇ receptor ligands	36
3.6 Synthesis of bivalent 5-HT ₇ receptor ligands.....	40
4 MODELING	43
4.1 Calculation of models for 5-HT ₇ and 5-HT _{2a} receptors.....	43
4.1.1 Validation of QSAR methods.....	44
4.1.2 Statistical parameters	45
4.1.3 Ligands used to calculate the models.....	46
4.1.4 Binding mode conformation	55
4.1.5 Alignment of structures	59
4.2 Presentation of QSAR models.....	60
4.2.1 Pharmacophores.....	60

4.2.2	The model for affinity to the 5-HT ₇ receptor	65
4.2.3	Calculation of a model for affinity to the 5-HT _{2a} receptor	69
4.3	Analysis of each set of compounds according to the calculated models	74
4.3.1	Steric interactions	76
4.3.2	Electrostatic Interactions	77
4.3.3	Hydrophobic interactions	79
4.3.4	Hydrogen bond donor interactions.....	80
5	CONCLUSIONS.....	82
6	EXPERIMENTAL	84
	REFERENCES.....	106
	APPENDICES	119
A.	List of abbreviations.....	119
B.	Glossary.....	120
C.	Spectra	124

LIST OF TABLES

Table 1-1. A summary of conditions in which a serotonergic effect is proposed.....	7
Table 2-1. Compounds showing high affinity and selectivity to 5-HT ₇	22
Table 2-2. Currently available 5-HT ₇ receptor ligands	24
Table 4-1. Disubstituted pyrimidines used to calculate the 3D-QSAR models.....	49
Table 4-2. <i>N</i> -substituted piperazino compounds used to calculate the 3D-QSAR models.....	51
Table 4-3. Alternatively substituted pyrimidines at the 2-position used to calculate the 3D-QSAR models	52
Table 4-4. Benzenes and pyridines used to calculate the 3D-QSAR models	53
Table 4-5. Benzofurans used to calculate the 3D-QSAR models	54
Table 4-6. Compounds with substituents to the central aromatic ring in the para-position to <i>N</i> - methylpiperazine used to calculate the 3D-QSAR models	55
Table 4-7. Compounds used for pharmacophore calculation	61
Table 4-8. Calculated distances between pharmacophore regions.....	64
Table 4-9. Predicted pK_i and experimental pK_i to the 5-HT ₇ receptor	68
Table 4-10. Predictivity statistics of the 5-HT ₇ model for affinity.....	69
Table 4-11. Predicted pK_i and experimental pK_i to the 5-HT _{2a} receptor.....	73
Table 4-12. Predictivity statistics of the 5-HT _{2a} model for affinity.....	73

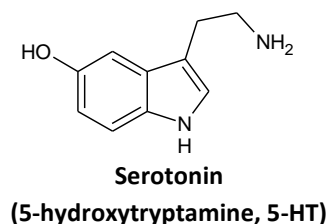
LIST OF FIGURES

Figure 1-1. Biosynthetic and metabolic pathway of serotonin.....	2
Figure 2-1. Homology model of the 5-HT _{2a} receptor	15
Figure 2-2. A calculated model for affinity to the 5HT ₇ receptor	18
Figure 2-3. Comparisons between recent pharmacophores for agonism and antagonism of the 5-HT ₇ receptor	19
Figure 2-4. Most recent calculated pharmacophore for antagonism of the 5-HT ₇ receptor	21
Figure 3-1. The catalytic palladium cycle.....	38
Figure 4-1. Conformational analysis of furylpyrimidines.....	57
Figure 4-2. Conformation of substituents (AR13).....	58
Figure 4-3. Alignment of all structures.	59
Figure 4-4. Pharmacophore models for antagonism of the 5-HT ₇ receptor.....	64
Figure 4-5. Dendrogram calculated from 5-HT ₇ ligand database of structures.....	66
Figure 4-6. Predicted pKi vs. experimental pKi for 5-HT ₇ ligand structures.....	67
Figure 4-7. Dendrogram calculated from 5-HT _{2a} ligand database of structures.....	70
Figure 4-8. Predicted pKi vs. experimental pKi for 5-HT _{2a} ligand structures.	72
Figure 4-9. 3D-QSAR models for affinity to the 5-HT _{2a} and 5-HT ₇ receptors.....	75
Figure 4-10. Field contours for steric regions calculated for 5-HT _{2a} and 5-HT ₇ receptors.....	76
Figure 4-11. Field contours for steric regions calculated for 5-HT _{2a} and 5-HT ₇ receptors.....	78
Figure 4-12. Field contours for steric regions calculated for 5-HT _{2a} and 5-HT ₇ receptors.....	79
Figure 4-13. Field contours for steric regions calculated for 5-HT _{2a} and 5-HT ₇ receptors.....	80

1 INTRODUCTION

1.1 The characterization of serotonin

Research on serotonin began with its discovery [6] which is credited to Erspamer [7] whose work with smooth muscle contraction led him to observe an amine in cells of the gut. Erspamer observed that this compound was responsible for muscle contraction seen in his experiments and named it enteramine (enteric¹ amine) without full characterization [8]. In separate research, serotonin was isolated from blood [9] and named such for its properties as a vasoconstrictor². Rapport succeeded in the crystallization and characterization of serotonin, defining the structure as



5-hydroxytryptamine and identical to the enteramine described by Erspamer [10,11]. Two years later, serotonin was synthesized and made commercially available, and research on serotonin grew rapidly. Several reports followed which described serotonin prevalent throughout the periphery. The presence of serotonin in the central nervous system³ (CNS) [12] quickly led to its identification as a neurotransmitter [13]. These studies are the foundation for the current understanding of the serotonergic system. This understanding has been advanced significantly, but there remains much to be desired. This research aims to further the knowledge of the serotonergic system by synthesizing novel ligands to be used in physiological⁴ studies. Research using these compounds promises to extend the knowledge of the serotonergic system and help to identify therapeutic uses, such as antidepressants.

¹ enteric – pertaining to the intestines

² vasoconstrictor – a compound which causes the blood vessels to contract

³ central nervous system – a broad characterization of the structures which allow for communication with the periphery and the environment and includes all of the brain and spinal cord

⁴ physiological – referring to the biological purpose of a receptor as it relates to the process it affects within the body

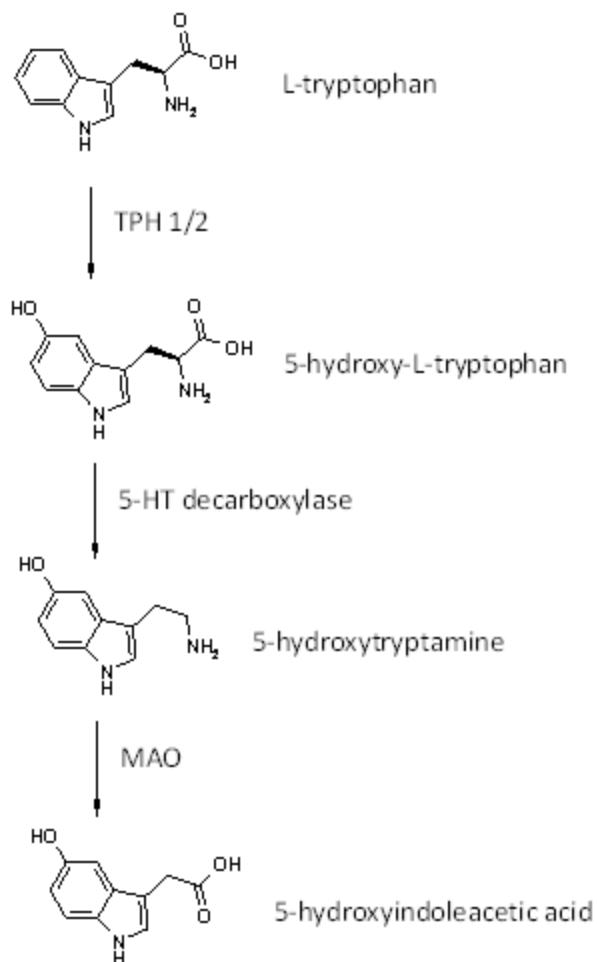


Figure 1-1. A summary of the biological pathway for synthesis and metabolism of serotonin.

1.2 The serotonergic system

The prevalence of serotonin within the central nervous system (CNS) provides a biological pathway for controlling a diverse set of physiological functions. Understanding the biological means for the release and reuptake of serotonin illuminates the reasoning for current drug strategies. Serotonin is a neurotransmitter and takes action upon serotonin receptors within the CNS. The concentration of serotonin at the receptor site is governed by a complex network of cells and proteins. It is the control over this concentration which is desired and the biological

routes for doing so are described. It is prudent to note that the whole of serotonin producing and binding cells is often called the serotonergic system. This is somewhat misleading however, as serotonergic neurons in the body do not act cohesively, but act largely independent of one another [14]. This flexibility allows for serotonergic pathways to simultaneously illicit a multitude of distinct physiological responses.

Each serotonergic neuron is linked to another neuron capable of detecting serotonin through receptors on its surface. The release of serotonin is controlled by the firing rate of the neuron. The serotonin diffuses into nearby 5-HT receptor sites. This binding event causes a conformational shift of

the receptor and results in signal transduction⁵. Controlling this binding event is a major step toward gaining control over the end result of 5-HT receptors.

Serotonin is synthesized biologically by a short pathway beginning with the amino acid L-tryptophan, shown in Figure 1-1. Two enzymes⁶ carry out this biosynthesis and it is the first of these two, tryptophan hydroxylase (TPH) which is the rate limiting step [15]. Therefore, the second enzyme involved in the biosynthesis, 5-HT decarboxylase, is a less attractive therapeutic target. The level of research on the inhibition of this enzyme reflects this observation. TPH introduces a hydroxyl group on the aromatic region of the amino acid and exists in two different isoforms, TPH1 and TPH2. These different forms exist almost exclusively in isolation from each other with TPH1 acting in the periphery while TPH2 acts in neuronal⁷ cells. Inhibition of TPH1 has the potential to allow control of serotonin levels in the blood and gastrointestinal⁸ tract. This may prove to be therapeutically useful in hypertension [16] and gastrointestinal disorders such as irritable bowel syndrome [17]. Inhibition of TPH2 has been shown to reduce brain serotonin levels [18]. However, therapeutic use for TPH2 inhibitors⁹ is limited, due to the global nature of the serotonin depression throughout the CNS. This decreased level of serotonin likely causes many unwanted side effects. Most therapeutic targets in the CNS are aimed to increase synaptic serotonin levels. Inhibiting TPH2 would have the opposite effect, making even the targeted effect opposite of that desired. Thus, the selective inhibition of TPH1 to alter serotonin levels in the blood and gastrointestinal tract is likely the only viable therapeutic strategy for these biological pathways [19].

⁵ signal transduction – the process of relaying an extracellular signal, such as increased concentration of a neurotransmitter, into intracellular changes

⁶ enzyme – a protein which catalyzes a chemical reaction

⁷ neuronal – pertaining to the cells (neurons) which regulate the release and reuptake of neurotransmitters for the purpose of signal transmission between nerve cells

⁸ gastrointestinal – pertaining to the entire system which is used to extract nutrients from ingested food, beginning at the oral cavity and ending at the anus

⁹ inhibitors – a compound which the activity of a specific protein upon binding

Serotonergic drugs have been focused on artificially increasing serotonin levels *in vivo*. This has been accomplished most successfully by blocking the clearance of serotonin. This clearance occurs by two different routes, reuptake into a neuronal cell or metabolism. Inhibiting the enzymes responsible for serotonin clearance has resulted in several commercially successful drugs. The main protein responsible for the reuptake of serotonin is the serotonin transporter (SERT). Inhibition of this transporter has led to the most commercially successful products of serotonin research [20]. By blocking the reuptake into the neuronal cells, serotonin levels are artificially raised. This has led to use as anti-depressants [21] and for other mood related conditions. Marketed as serotonin specific reuptake inhibitors (SSRIs), these compounds amplify the amount of serotonin throughout the CNS. This results in many side effects due to poorly defined physiological profiles. There is evidence to support an additional transporter that plays a significant part in serotonin reuptake, the plasma membrane monoamine transporter (PMAT). This protein does not transport serotonin as efficiently as SERT, but does so with a much greater capacity. It is therefore possible that PMAT plays a significant role in serotonin reuptake [22]. The efficiency of current SSRIs may be improved by analyzing their effect on PMAT and optimizing the ligands for dual inhibition to these transporters.

Much like blocking the reuptake of serotonin, inhibiting monoamine oxidase (MAO) effectively raises global serotonin levels by blocking its metabolism [23]. Drugs targeting MAO represent another commercially successful class of compounds. As with the TPH enzyme, MAO enzymes also exist in two forms, MAO-A and MAO-B, both of which are present in the CNS. MAO-A preferentially metabolizes serotonin into 5-hydroxyindoleacetic acid along with other monoamines. Since the end result of MAOIs is much the same as SSRIs, they are susceptible to the same faults such as multiple side effects due to poor physiological profiling. MAOIs have the added difficulty of increasing the concentration of other monoamine neurotransmitters as well, as they are not specific to serotonin.

A seemingly more advantageous approach to controlling the serotonin signal is to design selective ligands for the receptor subtype responsible for mediating a specific function [24]. The ability to discern between different types of serotonin receptors adds another level of selectivity¹⁰ to the SSRI class of compounds. This may ultimately allow for the serotonin signal to be more discretely directed toward the functions of a particular serotonin receptor, as opposed to universally altering the level of post-synaptic serotonin, as is the case with SSRIs and MAOIs. Ideally, the administration of serotonin receptor ligands selectively activates or inhibits the functions specific to that receptor. The development of such selective ligands offers an improvement over current drug treatments, although the functions regulated by each subtype are not singular and may still produce unwanted side effects. Existing serotonin ligands and their therapeutic uses and relevance is discussed in detail.[‡]

1.3 Therapeutic relevance

Manipulation of the serotonergic system has been established as a valid method for regulating biological functions. The prevalence of serotonin throughout the brain and body has been well documented [25]. It has been shown that serotonin plays a major role in several vital functions which implicate the neurotransmitter in many biological processes. Each of these biological processes represents an opportunity for therapeutic use. Table 1-1 below shows the most accepted processes which serotonin is thought to regulate to some degree. The regulation of visceral motor response is most noted in the gut, where serotonin is responsible for initiating the migrating contractions of the bowel [26]. The electrical impulses of serotonergic neurons have also been shown to be in step with the

¹⁰ selectivity – describes a ligand which binds to only one (or a limited amount) of receptors; in this case, 5-HT receptor subtypes and other monoamine receptors

circadian pacemaker¹¹, which regulates sleep-wake cycle among other things. It has also been shown that differing levels of serotonergic activity in a developing brain can significantly affect the function of the adult. This also includes conditions related to sexual behavior [27], mood [28], regulation of the body standards (temperature [29], blood pH [30], blood pressure [31], appetite[32]), learning and memory [33], gastrointestinal disorders [34], perception of pain [35], and neurological disorders [36-40]. The involvement of serotonin in regulation of behavioral aspects is more difficult to describe, largely due to the lack of precision in the definition of these disorders. Altered serotonin levels and expression of serotonin receptors, transporters, and neurons in the brain have been associated with abnormal behaviors. The regulation of behavior has been the most successful area of serotonin research, yielding many commercially successful drugs aimed at depression and schizophrenia. However, the action of these drugs is not sufficiently understood. The synthesis of ligands in order to better understand these processes is a major focus of this research.

¹¹ circadian pacemaker – refers to the structures which maintain daily rhythms such as feeding and sleeping

Table 1-1. Serotonergic pathways have been implicated in the regulation of the listed conditions.

Processes which may be regulated by 5-HT	Conditions arising from regulated processes of therapeutic relevance	Proposed method of serotonergic involvement
mood	anxiety [41,42], conduct disorders (ADD, OCD, etc.) [43], depression [44], locomotion/energy balance [45]	serotonergic innervations to forebrain structures ¹²
body standards	blood pressure [31], internal temperature [29], body fluid homeostasis [30], appetite/obesity [32], sleep disorders [46]	serotonergic neurons in the hypothalamus and brainstem projections from raphe nuclei ¹³
learning and memory	schizophrenia [39], Alzheimer's disease [40]	ascending serotonergic neurons into the frontal cortex, hippocampus and other brainstem projections from the raphe nuclei
perception of pain	nociception [35], migraine [47, 48]	descending serotonergic pain inhibitory system
neurological disorders	Parkinson's disease [37], epilepsy [38]	inhibition of dopamine release and methods of cognition
gastrointestinal disorders	dyspepsia ¹⁴ [49], irritable bowel syndrome [50], heartburn [51], gastroparesis [52]	gastrointestinal motility, fluid secretion in the bowel

1.4 The need for more selective serotonin receptor ligands

A common theme present in many physiological studies on 5-HT receptors used to produce the functional theories is the incomplete nature of the studies due to lack of sufficiently potent and selective ligands [27, 34, 43, 53]. The need for selective ligands comes from the diversity of serotonin receptor subtypes. There are fourteen subtypes of 5-HT receptors characterized to date, all binding the same ligand. The selective interaction of ligands with individual subtypes allows for research on their distinct

¹² forebrain structures – refers to structures implicated in higher order thought processes

¹³ raphe nuclei – portion of the brain which houses an overwhelming majority of serotonergic neurons; near the brainstem

¹⁴ dyspepsia – a loosely defined stomach ailment similar to an upset stomach or indigestion

physiological properties. While the challenge to synthesize the ligands which are selective to each subtype has been daunting, the aim is to achieve a greater level of control over the broad spectrum of functions. Complicating the issue further is the need for selectivity not just over other serotonin receptor subtypes, but other similar neurotransmitter receptors, such as noradrenergic, cholinergic, and dopaminergic receptors [3]. This research has produced effective ligands for some of the receptor subtypes [34], which has led to important discoveries regarding those subtypes. There are several receptor subtypes for which improvements on the currently available ligands are needed. Ongoing efforts to this end have produced many novel classes of ligands [54] and several binding studies to elucidate the requirements for the desired selectivity and potency [3]. The evolution of these ligands has helped clarify the physiological profile for serotonergic receptors and the therapeutic value of 5-HT receptor ligands.

2 LITERATURE REVIEW

2.1 Serotonin receptor subtypes and other related G-protein coupled receptors (GPCR)

As mentioned, synthesizing ligands which interact at the serotonin receptors allows the greatest control over serotonergic function. This is due to the diversity of serotonin receptor subtypes which are expressed throughout the CNS. Each of the fourteen 5-HT receptor subtypes exhibits a unique pharmacology and expression in the body. These include 7 groups of receptor subtypes: 5-HT₁ (5-HT_{1a}, 5-HT_{1b}, 5-HT_{1d}, 5-HT_{1e}, 5-HT_{1f}) 5-HT₂ (5-HT_{2a}, 5-HT_{2b}, 5-HT_{2c}), 5-HT₃, 5-HT₄, 5-HT_{5A} (5-HT_{5B} found in rats), 5-HT₆, and 5-HT₇. All 5-HT receptors (except for the 5-HT₃ receptor, which is a ligand gated ion channel) belong to a large family of receptors known as G-protein¹⁵ coupled receptors (GPCRs). Therefore, affinity to a single 5-HT receptor subtype must be evaluated against all other subtypes as well as other monoaminergic receptors, in order to determine its selectivity. These receptors are characterized by a seven transmembrane, alpha-helical structure which enables their function as membrane bound receptors. This general structure is shown by the model in Figure 2-1 (page 11). When a receptor ligand binds to the extracellular region of the receptor, a conformational shift within the receptor takes place. This conformational change in the receptor has been proposed to be very similar for all GPCRs and especially among 5-HT receptors [55]. It is this shift that activates the intracellular region of the receptor and results in the signaling event. The three-dimensional structure of these proteins has been difficult to obtain experimentally due to many factors including difficulties with crystallizing the membrane protein [56]. The crystallization of the GPCR bovine rhodopsin [57], allowed for structural comparisons to other GPCRs. Much of the information about the binding site of 5-HT receptors and the conformational changes that take place upon binding is inferred from this crystal structure.

¹⁵ G-protein – a guanidine binding protein; commonly seen with G-protein coupled receptors and use alternate phosphorylation states of guanidine as a switch in signal transduction

Comparisons between this receptor and others must take some liberties in their assumptions, but draw from the fact that while most 5-HT receptors share a sequence homology¹⁶ of about 35%, there are conserved regions which are practically identical. These regions are thought to be involved in the binding event of most GPCRs, including the thirteen 5-HT receptor subtypes [58].

In addition to the complexity contained within the serotonergic family of receptors, other receptors and ion channels can bind 5-HT receptor ligands. Adrenergic receptors are a class of monoamine receptors which exhibit similarities in their physiological profile to some 5-HT receptors. In fact, some ligands that were thought to be selective for certain 5-HT receptor subtypes have shown high affinity to the adrenergic α_2 receptor [59]. Similarly, dopaminergic receptors are often conflated with serotonergic receptors in their functions. Selectivity for dopaminergic receptors with respect to 5-HT receptors has been shown to be a significant concern addressed in recent research [60]. It is therefore necessary to be mindful of this relationship when designing new selective 5-HT receptor ligands. Other receptors which have shown some similarity to 5-HT receptor ligands include ion channels, monoamine (GABA, norepinephrine, etc.) receptors and transporters [61]. This apparent complexity is somewhat simplified in practice by focusing on achieving selectivity over the most similar receptor subtypes and subsequently testing the affinity for a wide range of receptors. This approach has been shown to be reasonable, resulting in the synthesis of increasingly selective 5-HT receptor ligands in recent years.

2.2 The 5-HT₇ receptor

Being the most recently discovered 5-HT receptor subtype [62], the 5-HT₇ receptor has become increasingly distinguished from other 5-HT receptor subtypes according to its locations, mechanism of signal transduction, primary sequence¹⁷ and higher order structure¹⁸. The 5-HT₇ receptor was initially

¹⁶ sequence homology – a measure of the similarity between the sequence of residues in two related proteins

¹⁷ primary sequence – the order of amino acid residues in a protein

characterized as a 5-HT₁ receptor subtype based on its affinity to certain ligands thought to be selective for 5-HT₁ receptors. Although later studies on its signal transduction method revealed that this receptor was significantly different [63], the similarity between these subtypes was an early indicator that selectivity with regard to these subtypes would be problematic. This finding also somewhat invalidated previous research on the functions of existing subtypes which used ligands shown not to be selective. As a result, the newly discovered 5-HT₇ receptor was implicated in several conditions thought to be regulated by 5-HT₁ receptor subtypes. Its full potential as a therapeutic target remains unclear due to the inability to separate its functions from those of other similar receptor subtypes.

In addition to comparisons with other receptors, comparisons with splice variants¹⁹ of the 5-HT₇ receptor have been made [64]. There are four splice variants of the mammalian 5-HT₇ receptor, only three of which have been found in humans. These variants of the receptor are thought to differ only near the intracellular carboxy terminal, meaning that selectively binding these isoforms is not practical [65]. These differences may affect the overall action of the receptor, but likely only modify the signal transduction mechanism after the binding event concerning the coupling of the intracellular G-protein. Therefore, the effects of differences between these variants go largely overlooked in the attempt to produce selective binding agents to the receptor. The validity of this approach is established as more becomes known about the structure of the 5-HT₇ receptor and its splice variants.

¹⁸ higher order (protein) structure – the complex three-dimensional folding patterns of proteins which form common structures, such as alpha helices

¹⁹ splice variants – refers to the proteins which are encoded from the same DNA sequence, yet have different primary sequences; in the case of the 5-HT₇ receptor, splice variants exist in which the protein sequence is truncated

2.2.1 Biological expression and functions of 5-HT₇ receptors

While there is not a perfect correlation between location and function, observing the primary locations of the 5-HT₇ receptor gives some insight to the receptor's role and possible therapeutic relevance. Expression of the 5-HT₇ receptor in several different species has been thoroughly examined and reviewed [66]. Although the locations and concentration of the 5-HT₇ receptor vary largely from species to species and according to the methods used in each study, there is still enough evidence in the current literature to make some meaningful assumptions about the presence of this receptor in certain organs. These assumptions lead to theories and research about the specific physiology of the 5-HT₇ receptor.

The precursor for the 5-HT₇ protein, 5-HT₇ mRNA, has been studied through molecular biology approaches [66]. These methods have found that mRNA for the 5-HT₇ receptor is mainly found in the CNS; more specifically in the hypothalamus, thalamus and hippocampus [66]. This supports the idea that the 5-HT₇ receptor is most concentrated in these brain structures. It may also be noted that this assumption falls in accord with the long-standing implication of 5-HT₇ receptors in processes believed to be regulated by these structures, such as cognition and higher-order brain function. In additional studies on the distribution of the receptor, the correlation between mRNA and receptor concentration is supported. The methods of determination are more direct as they measure the concentration of the receptor directly, but also have innate flaws relating to the binding selectivity of ligands to the 5-HT₇ receptor. Several studies [67] have shown the distribution of the receptor to be consistent with that of the mRNA. It is also worth mentioning that while the highest concentration of 5-HT₇ receptors is found within the CNS, this receptor is also involved in functions throughout the periphery. This involvement is evidenced by its widespread presence in smooth muscle cells. The 5-HT₇ receptor has thus become

included in the possible treatment of conditions related to the relaxation of blood vessels such as migraine [68] and irritable bowel syndrome [69].

As more research is conducted on the functions of the 5-HT₇ receptor, it has become reasonable to assume that these receptors have a significant and unique role in many essential brain functions. However, as this receptor becomes increasingly implicated in brain function, it may be important to note the correlation with ligand availability and this observed increase. There are several processes which are now believed to be mediated specifically by 5-HT_{1a} and 5-HT₇ receptors. It is possible that this correlation is observed due to availability of ligands which selectively bind only these receptors. In reality, these functions may be mediated by a much more complex response from several serotonin receptor subtypes. Research with novel selective ligands will help to advance this research.

2.2.2 Mechanism of signal transduction

The mechanism of action of the 5-HT₇ receptor follows that of the general mechanism of the superfamily of receptors to which it belongs (see review [67] and references therein), known as G-protein coupled receptors (GPCR). These receptors transmit their signal through an association with an intracellular protein (G-protein). This association initializes a signal cascade when the receptor is bound with an agonist²⁰. In summary, activation of the 5-HT₇ receptor causes an increase in intracellular cyclic AMP (cAMP) [70]. This increase can then influence several different signaling cascades depending on the particular cell type in which the receptor is expressed. These signaling pathways provide more clues to the function and importance of the 5-HT₇ receptors. Observing the end results of these pathways allows insight into what the end result of receptor activation may affect. As an example, it has been

²⁰ agonist – a compound which upon binding to a receptor causes activity identical to when the receptor is bound with the natural ligand

reported that the 5-HT₇ receptor can activate a kinase²¹ (ERK) in hippocampal neurons [71], further supporting the receptor's role in mood regulation [67].

It may also be the case that the 5-HT₇ receptor does not operate on the strict axis of activation and inactivation put forward by the ternary complex model²². Recent research shows that many GPCRs, including the 5-HT_{2a} receptor, may operate according to the agonist-trafficking theory [72]. This theory postulates that different agonists may cause different structural changes in the receptor, and thus, affect different signaling cascades [73]. This has been proposed to be the mechanism by which hallucinogens such as LSD have a profoundly differing effect when bound to the 5-HT_{2a} receptor than other agonists [74]. If this is indeed the case for the 5-HT₇ receptor, the physiological profile of this receptor is only made more complex. Further studies on the structure of agonist bound receptors are needed to make conclusions on how this information modifies the attractiveness of GPCRs as a therapeutic target.

2.2.3 Conformational changes upon binding

Research has recently provided detailed pharmacophores²³ of the binding site from X-ray crystallography and molecular modeling methods. Due to the fact that GPCRs are transmembrane proteins, they have proven difficult to crystallize [56]. While some GPCRs have been crystallized in their activated and inactivated states, structural data from X-ray crystallographic techniques is limited. However, this information about similar GPCRs along with molecular modeling research [75,76] has produced a reasonable understanding for structural changes which take place after the ligand binds to

²¹ kinase – an enzyme which modulates the transfer of a phosphate group between two structures

²² ternary complex model – a model for ligand binding which assumes a direct relationship between the dissociation constants of two ligands with respect to a receptor; used to determine the affinity of novel compounds to a receptor

²³ pharmacophore – a map of regions which describe the necessary characteristics for binding a receptor; a complete pharmacophore will include all necessary regions for binding and describe the nature of those interactions

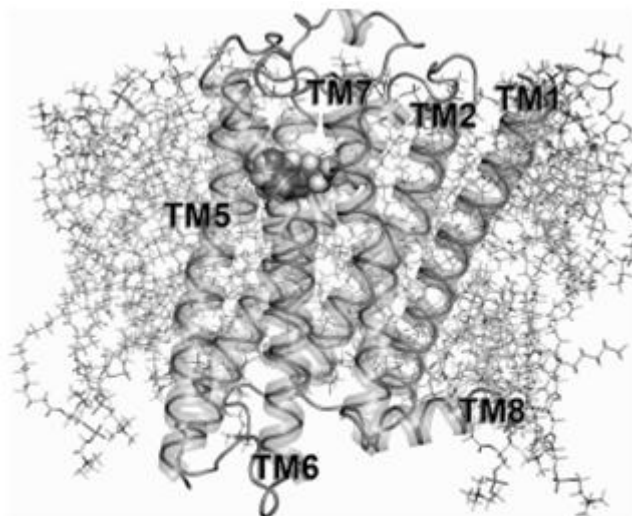


Figure 2-1. Modeled structure of serotonin bound to the 5-HT_{2A} receptor based on the crystal structure of the β_2 -adrenergic receptor [55]. Comparisons between this receptor and other 5-HT receptors have proven valuable in understanding binding site interactions which confer activity and selectivity between different receptor subtypes.

GPCRs. As before, these observations are likely common to all GPCRs, including the 5-HT₇ receptor and other serotonin receptor subtypes. More information about how these proteins realign their structures upon binding gives further insight into the design of novel 5-HT receptor agents. The difficulties in selectively binding 5-HT receptors due to their high similarity have been discussed. Modeling calculations take advantage of these similarities

to estimate a binding site structure. Because the GPCR family is highly conserved in certain areas, including the binding site, the overall structural changes that take place during binding an agonist are assumed to be similar for all 5-HT receptors. While the resolution resulting from these methods may not be sufficient for describing precise spatial differences between 5-HT receptor subtypes, it is assumed to be adequate for studying the binding mechanism. Researchers have taken advantage of this using several different structures and calculated models to make comparisons. This information has been reviewed in detail [55] and is summarized below.

The transmembrane region of the 5-HT₇ receptor consists of seven alpha-helical domains (TM 1-7, Figure 2-1) which serve as the core structural element of all GPCRs. These alpha helices alter their alignment with each other after binding an agonist. This conformational shift greatly alters the overall structure of the protein. This realignment causes the G-protein to exist in an activated state and is the basis of the signal transduction ability of the protein. As labeled by Nichols[8] [3], TM 1-4 serve as the rigid core of the receptor, while TM 5-7 are thought to be responsible for inducing structural changes in the intracellular region. The intracellular loops connecting the TM regions (IL 1-3) are proposed to

couple to the G-protein, and therefore, changes in the position of these loops affect receptor activation. The specific cascade of conformational changes which takes place is largely hypothetical and extremely complex, but there are a few steps in this process which are generally accepted mechanisms of GPCRs. The mechanism is thought to involve the movement of TM 3, 6 and 7. These regions are set into motion as serotonin binds to the conserved Asp 3.32 residue (nomenclature as in [55], Res 3.50 is the most conserved residue of TM 3). As the protonated amine of serotonin forms a salt bridge with Asp 3.32, the ligand is further positioned by interactions between the hydroxyl group and Ser 5.43. This positioning step has been proposed to be where binding selectivity is conferred. After these groups become associated with each other, several interactions which serve to stabilize the receptor in its inactive state are disrupted by concerted movements within the core of the receptor. These interactions have been summarized in great detail [55] and are discussed in the following section as they correspond with pharmacophoric regions proposed by several different groups. The combined effect of these destabilizing interactions causes TM 6 to move away from TM 3, causing a key interaction between Glu 6.30 and Arg 3.50 to dissociate. These residues are stabilized when dissociated from each other, minimizing the strain on the activated receptor caused by the separation of these oppositely charged residues. This triggers movement of TM 5, disrupting interactions with IL 3 that keep it closely tethered to the receptor while inactive. Once IL 3 is allowed to move away from the receptor, the G-protein takes its activated heterotrimeric form and the signal transduction circuit is completed.

The actions of the binding mechanism can be related to pharmacophore hypotheses projecting the need for certain functional groups in specific regions in the binding site. These vital binding site requirements all seem to actively participate in receptor activation. In the proposed pharmacophore hypothesis there are five possible ligand interactions with the binding site. These include a protonated amine (PA), hydrogen bond acceptors (HBA), and hydrophobic/aromatic regions (HYD/AR). These interactions between the binding site regions and several different classes of ligands are illustrated well

by a recent pharmacophore model by Kolczkowski [77]. These studies were performed on calculated models of the receptor, so they are not useful for high resolution considerations. They do, however, serve the purpose of illustrating possible interactions within the binding site. The next section details how interactions between these residues may be advantageous for design of novel selective ligands of the 5-HT₇ receptor.

2.2.4 Pharmacophores of 5-HT_{1a}, 5-HT_{2a}, and 5-HT₇ receptors

The necessary binding site interactions between ligands and 5-HT receptors were mentioned in the previous section. It is prudent to discuss calculated pharmacophores which describe these interactions visually, and in greater detail. These models have been calculated from several groups of high affinity ligands, with differing degrees of selectivity to the 5-HT₇ receptor. It is a major goal of this research to improve on the selectivity and affinity of ligands to serotonin receptor subtypes, namely the 5-HT₇ receptor. In order to derive more detailed information about the differences between the receptor subtypes and how to exploit those differences, it is useful to calculate a pharmacophore. These studies compare high affinity ligands and use their structural similarities to make quantitative observations about the binding interactions between the ligand and the receptor. Although these methods have drawbacks, this research has continually improved upon pharmacophores for selectively binding to the 5-HT₇ receptor. Calculation of pharmacophores and subsequent optimization of ligands has resulted in thousands of novel 5-HT₇ receptor ligands. A summary of the evolution of the pharmacophore for the 5-HT₇ receptor follows.

The development of a pharmacophore hypothesis for the 5-HT₇ receptor began with simple observations about the database of 5-HT₇ receptor ligands and their affinity. It was initially assumed from analysis of a small set of benzindoles that a central aromatic group must be present for affinity [78]. Although a somewhat narrow prediction, this observation has contributed to the current definition

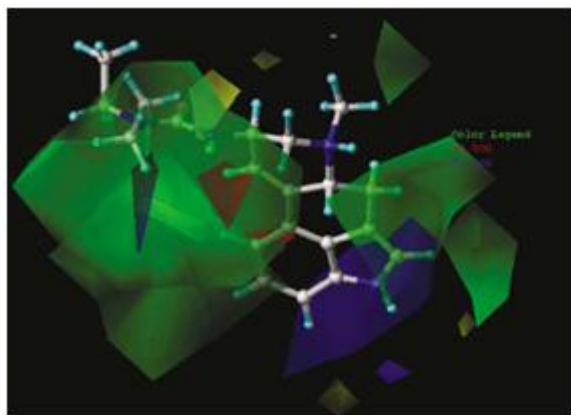
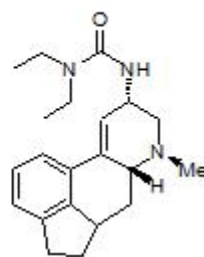


Figure 2-2 A calculated model for affinity to the 5HT₇ receptor [80]. R-lisuride is shown in the figure. Positive electrostatic charge is favored (blue) or not favored (red) for high-affinity. Steric bulk is favored (green) or not favored (yellow) for high-affinity.



R-lisuride

of the 5-HT₇ receptor pharmacophore. As the database of ligands grows, the pharmacophore calculations become more detailed. The first significant pharmacophore hypothesis to include a quantitative projection of

ligand functional groups was published by Lopez-Rodriguez, et al [79]. Their proposed pharmacophore (similar to Figure 2-3) predicted antagonism of the 5-HT₇ receptor by analyzing 30 previously synthesized compounds. These calculations described the initial scaffold for antagonists²⁴ of the 5-HT₇ receptor. As more ligands have been synthesized, the optimal spatial arrangement of these interactions has become more precise.

A subsequent study on the 5-HT₇ receptor [80] yielded information about similarities between 5-HT₇ and 5-HT_{1a} receptors (Figure 2-2). In doing so, a pharmacophore was calculated for selectivity to 5-HT₇ relative to 5-HT_{1a} receptors. Increased detail in the field contours and regions show that the hydrophobic group adjacent to the positively charged amine may play a crucial role in receptor selectivity. There is evidence of a hydrophobic interaction (large green contour) as well as a region corresponding to a protonated amine. Also present are electrostatic favored and disfavored regions within the large green contour. This presence of these regions foreshadows a possible hydrogen bonding interaction which is shown more clearly in the following models.

²⁴ antagonist – a compound which upon binding to a receptor blocks activity identical to when the receptor is bound with the natural ligand

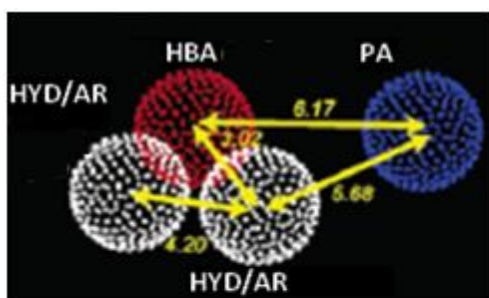
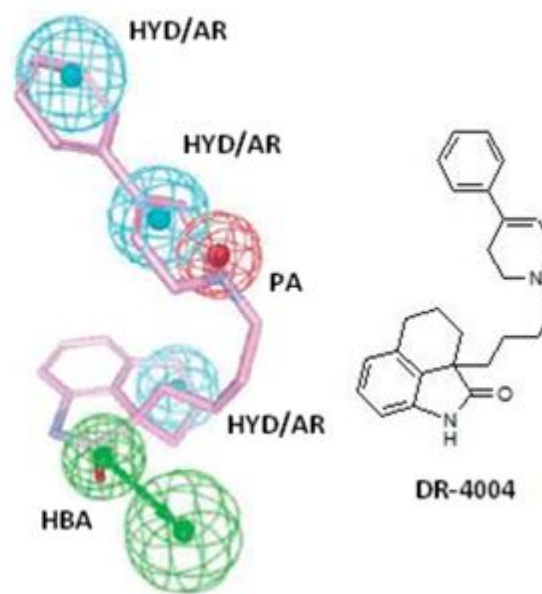


Figure 2.3. Models for agonism (above, [81]) and antagonism (right, [4]) of the 5-HT₇ receptor. The antagonist DR-4004 is superimposed onto the model for antagonism and its structure is represented at the far right. Comparing the two models shows that the regions occupied by the phenyl-tetrahydropiperadine moiety of DR-4004 likely coincide with the HYD/AR groups in the model for agonism.



A pharmacophore for agonism [81] is shown in Figure 2-3. This study details a median distance of 6.2 angstroms between the required protonated amine and a hydrogen bond acceptor, which disagrees with the 7.1-8.1 angstroms proposed by the previous study [79]. This paper goes further to suggest that the hydrogen bond acceptor group is not crucial to agonism, as was suggested for antagonism. It was also suggested that compounds showing high affinity for the receptor could overcome the lack of a hydrogen bond acceptor with an aromatic ring 4-4.3 angstroms from the central aromatic ring. This hints at ligand interactions with either Ser 5.42 or Phe 6.51 and Phe 6.52. These residues are all in the same region of the binding site, as is shown by later studies, and could accommodate either a HBA or HYD/AR interaction. These findings hint at the possibility that the hydrogen bond acceptor regions described by these two models do not result from the same binding site interaction. It is possible that after forming the salt bridge in the PA region, an HBA interaction may be possible in two different conformations. These calculations provide support for multiple possible binding modes for ligands.

Lopez-Rodriguez et al. [4] amended their initial research with a revised model (Figure 2-3) for antagonism which includes five regions, all deemed necessary for the antagonists to bind to the 5-HT₇ receptor. This model improves on the previous calculation by including the aromatic groups mentioned

in Wilcox's model in Figure 2-2 [80]. However, this model only describes one HBA interaction and it is away from the region of the binding site containing Ser 5.42, unlike that proposed by Vermeulen in Figure 2-3 [81]. This model did also not include the region which noted favorable steric bulk, but this feature is present several of the ligands used in the calculation.

A subsequent study proposed which agrees with the evidence for two possible HBA interactions in the binding site suggests that there are two binding pockets of the receptor [5]. Docking studies confirmed the binding mode of the ligands used in the calculation. They are conformed in a similar manner as previous research [4] as shown by the overlaid structure in Figure 2-4. This recent pharmacophore describes in detail two different HBA interactions as described separately in previous research. Shown near the right side of Figure 2-4 is the HBA interaction proposed to affect agonism of the 5-HT₇ receptor. Few ligands have been synthesized previously which explore this region for affinity and selectivity advantages. Of these ligands include arylpiperazines, which is a common moiety in the library of ligands synthesized for the current study. It was a goal of this research to synthesize ligands which exploit the interactions described at this secondary HBA region based on these projections. A region corresponding with the hydrophobic interactions seen in the model in Figure 2-2 is also present, shown as a HYD/AR region on the left side of the presented model in Figure 2-4. The central protonated amine region is also present.

Many ligands exhibiting high affinity to the 5-HT₇ receptor have been synthesized based on the predictions of these models. Table 2-1 shows a few compounds whose affinity can be described by these pharmacophores. The compounds listed show features of many previous 5-HT₇ receptor ligand classes. These efforts are continued, as detailed in the next chapter, with the synthesis of a series of compounds which combines the most advantageous groups from each of the previously published ligand classes, as well as those synthesized in this lab.

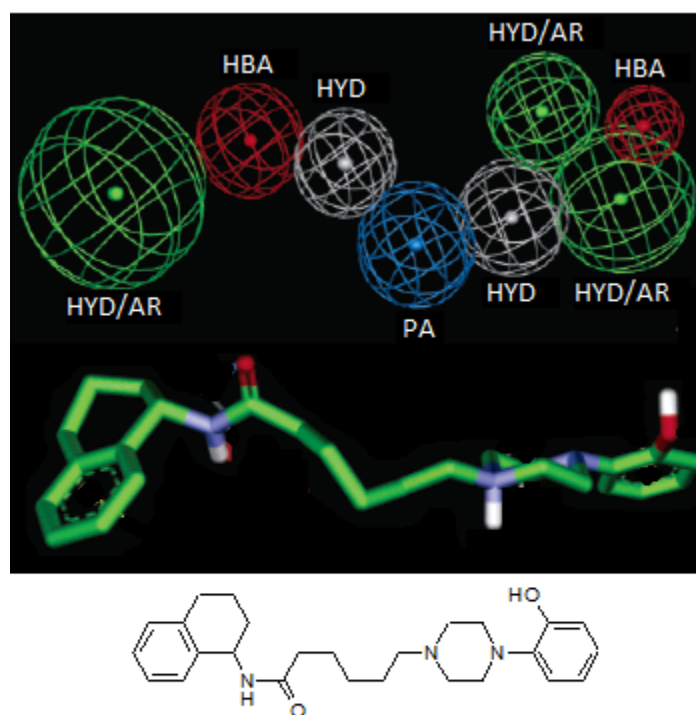
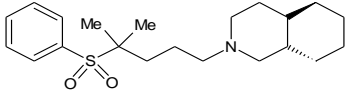
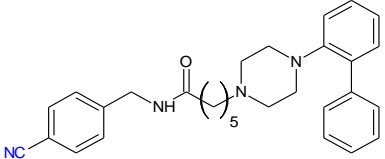
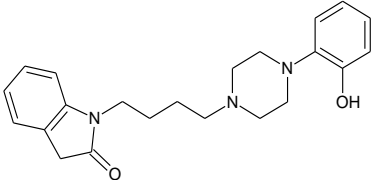
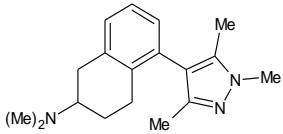
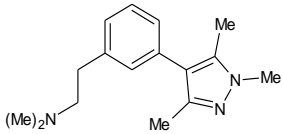


Figure 2-4. A pharmacophore for antagonism of the 5-HT₇ receptor (74). The long-chain amino piperazine (156) shown was minimized within a model of the 5-HT₇ binding site. The structural features of the ligand correlate well with the predicted regions of favorable binding site interactions. The long-chain aminopiperazine compound is drawn below.

Table 2-1. A few compounds with high affinity and selectivity to 5-HT₇ are listed. This affinity is due to optimized interactions between the ligands and the binding site, as described by the above pharmacophore models.

Structure	Action	K _i (nM) to 5-HT ₇ receptor	pK _i (5-HT ₇ receptor)	Selectivity advantages
	antagonist	7.9	8.1[8][6]	>100 fold over 5-HT _{1a} and 5-HT _{2a} receptors
	antagonist	0.63	9.2[8][7]	>100 fold over 5-HT _{1a} and D ₂ receptors
	antagonist	32	7.5[8][8]	>100 fold over 5-HT _{1a} receptor
	agonist	0.63	9.2[8][9]	>100-fold over most, except some 5-HT ₁ receptor family
	agonist	2.5	8.6[8][10]	complete selectivity over 140+ receptors

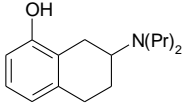
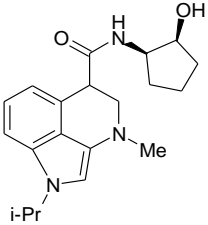
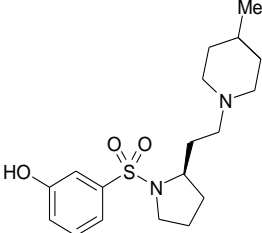
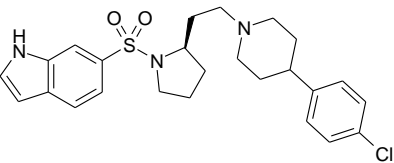
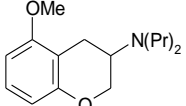
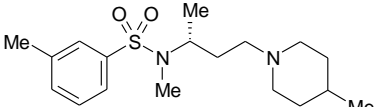
2.3 Current 5-HT₇ receptor ligands

Using the models and projections described in the previous section, as well as other methods, several thousands of 5-HT₇ receptor ligands have been designed and synthesized. These compounds represent many different classes of 5-HT₇ receptor ligands. These ligands are the result of decades of research, which has been reviewed by Leopoldo [66]. This review contains a detailed account of how the current database of ligands came about, including the drug design strategies employed and specific

modifications to ligands as they developed. These strategies are summarized, including only the most successful strategies and methods used to develop these ligands.

When the 5-HT₇ receptor was characterized, the only known ligand was its natural ligand, serotonin. This led several investigators to use serotonin as a scaffold for further modifications. These studies attempted to explore the binding site of the 5-HT₇ receptor by expanding the natural ligand to test the spatial limits of the binding site. These studies relied on the 5-HT structure as a scaffold for modifications which would relay information about the nearby binding site structure. While compounds designed by this method had very limited success in physiological studies, they exhibited some affinity to the 5-HT₇ receptor. These ligands always showed higher affinity to other receptor subtypes making them useless for physiological studies on the 5-HT₇ receptor.

Table 2-2. Previously synthesized 5-HT₇ receptor ligands. These compounds were important in the evolution of pharmacophores and the understanding of the 5-HT₇ receptor binding site. There is still room for improvement of these ligands, as noted in the far right.

Compound Name	Structure	K _i (nM) to 5-HT ₇ receptor	pK _i (5-HT ₇ receptor)	Main receptors with selectivity problems	Comments
8-OH-DPAT		500	6.3	5-HT _{1a}	Useful in its radiolabeled form for binding assays
LY215840		16	7.8	5-HT _{2a-c}	Also affected other monoamine receptors in animal studies
SB-269970		5.0	8.3	HT _{1a} , HT _{2a}	Metabolized very quickly, no oral bioavailability ²⁵
SB-656104		2.0	8.7	-	-
S20244		16	7.8	5-HT _{1a}	Previously designed as 5-HT _{1a} antagonist
SB-258719		32	7.5	-	-

Another strategy utilized in the early stages of 5-HT₇ receptor ligand development involves testing ligands for other receptor subtypes for affinity to the 5-HT₇ receptor. These studies showed that

²⁵ bioavailability – a measure of the percentage of a dosage which enters systemic circulation. Considerations relating to bioavailability include metabolism and absorption into the bloodstream

compounds thought to be selective to other receptor subtypes, such as 8-OH-DPAT, also showed affinity to the 5-HT₇ receptor [87]. This affected years of research on the 5-HT_{1a} receptor, and immediately implicated the 5-HT₇ receptor in many processes previously thought to be mediated specifically by the 5-HT_{1a} receptor [88-89]. Later studies would repeat this strategy by using existing ligands to other receptors as leads for new 5-HT₇ receptor ligands. In this manner, ergolines were used to explore the 5-HT₇ receptor binding site. Optimization of these compounds led to LY-215840, as well as many others which showed high affinity to the 5-HT₇ receptor [90]. Guillemet also used ligands to other 5-HT receptors as leads, such as S20244, which were modified to yield compounds showing high affinity to the 5-HT₇ receptor [91]. These studies expanded the pool of high affinity 5-HT₇ receptor ligands. However, the major drawback of this approach is the difficulty in achieving selectivity over the receptor for which the lead compound showed affinity. Indeed all compounds derived from 5-HT₁ and 5-HT₂ receptor ligands showed lower affinity to the 5-HT₇ receptor than the original receptor.

The first studies on binding site structure were used in research such as that resulting in a patent published by SmithKline Beecham [92]. The authors used high-throughput screening (HTS) methods to identify a lead for the first novel class of 5-HT₇ receptor antagonists, sulfonamides. This study optimized a series of sulfonamides yielding SB-258719 which exhibited modest affinity and selectivity to the 5-HT₇ receptor. The sulfonamides were optimized further, resulting in SB-269970, which has been widely used for *in vitro* research. Although this compound was a significant breakthrough, SB-269970 showed no oral bioavailability and was shown to be metabolized almost immediately *in vivo*. Resulting metabolism research indicated this may be due to the nature of the cyclic amine (instead of the phenolic group, as initially thought). This prompted modifications to the cyclic amine and resulted in the introduction of an arylpiperazine to the sulfonamide class of compounds. The arylpiperazine moiety has since been seen throughout several ligand classes due to its affinity to the receptor. Arylpiperazine analogs, namely SB-656104, demonstrated slower metabolism and increased oral bioavailability. This compound showed

higher affinity and selectivity than its predecessors, with only selectivity to 5-HT₁ and 5-HT₂ receptor subtypes remaining problematic. A large library of arylpiperazine 5-HT₇ receptor ligands have been synthesized in order to optimize the selectivity over these receptors and are discussed in the following sections.

After a decade of research developing new ligands and analyzing their binding profiles, the binding site of the 5-HT₇ receptor has become more precisely defined. Pharmacophore studies mentioned previously are testament to this and the general structure is thought to include aromatic/hydrophobic regions, hydrogen bond acceptors, a hydrophobic linker region and an interaction with a protonated amine. With a significant amount of information about the 5-HT₇ receptor, it is now possible to rely less on information gleaned from other receptors. Research has become focused on optimizing the pharmacophore for antagonism and agonism, as is reflected by recent publications at this time. Additional computational methods are now available, including homology modeling of the receptor site due to available crystal structures of rhodopsin and α_2 adrenergic receptors. In this manner, investigators focused on analyzing each region of the pharmacophores to present novel leads through HTS, classes through lead optimization, and selective ligands through pharmacophore optimization. The optimization of several classes of compounds has yielded several novel selective antagonists and at least one selective agonist. Currently, many successful ligands to the 5-HT₇ receptor have been developed from leads representing many different classes of compounds. These are summarized in Table 2-2. Each of these compounds has drawbacks and advantages but to date there is no universal 5-HT₇ receptor ligand which possesses all advantageous properties necessary for complete physiological profiling. The available binding requirements are used to design ligands with better pharmacological²⁶ attributes, affinity and selectivity over other subtypes.

²⁶ pharmacological – relating to the actions of biological systems on a specific compound

3 SYNTHESIS

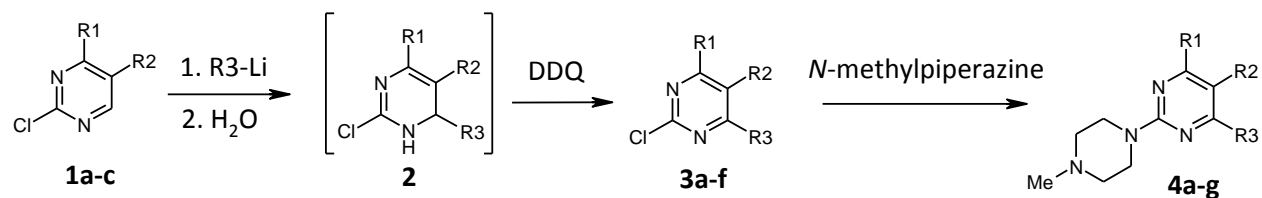
3.1 Synthesis of substituted pyrimidines as a diverse set of 5-HT receptor ligands

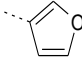
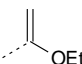
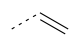
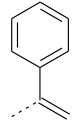
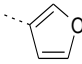
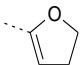
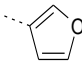
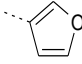
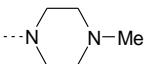
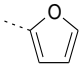
Initial studies on pyrimidine ligands demonstrated that pyrimidines exhibit high affinity to 5-HT receptors [93]. Pyrimidines are an optimal moiety for synthesizing a diverse set of substituted arylpiperazine compounds, as shown in Scheme 1. This synthetic pathway has demonstrated to be effective in synthesis of substituted pyrimidines [1,2]. The commercially available pyrimidines **1a-c** were used as starting materials in the synthesis of a novel library of 5-HT receptor ligands. Pyrimidines undergo a nucleophilic attack at the partially positive 2-, 4-, and 6- positions when treated with carbon nucleophiles, which makes these compounds an attractive scaffold for introducing variable substituents to the aryl ring. Additionally, the use of 2-chloropyrimidines **1a-c** allow for the substitution to proceed exclusively at the 4/6-position. This is accomplished by performing the nucleophilic addition to the aromatic ring at low temperatures. These conditions ensure the reaction proceeds through addition at the 4/6-position as opposed to the substitution of chlorine at the 2-position of pyrimidine, due to the size of the 2-chloro substituent. The substitution product was not observed as a product of any reaction. A diverse library of 4- and 4,6- substituted 2-chloropyrimidines **3a-f** were synthesized by nucleophilic addition of nucleophiles at low temperatures. The nucleophiles were either commercially available or generated in situ. This was achieved either by the abstraction of an acidic hydrogen or a lithium-halide exchange using a lithiated base, most commonly *n*-butyllithium. During the dropwise addition of the appropriate chloropyrimidine dissolved in dry THF, the temperature was kept at -78° C. The temperature was then slowly raised until no starting material was detected by TLC. After completion, the mixture was slowly quenched with a water/THF solution. The resulting dihydro intermediate **2** was oxidized quantitatively with a solution of 2,3-dichloro-5,6-dicyanoquinone (DDQ). A

basic workup using 1M sodium hydroxide in order to remove excess DDQ followed which allowed for the extraction of substituted pyrimidines **3a-f** into an ethereal solution. Compounds **3a-f** were then isolated by preparative chromatography using a chromatotron and a mobile phase of hexanes/dichloromethane (typically 4:1) The substitution product was not observed as a product of any reaction. The substitution product was not observed as a product of any reaction.. Addition to substituted pyrimidines is also possible, such as shown in the synthesis of **4f**. Yields of the addition were in the range of 44-59% which is typically lower than previously reported for alkyl substitutions. In the previous paper which details aryl substitutions to pyrimidine [2], the yields were comparable to those found here.

A subsequent nucleophilic aromatic substitution of the chlorine provides facile entry to compounds **4a-g**. This aromatic nucleophilic substitution has typically been carried out in ethanol, although the compounds reported showed higher yields when carried out in toluene. In cases where toluene was dried using sodium metal prior to the reaction, yields were often significantly higher. This substitution was effected by treating the appropriate chloropyrimidine **3a-f** with an excess of *N*-methylpiperazine. The mixture was heated under reflux in toluene until the starting material was no longer detected by TLC. The products were then separated into ether and purified on the chromatotron yielding compounds **4a-g**. The conditions of this reaction were not optimized further and resulted in yields of substituted arylpiperazines ranging from 32-82%.

Scheme 1.



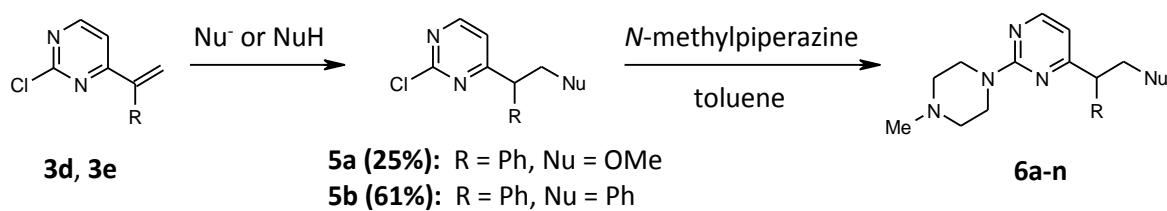
Compound	R ¹	R ²	R ³	Starting material	Yield (%)
1a	H	H	-	-	-
1b	H	<i>n</i> -propyl	-	-	-
1c	Cl	H	-	-	-
3a	H	H	<i>t</i> -butyl	1a	44
3b [2]	H	H		1a	57
3c	H	H		1a	40
3d [94]	H	H		1a	59
3e	H	H		1a	58
3f	H	<i>n</i> -propyl		1b	(17)
4a	H	H	<i>sec</i> -butyl	1a	32
4b	H	H	<i>t</i> -butyl	1a	52
4c	H	H		1a	53
4d	H	<i>n</i> -propyl	H	1b	82
4e	H	<i>n</i> -propyl		1b	44
4f	<i>n</i> -butyl	<i>n</i> -propyl		3f	73
4g		H		1c	37

3.2 Synthesis of substituted pyrimidines by 1,4 addition to vinyl-substituted pyrimidines

To further examine affinity increases seen by compounds with a hydrogen bond acceptor in a position analogous to that of the oxygen in 4-(3-furyl)-2-(piperazino)pyrimidine, the series of substituted pyrimidines was further explored. The addition of a nucleophile to vinyl substituents, such as found in **3d** and **3e** was achieved both before and after the substitution of chlorine. In the case of compounds containing a vinyl moiety such as **3d** and **3e**, it was observed treatment with an excess of a nucleophilic species resulted in both substitution of the chlorine and conjugate addition to the vinyl moiety. The conjugate addition of nucleophiles to pyrimidines has only been reported recently [5] despite the great potential for synthetic applications. The competing substitution reaction allowed for us to observe the relative reactivity of the vinyl groups during conjugate addition. When Grignard reagents were employed in the presence of copper(I) iodide, the substitution product was not observed. In all other cases, some amount of the substitution product was observed, though typically the 1,4-conjugate addition was the major product. Only in the case of nucleophiles sodium methoxide and sodium ethylthiolate was there no major product. In the case of sodium methoxide addition, the substitution product, the conjugate addition product, and the diaddition product were observed in 19-22% yields. Reaction with sodium ethylthiolate only produced significant yields of the diaddition product when treated in excess, otherwise, low yields and many product resulted. Treatment of the pyrimidines with the nucleophiles typically occurred in refluxing toluene with the exception of Grignard reagents, which were used at low temperatures. Although first attempted with a catalytic amount of copper (I) iodide, the optimal ratio of Grignard reagent to copper iodide was determined to be 2:1. The appropriate pyrimidine was then added and the mixture was stirred. These reactions were quenched after the presence of starting material was no longer detected by TLC. The products of these reactions were extracted into ether, concentrated, and purified on the chromatotron. Care was taken to ensure that

products were analyzed for nucleophilic aromatic substitution and diaddition products. Similar treatment of compounds with electron donating groups did not undergo the analogous conjugate addition and resulted only in the substitution product. This is exemplified by compounds **3c** and **4c**. Resulting arylpiperazine compounds are summarized by Scheme 2 and listed in the table below. This synthetic pathway is especially helpful in the optimization of 5-HT₇ receptor ligands as it addresses the necessity of a hydrogen bond acceptor in compounds such as **6i**. Modifications of this group have supported current hypotheses about the nature of this interaction. Further study may reveal additional information unique to the 5-HT₇ receptor resulting in a ligand with increased selectivity..

Scheme 2.



Compound	Nucleophile	R	Yield (%)
6a		H	22
6b		Ph	57
6c	EtS ⁻ Na ⁺	Ph	37
6d^a	Me ₂ NH	H	55
6e^b	<i>n</i> -BuNH ₂	H	
6f^b	<i>t</i> -BuNH ₂	H	
6g^a		H	62
6h^b		H	
6i^a	MeO ⁻ Na ⁺	H	55
6j^a	EtS ⁻ Na ⁺	H	25
6k^b		H	
6l	MeMgBr	Ph	39
6m^a	MeMgBr	H	56
6n^a	PhMgBr	H	77

Synthesized under the direction of Dr. Lucjan Strekowski by Elizabeth Raux^a or Ava Blake.^b

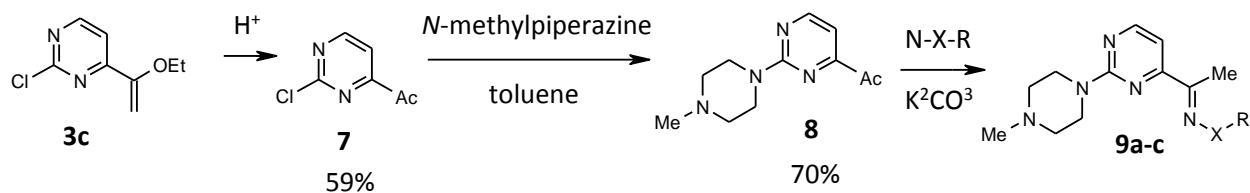
3.3 Synthesis and facile modification of 2-chloro-4-(acetyl)pyrimidine

Although compound **3c** did not undergo conjugate addition, as with other pyrimidines with a vinyl moiety, further modifications to this substituent were available. The resulting analogs are summarized in Scheme 3. As shown, **3c** can be hydrolyzed to 4-acetylpyrimidines in high yields, such as **7**. This was

achieved by treatment of either **3c** or the substitution product 2-(*N*-methylpiperazino)-4-(1-ethoxyvinyl)pyrimidine with 10% methanolic HCl. The acidic mixture was stirred at room temperature until the presence of starting material was no longer detected. The hydrolysis of **3c** was performed prior to the substitution with *N*-methylpiperazine in order to avoid forming salts of the products during the reaction. For all products **5** and **6a-c**, compound **3c** was hydrolyzed before the nucleophilic aromatic substitution of chlorine as before. This gave the acetyl compound **8** which is highly functionalizable and gives access to a diverse set of ligands such as compounds **9a-c** in yields comparable to those previously reported. As with compounds **6a-6c**, this synthesis allows for a heteroatom to be inserted into the analogous position of previous high affinity 5-HT₇ ligands. Examining the affinity of these compounds will give further information on the nature of binding site interactions with currently available ligands. This information will lead to further optimizations.

Compounds **9a-c** were synthesized by treatment of **8** with the appropriate hydroxylamine or hydrazine compounds. This reaction was carried out in refluxing methanol with potassium carbonate. After no starting material remained, the products were extracted into ether and purified on a chromatotron. The aim was to synthesize both *E* and *Z* stereoisomers of compounds **9a-c** by varying the size of the base used in the reaction, but this was not the case [95]. Compound **9a** was synthesized using both sodium hydroxide and sodium acetate as the base. The ¹H NMR spectra for both products were identical, indicating that only one isomer was synthesized. In order to determine which isomer was synthesized, the structure of compound **9a** was analyzed by NOESY. No crosspeaks between the hydroxyl group and the aromatic proton or methylene protons of the piperazine were observed. Crosspeaks in the spectra are seen between the protons of adjacent methylene protons of the piperazine. While the absence of expected crosspeaks correlating to the *Z*-isomer structure may be due to proton exchange with the solvent, compounds **9a-9c** are assumed to exist exclusively as *E*-isomers. This is in accordance with their lowest energy conformation.

Scheme 3.

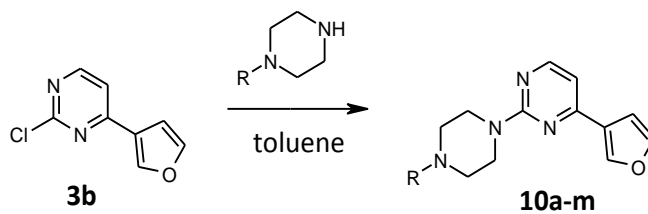


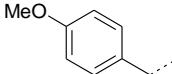
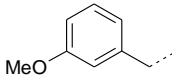
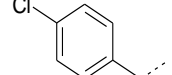
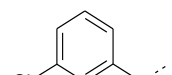
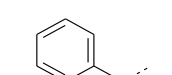
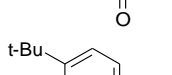
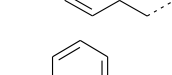
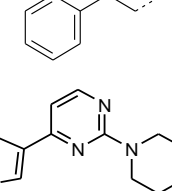
Compound	X	R	Yield (%)
9a	O	H	76
9b	N	H	76
9c	O	Et	29

3.4 Synthesis of 5-HT₇ receptor ligands with piperazine extensions

In addition to synthesizing analogs with substitutions at positions around pyrimidine, it is prudent to further explore the binding site of the 5-HT receptors by extending the piperazine substituents. Previous studies have shown that extending these ligands result in active compounds. Indeed, some of the most active and selective compounds belong to the class of long chain aminopiperazines, as classified by Kolaczowski [77]. It is also hypothesized that by increasing the size of the ligands, the interactions with the binding site can be maximized. This should have the effect of increasing selectivity as well as affinity. These compounds were synthesized by treating the highly active 2-chloropyrimidine **3b** with several commercially available *N*-substituted piperazines. This substitution yielded compounds **10a-m** in 16-87% yields.

Equation 1.



Compound	R	Yield (%)
10a	H	56
10b	Et	61
10c	propyl	39
10d	benzyl	73
10e		87
10f		40
10g		36
10h		60
10i		33
10j		45
10k		22
10l		16
10m^a	phenyl	

Synthesized under the direction of Dr. Lucjan Strekowski by Sam Barnes^a

3.5 Synthesis of fused ring 5-HT₇ receptor ligands

Benzofuran derivatives of arylpiperazino compounds were synthesized in order to increase the rigidity of the structure compared to furyl-substituted pyrimidines which showed high affinity. Specifically, by eliminating the possibility for rotation between the heteroaryl rings, more detailed information could be obtained about the binding interaction resulting in high affinity to 5-HT₇ and 5-HT_{2a} receptors. As before, this information gives insights into designing future ligands with increased affinity and selectivity to the 5-HT₇ receptor. These benzofurans were synthesized according to Scheme 5. The appropriate bromophenol was treated with an aqueous solution of potassium hydroxide in DMSO to form the bromophenoxide. This basic solution was then treated with 2-bromo-1,1-diethoxyethane and heated under reflux until no starting material remained. Extraction into ether and subsequent washings with 5% aqueous sodium hydroxide gave the substitution products **12a-e**, in quantitative yields. In most cases the products were used without purification. This was followed by a ring closure reaction under acidic conditions. Compounds **12a-e** dissolved in a solution of chlorobenzene and polyphosphonic acid. This solution was refluxed for 12h resulting in a thick black solution. The acid enables the benzene ring to exist with a positive charge as an aromatic bond attacks the partially positive carbon of the diethoxy group. Two intramolecular eliminations of ethanol oxidize the intermediate to the benzofurans **13a-e**. The products were decanted from a large amount of remaining tar, which was washed several times with diethyl ether. This organic solution was then neutralized by washing with a 1M aqueous sodium hydroxide solution. Purification on a chromatotron yielded the bromobenzofurans **13a-e** in 23-31% yields, which are comparable to those previously reported for the synthesis of benzofurans[8][11].

These halogenated benzofurans were then subjected to a Buchwald-Hartwig coupling [97] with *N*-methylpiperazine to give the arylpiperazino analogs **14a-e**. The Buchwald-Hartwig coupling reaction exploits a palladium catalyst which inserts into an aryl halide bond, such as those found in **13a-e**, leaving

the aromatic group susceptible to substitution by *N*-methylpiperazine. This reaction was carried out in dry toluene by treating compounds **13a-e** with *N*-methylpiperazine in the presence of tert-butoxide, the catalyst tris(dibenzylideneacetone) dipalladium(0) and the ligand racemic 2,2'-bis(diphenylphosphino)-1,1'-binaphthyl. These reagent participated in the catalytic cycle illustrated below. To summarize, the palladium catalyst undergoes oxidative addition to insert into the aryl halide bond. This results in oxidation of the palladium(0) complex to palladium(II). A t-butoxide ion then replaces the more stable halide. A reversible proton exchange between the t-butoxide group and *N*-methylpiperazine results in the secondary amine and the aromatic group bound in complex with palladium. As the amine and the electron deficient aromatic group are coupled, the palladium(II) complex undergoes reductive elimination to give the final product. Altering the conditions of the reaction with consideration to the base and the ligands used often results in increased yields. This was not the focus of this study, however, and the yields were found to be acceptable. Due to this, the yields are comparatively low with other similar syntheses, but would likely increase were the reaction conditions optimized. After refluxing until the starting material was no longer detected, water was added and the products were separated into diethyl ether. Purification of the products on a chromatotron yielded arylpiperazines **14** in 34-46% yield. The yields of these coupling reactions can be improved through optimization of the ligand and base used. However, optimization of this coupling reaction was outside the scope of this project.

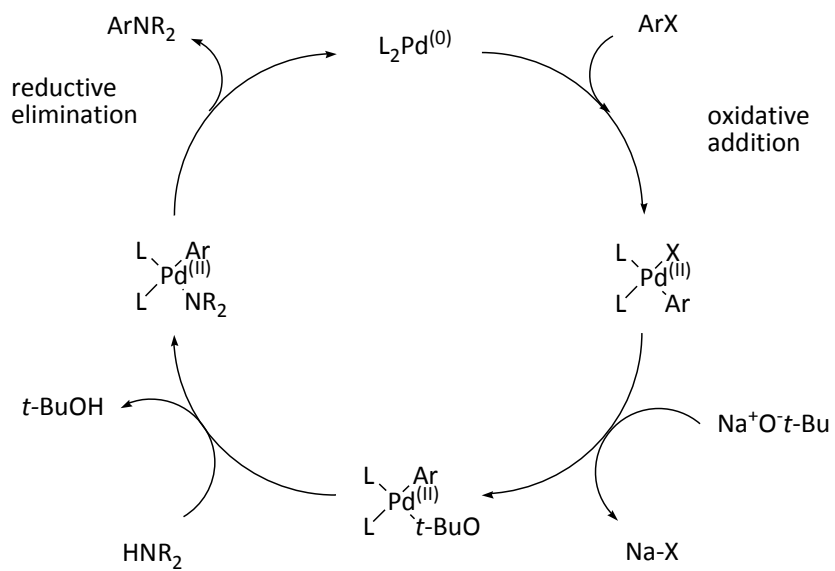
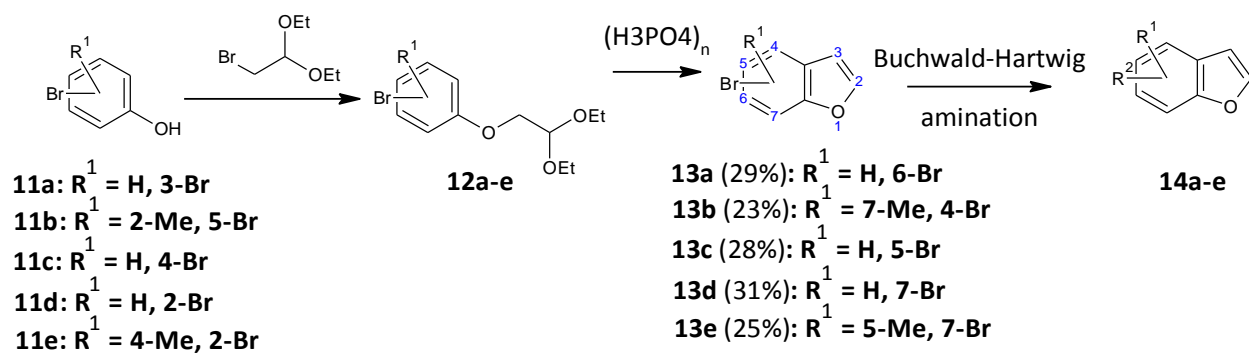


Figure 3-1. The catalytic palladium cycle.

Scheme 4.



Compound	R^1	Starting Material	Yield (%)
14a		11a	38
14b		11b	38
14c		11c	34
14d [12]		11d	39
14e		11e	46

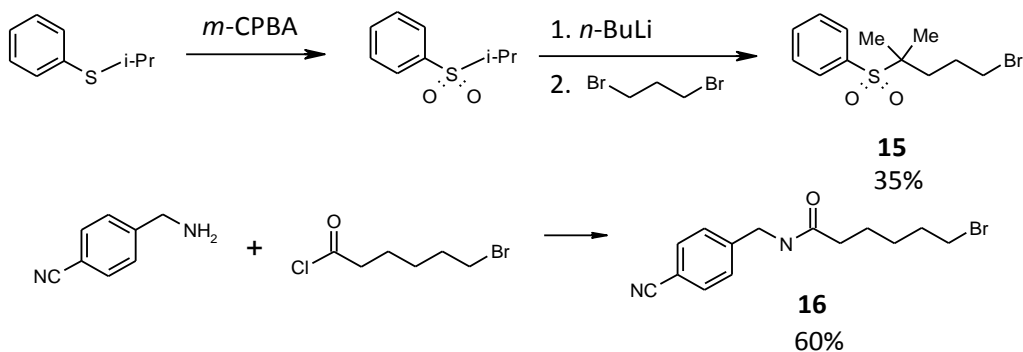
3.6 Synthesis of bivalent 5-HT₇ receptor ligands

Many previously synthesized *N*-substituted arylpiperazines have shown high affinity to 5-HT receptors. In fact, several classes of compounds exist which exploit the arylpiperazine moiety in selective 5-HT₇ receptor ligands. This research has focused on the optimization of the arylpiperazine interaction with the 5-HT₇ receptor to increase affinity and selectivity. It is logical to combine the most successful arylpiperazine moieties with previously noted classes of compounds such as sulfonamides, oxindoles and hexanamides. This strategy has resulted in the design of a novel set of ligands which contains moieties optimized for each proposed binding site interaction. Ongoing research on the activity of these compounds will clarify which structural characteristics are required for selective agonism and antagonism of the 5-HT₇ receptor. Study of these ligands may also yield information about the receptor mechanism for agonism and antagonism by comparing the activities of agonists such as AS-19 with their extended analogs. Synthesizing a series of extended ligands based on known agonists will test this theory.

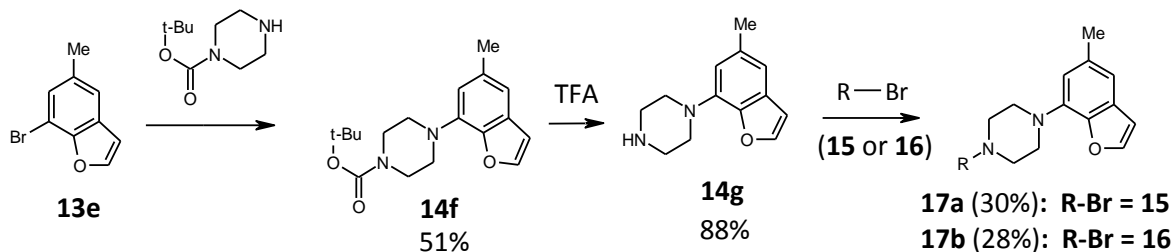
New analogs to existing classes of compounds have been synthesized and shown to bind to the 5-HT₇ receptor. These classes contain previous examples of arylpiperazine moieties. Replacing these arylpiperazines with the optimized ligands synthesized as above, such as **10a**, is expected to produce ligands with much higher affinity to the 5-HT₇ receptor while decreasing affinity to other similar receptors. These compounds (**17a-b**) are shown in Scheme 6 below and were prepared from the previously described precursors. For each of these compounds, the synthetic strategy was to prepare the corresponding halide to compounds representative of each ligand class. These halides are shown in Scheme 5 and were synthesized according to the literature. The relative length of the alkyl linker differs in all cases, and gives a more accurate description of the overall binding site size. All compounds have groups which represent the proposed interactions for this region of the binding site, such as the

aromatic/hydrophobic region of the benzene groups and an adjacent hydrogen bond acceptor as was described in the pharmacophore review.

Scheme 5.



Scheme 6.



The synthesis of these precursors to the eventual 5-HT₇ receptor ligands has been reported previously. These procedures were repeated, modifying when necessary. The synthesis of the sulfone followed Scheme 6. The sulfone was synthesized beginning with the oxidation of isopropyl phenyl sulfide. This was achieved by treating a solution of isopropyl phenyl sulfide in dichloromethane with *m*-chloroperoxybenzoic acid. This reaction typically proceeds at room temperature, but in this case mild heating was used in order to ensure the efficient reaction of the oxidizing agent. After the reagents were consumed, the reaction was quenched with sodium sulfite and the products were separated and washed with subsequent portions of aqueous basic, acidic, and brine solutions. The products were then distilled to give the sulfone in good yield. This oxidized species was then treated with *n*-butyllithium in the next step to yield the carbon nucleophile. Once generated, this nucleophile was treated with 1,4-

dibromopropane at low temperatures, similar to the previous additions of carbon nucleophiles, to give the substitution product.

The remaining precursors were prepared by nucleophilic substitution of a halide with a commercially available amine. In the case of the hexanamide, a basic solution of the amine was stirred during the addition of acyl chloride. This readily gave the product as a white precipitant in the reaction mixture, as the pH of the solution was maintained by continuous addition of an aqueous sodium hydroxide solution. The products were separated into dichloromethane and purified by recrystallization to give the hexanamide precursor in good yield. The oxindole followed a similar procedure by treating the a solution of commercially available oxindole in acetonitrile with 1,4-dibromobutane. This was done in the presence of potassium carbonate to enhance the nucleophilicity of the amide. The mixture was heated until the presence of starting material was no longer detected by TLC. Purification on a chromatotron yielded the substitution product in adequate yield. It was found that when concentrated, this product decomposed into an intensely magenta colored compound. This decomposition occurred over the span of minutes and therefore, the product was stored as a solution in acetonitrile. This method sufficiently prevented decomposition.

These bromides were then treated with the appropriate amines, whose preparation has been detailed elsewhere. This was achieved by refluxing the reagents in the presence of base until the only product was detected by TLC. The dimeric substitution products **17a-b**, were then separated into ether and purified on a chromatotron.

4 MODELING

4.1 Calculation of models for 5-HT₇ and 5-HT_{2a} receptors

Three-dimensional quantitative structure-affinity relationship (3D-QSAR) analysis is a powerful strategy to elucidate interactions between ligands and the binding site [99]. The objective of this analysis is to calculate a statistically significant correlation between the structural properties of a large set of ligands and the binding affinity to serotonin receptors. In order to determine a meaningful correlation, the structure of each ligand must be represented accurately and quantitatively. The structure can then be analyzed mathematically and the results can be represented in a straightforward manner allowing for prediction of ligands with higher affinity and more detailed descriptions of the receptor binding site. While 3D-QSAR methods are a powerful tool for analyzing binding site structure and interactions, there are drawbacks which arise from necessary assumptions. Among these is the assumption that there is only one binding mode for a group of ligands due to the dependence of 3D-QSAR on the alignment of all compounds in an analogous manner. If two compounds do not bind in the same way, then comparing their affinity based on a common set of binding site interactions is not valid. In the same manner, it is assumed that each compound binds the receptor in its lowest energy conformation. Ligands which bind in other conformations observe a decrease in apparent binding affinity corresponding to the resulting energy change. This may significantly affect the affinity and result in skewed results. Also, it is common to assume that the ligands bind to the receptor in their lowest energy conformation. Any perturbations from this conformation upon binding are reflected as an increase in the experimental K_i and result in the generation of artificial regions in the model. This is a concern in this study, and is discussed further.

4.1.1 Validation of QSAR methods

These 3D-QSAR methods assign values to ligand structures by evaluating potential energy functions at many points in a regularly spaced grid. A probe atom [100] is placed at each lattice point of the grid and the overall potential energy of the probe and the ligand is calculated. The systematic evaluation of the energy function at all points in the grid results in a numerical representation of the three-dimensional steric and electrostatic features of each ligand. These values can then be correlated with the experimental data to determine which combinations of structural properties are most effective. 3D-QSAR has been most effective when undertaken by either comparative molecular field analysis (CoMFA) or comparative molecular similarity index analysis (CoMSIA) methodologies [101]. Both CoMFA and CoMSIA methods operate on the same basic principles, however they differ in the way structural data is assigned and evaluated [102]. CoMSIA methods rely on functions which eliminate the possibility of unreasonably large calculated energy potentials at grid points. This poses a significant challenge in CoMFA studies [103]. The end result of these field calculations is a much smoother function, which leads to contour maps that are more contiguous and easier to interpret [104]. Many studies have analyzed data by both methods [105-107]. In the vast majority of these studies, the predictivity of calculated CoMSIA models was comparable or exceeded that of CoMFA models. CoMSIA models are also more resistant to small changes in the absolute positions of the ligands by systematic shifts and rotations of the aligned database of ligands [108]. CoMSIA methods also have the advantage of using several functions which are typically not included in CoMFA studies, such as hydrophobicity, and hydrogen bond donor and acceptor fields [109]. The separation of these characteristics from steric and electrostatic fields calculated in CoMFA studies provides more detailed information about the ligand structure and subsequently the receptor binding site. For these reasons, CoMSIA methods were used to evaluate the data.

4.1.2 Statistical parameters

In essence, calculating a 3D-QSAR model is a problem of multivariate regression analysis. This is to say that a dependent variable (the pK_i of the ligand) is to be calculated from a set of many independent variables (the set of coefficients used to describe the ligand structure) [110]. This correlation is typically calculated by means of a partial least squares (PLS) analysis and can be represented by the formula $y = f(x)$, where the calculated QSAR model is the function [111]. PLS is popular for this type of calculation due to its ability to handle a large amount of dependent variables. Using only the most significant of the dependant variables allows most of the noise to be removed from the model. This is achieved by a complex series of functions which compiles the most relevant structural data into a minimum number of dependent variables, or principal components²⁷ (N) [112]. A model that uses fewer principal components to accurately describe a function is more predictive, based on the input information. However, if too few components are used, the model may not reflect vital information to describe all the regions present. The optimum number of components is determined by a calculating the r^2 of the experimental vs. predicted activity across a range of principal components. The leave-one-out (LOO) procedure was chosen for internal validation of the data set and has been shown to be effective [113]. This analysis calculates the predicted residual sum of squares (PRESS) along with cross-validated r^2 (q^2) using a range of components. The number of components which corresponds to the lowest PRESS is typically used in calculations. However, if reasonably similar PRESS values are returned from a smaller number of components, this number may be used in order to reduce noise in the model. The predictivity of the PLS analysis can be evaluated by several statistical factors, most importantly q^2 , the correlation constant (r^2), and F-value [114]. Values of q^2 higher than 0.5 are considered to be acceptable for a significant model, although this parameter along does not adequately

²⁷ principal component – an algebraic matrix which represents compiled information about ligand structure for QSAR analysis

describe the predictivity of the model [115]. The F-test provides further support of a model, with higher values signaling a more predictive model. This statistical test gives the explained variance relative to the unexplained variance in the calculated model. The correlation coefficient shows the linearity of the data and is typically between 0.7 and 0.9 for predictive models. In addition to these parameters, a qualitative analysis of the graph of predicted vs. observed activity is common. Also, discussions of residuals and outliers help to support the evidence for a predictive model. The strength of this analysis directly corresponds to the confidence with which future ligands' activity can be predicted. These conventions are followed in this research and have showed these models to be statistically valid for predicting ligands with higher affinity and selectivity to the receptor being studied.

4.1.3 Ligands used to calculate the models

The structures used to calculate the 3D-QSAR models are listed in Tables 4-1 through 4-6 below. These tables have been organized based on their structural features. Ligands and their experimental data were obtained from the 5-HT₇ receptor ligands previously synthesized at Georgia State University. Compounds which were not included in the synthesis of this project are labeled as they were named by their author. The binding assay calculated the affinity as either K_i or K_s , the former of the two being more precise, with a reported standard error of measurement of 20% [116]. The error associated with K_s values is quite large and therefore, only compounds with experimental K_i values were used in the QSAR study. Ligands whose pK_i was less than 5 were not included. To calculate a robust QSAR model, it is necessary to consider ligands exhibiting a large range of affinity to the receptor. The database of compounds shows affinity ranging over five orders of magnitude. This range has yielded predictive models in several other studies [117-120]. This exclusion left 67 of the 104 ligands synthesized at Georgia State University available for analysis. These compounds are shown in Tables 4-1 through 4-6 below.

Several ligands were omitted from the QSAR study for structural reasons, such as chirality. Chiral structures have been problematic in CoMSIA calculations [121] as enantiomers often can exhibit significantly different affinity to 5-HT receptors [122]. The only compound with a chiral center in the synthesized ligands (**JS47**) was omitted from the library. Compounds which could not be minimized to the alignment which was used for the analysis were also omitted. This is not meant to imply that these compounds cannot conform to fit the binding site for these receptors. Including misaligned compounds in a QSAR analysis can provide misleading regions of interactions in the calculated model. These compounds are **4f**, **SB14**, **SS05** and **10i**. Compound **JK11** contains a bulky alkyl substituent at the 5-position of pyrimidine which prevents the 6-position alkyl group from being minimized into an alignment similar to other alkyl groups at this region. Compound **SB14** was omitted due to its aromatic substituent. This structure contains adjacent aromatic groups in the 4-position of pyrimidine which cannot minimize into a planar arrangement, as in high affinity compounds such as **AR02**. Compounds which do not contain basic nitrogens were also excluded as this group has been previously shown to be crucial for binding and can be observed qualitatively by examining the large decrease in affinity of compound **10i** and **10m** compared to similar compounds. Compound **SS05** was also excluded due to the poor alignment of the crucial tertiary nitrogen which acts as the protonated amine at the receptor to form a salt bridge. This interaction is well known and used as a point of reference in the analysis of the calculated models. The remaining 63 compounds were used in the study where experimental affinity data was available. Omitted compounds are highlighted in gray.

All subsets of pyrimidine analogs were drawn using SYBYL's (Tripos, Inc) sketch editor and stored in a molecular spreadsheet. To calculate a meaningful correlation by CoMSIA methods, structures must be realistically represented with regard to several steric and electrostatic factors [123,124]. Representation of individual atoms and bonds by atom typing is one method of describing the local physiochemical features of a molecular structure. The atom types as defined by SYBYL represent atoms in different

environments such as carbons with differing hybridizations. In all cases, atom types assigned by SYBYL were deemed to adequately represent ligand structure. Protonation of the structures was also considered in drawing the structures as the active species of the compounds likely contains a protonated amine [77,79,81]. However, protonation often causes problems in QSAR methodologies arising from inaccuracies in calculating the molecular fields [125]. To determine whether ligands should be represented in their protonated or unprotonated forms, CoMSIA models were calculated from both protonated and neutral structures. The pK_a of the ligands was estimated based on previous studies [126], and in all cases, a positive charge on the tertiary nitrogen not adjacent to the pyrimidine ring was appropriate. Ligands containing amides or nitrogens adjacent to phenyl rings were not protonated due to the low basicity of these compounds at physiological pH [127]. Comparisons between the contribution of the calculated fields and the predictive r^2 of both models show that the neutral representation of ligands provides a reasonable model. Therefore, the structures were represented in their unprotonated form for the model calculations.

Table 4-1. Shown are 4- and 4,6- substituted 2-N-methylpiperazinopyrimidines used to calculate the 3D-QSAR model for affinity to the 5-HT₇ receptor. Compounds omitted from the analysis based on structural features are highlighted gray.

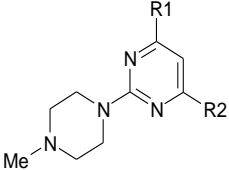
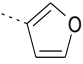
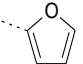
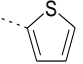
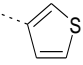
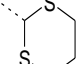
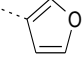
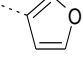
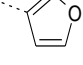
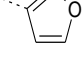
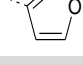

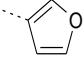
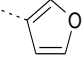
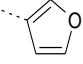
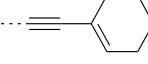
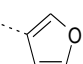
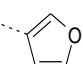
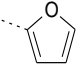
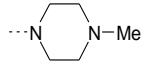
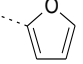
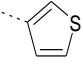
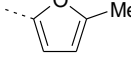
		R ₁	R ₂	Ki (nM) 5-HT _{2a}	Ki (nM) 5-HT ₇	pKi (5-HT _{2a})	pKi (5-HT ₇)
AR02	H	H		20	7	7.70	8.14
SS06	H	H		562	1023	6.25	5.99
LS104	H	H		209	631	6.68	6.20
NB45	H	H		191	209	6.72	6.68
AR43	H	H		-	1000	-	6.00
AR03	methyl	H		22	50	7.66	7.30
AR09	CF ₃	H		8	8	8.11	8.08
AR30	ethyl	H		12	7	7.92	8.15
AR13	<i>n</i> -butyl	H		2	2	8.72	8.80
JS41	<i>n</i> -hexyl	H		0	3	9.52	8.48
JS47	<i>sec</i> -butyl	H		4	27	8.44	7.57
AR04				-	22	-	7.66
JS49				0.1	-	10.00	-
EAR-II-62	ethyl	H		251	380	6.60	6.42
4g		H		871	1148	6.06	5.94
EAR-II-69(2)	<i>n</i> -butyl	H		7	15	8.15	7.82
GD01	<i>n</i> -hexyl	H		135	83	6.87	7.08

Table 4-1, continued.

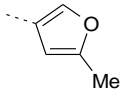
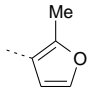
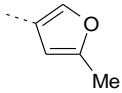
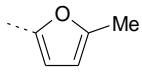
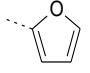
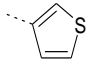
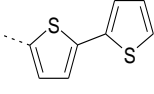
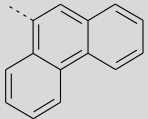
JS17	<i>n</i> -hexyl		41	12	7.39	7.92
JS06	H		389	1905	6.41	5.72
JS10	H		617	457	6.21	6.34
JS02	H		1905	4266	5.72	5.37
AR01	Cl		-	129	-	6.89
AR05	Cl		-	295	-	6.53
SB12	H		14125	1950	4.85	5.71
SB14	H		575	4074	6.24	5.39

Table 4-2. Shown are compounds containing substituents which extend from piperazine used to calculate the 3D-QSAR model for affinity to the 5-HT₇ receptor. Compounds omitted from the analysis based on structural features are highlighted gray.

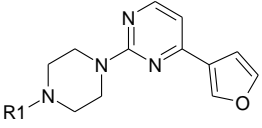
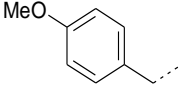
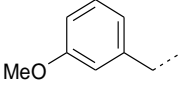
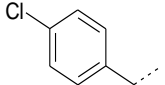
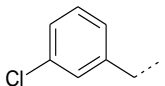
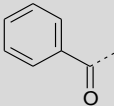
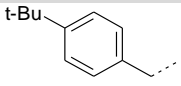
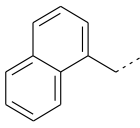
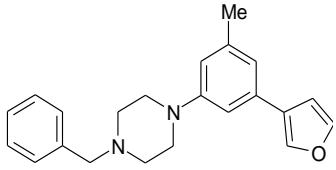
		R	Ki (nM)		pKi	
			5-HT _{2a}	5-HT ₇	(5-HT _{2a})	(5-HT ₇)
10a		H	14	9	7.85	8.05
10b		ethyl	19	10	7.72	8.00
10c		propyl	17	5	7.77	8.28
10d		benzyl	33	7	7.48	8.18
10e			776	74	6.11	7.13
10f			151	50	6.82	7.30
10g			2089	98	5.68	7.01
10h			2630	83	5.58	7.08
10i			6026	1479	5.22	5.83
10j			5754	7079	5.24	5.15
10k			288	49	6.54	7.31
E178			2951	209	5.53	6.68

Table 4-3. Shown are the compounds containing substituents other than N-methylpiperazine at the 2-position of the analogous central aromatic ring used to calculate the 3D-QSAR model for affinity to the 5-HT₇ receptor. Compounds omitted from the analysis are highlighted in gray.

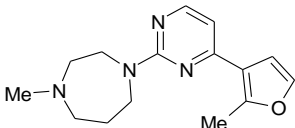
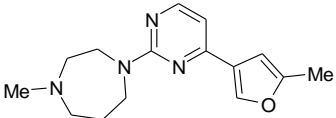
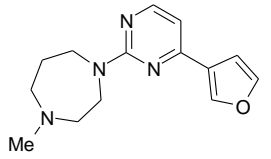
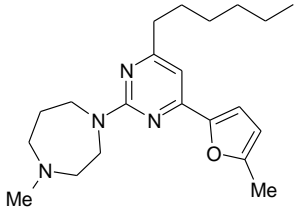
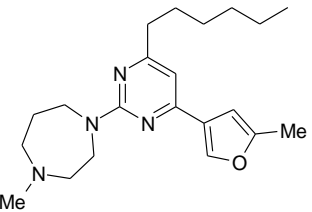
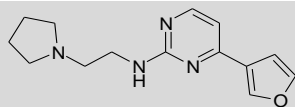
Compound	Structure	Ki (nM) 5-HT _{2a}	Ki (nM) 5-HT ₇	pKi (5-HT _{2a})	pKi (5-HT ₇)
JS07		-	9333	-	5.03
JS11		1122	2754	5.95	5.56
AR39		316	148	6.50	6.83
GD02		-	263	-	6.58
JS18		-	195	-	6.71
SS05		7413	8128	5.13	5.09

Table 4-4. Shown are the benzenes and pyridines used to calculate the 3D-QSAR model for affinity to the 5-HT₇ receptor. Compounds omitted from the analysis based on structural features are highlighted gray.

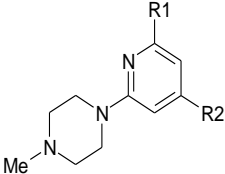
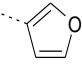
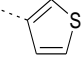
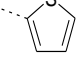
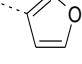
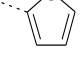
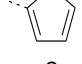
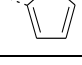
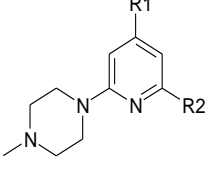
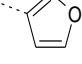
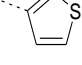
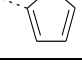
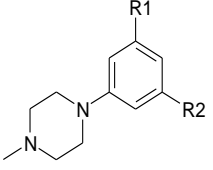
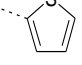
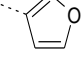
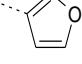
	R1	R2	Ki (nM) 5-HT _{2a}	Ki (nM) 5-HT ₇	pKi (5-HT _{2a})	pKi (5-HT ₇)
AB-B51	H		41	17	7.39	7.77
AB-B48	H		89	79	7.05	7.10
AB-B67	H		151	398	6.82	6.40
E1572	methyl		62	8	7.21	8.10
EAR-II-158(3)	methyl		115	117	6.94	6.93
AB-B72	H		331	309	6.48	6.51
EAR-II-166(8)	methyl		447	138	6.35	6.86
	R1	R2	Ki (nM) 5-HT _{2a}	Ki (nM) 5-HT ₇	pKi (5-HT _{2a})	pKi (5-HT ₇)
AB-B68	H		162	11	6.79	7.96
AB-B47	H		676	74	6.17	7.13
AB-B73	H		1950	1122	5.71	5.95
	R1	R2	Ki (nM) 5-HT _{2a}	Ki (nM) 5-HT ₇	pKi (5-HT _{2a})	pKi (5-HT ₇)
EAR-II-136(2)	<i>n</i> -butyl		195	741	6.71	6.13
E1712			33	339	7.48	6.47
EAR-II-173	methyl	phenyl	209	2884	6.68	5.54

Table 4-4, continued.

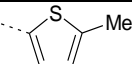
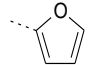
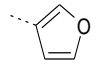
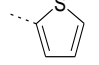
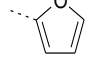
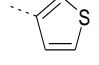
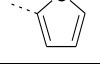
EAR-II-175(6)	methyl		851	2188	6.07	5.66
EAR-II-134	<i>n</i> -butyl		107	741	6.97	6.13
E129	<i>n</i> -butyl		68	107	7.17	6.97
E1032	methyl		331	295	6.48	6.53
E1052	H		646	912	6.19	6.04
E1262	<i>n</i> -butyl		46	263	7.34	6.58
E1352	methyl		912	309	6.04	6.51

Table 4-5. Shown are benzofurans used to calculate the 3D-QSAR model for affinity to the 5-HT₇ receptor. Compounds omitted from the analysis based on structural features are highlighted gray.

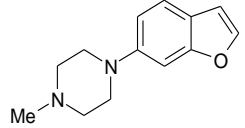
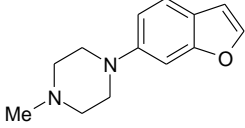
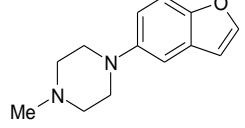
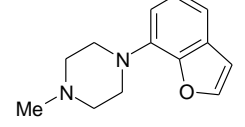
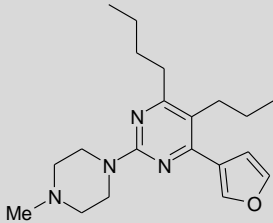
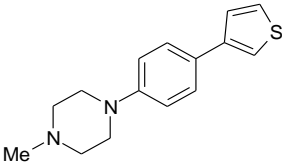
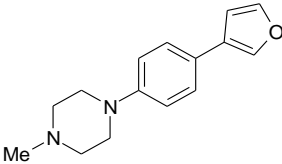
Compound	Structure	Ki (nM) 5-HT_{2a}	Ki (nM) 5-HT₇	pKi (5-HT_{2a})	pKi (5-HT₇)
14a		-	3631	-	5.44
14b		35	2291	7.46	5.64
14c		83	4677	7.08	5.33
14d		145	204	6.84	6.69

Table 4-6. Shown are the compounds with substituents to the central aromatic ring in the para-position to N-methylpiperazine used to calculate the 3D-QSAR model for affinity to the 5-HT₇ receptor. Compounds omitted from the analysis based on structural features.

Compound	Structure	Ki (nM) 5-HT _{2a}	Ki (nM) 5-HT ₇	pKi (5-HT _{2a})	pKi (5-HT ₇)
4f		240	1288	6.62	5.89
E1405		68	224	7.17	6.65
E149		1318	17378	5.88	4.76

4.1.4 Binding mode conformation

In order to make valid comparisons between ligand structures and the binding site, the conformation of the ligands represented in the model must mimic that of the receptor-bound conformation. The ligands synthesized for this study have been designed to limit the amount of conformational ambiguity present by including structurally rigid groups, such as pyrimidine. In most ligands, there are three regions where differing conformations must be considered. These correspond to the 2-, 4-, and 6-, positions of the central pyrimidine or analogous central ring. The rotation of each substituent with respect to the central ring is crucial to the resulting alignment. Similar substituents must be minimized to a similar conformation so that during alignment, optimal overlap of features is observed. Considerations with respect to the conformation of ligands are outlined below and thought to be reasonable based on previous research, cited where appropriate.

Each of the arylpiperazines have been minimized so that their basic nitrogens overlap in the same region. Any structures containing a similar group, such as homopiperazine, were minimized in a conformation which maximized the overlap of the basic nitrogens. Structures with extended piperazine groups (**10a-m**) were minimized to extend from the chair position of the ring in the equatorial position. A small displacement between analogous alkyl (**10c**) and benzyl (**10d**) piperazino substituents was observed, though these compounds likely bind in the same manner. This displacement was minimal and caused no disruption in the calculated model with respect to this region. In the same manner alkyl substituents were minimized in a planar arrangement with the central aromatic ring, and extended toward the piperazino substituent.

In order to distinguish between the symmetrical positions of substituents to pyrimidines and analogous aromatic groups, one side of the ring was designated to contain the best hydrogen bond acceptor. Alkyl and steric substituents were aligned to the opposite side of the central aromatic ring. The intention is to separate as best as possible hydrogen bond acceptors from hydrophobic groups to gain separate information about interactions with residues Ser 5.42 and Phe 6.51 and Phe 6.52. This was difficult in some cases, such as with **AR02**, where the furyl ring may be beneficial to both interactions. All aromatic substituents to the central ring were minimized in the hydrogen-bond acceptor position, giving furyl substituents priority in this region.

Conformation of aromatic substituents was complicated by differing lowest energy conformations of 2-furyl and 3-furyl substituents. Also, a large difference in K_i is observed between the two isomers. Compounds containing a 3-furyl substituent showed as much as a 100-fold increase in affinity to the 5-HT₇ receptor compared to their 2-furyl analogs. Conformational studies on these compounds have been performed previously [128] and have shown that these analogs exist in two different conformations, designated s-cis and s-trans, as shown in Figure 4-1 [129]. The energy profiles of these two isomers

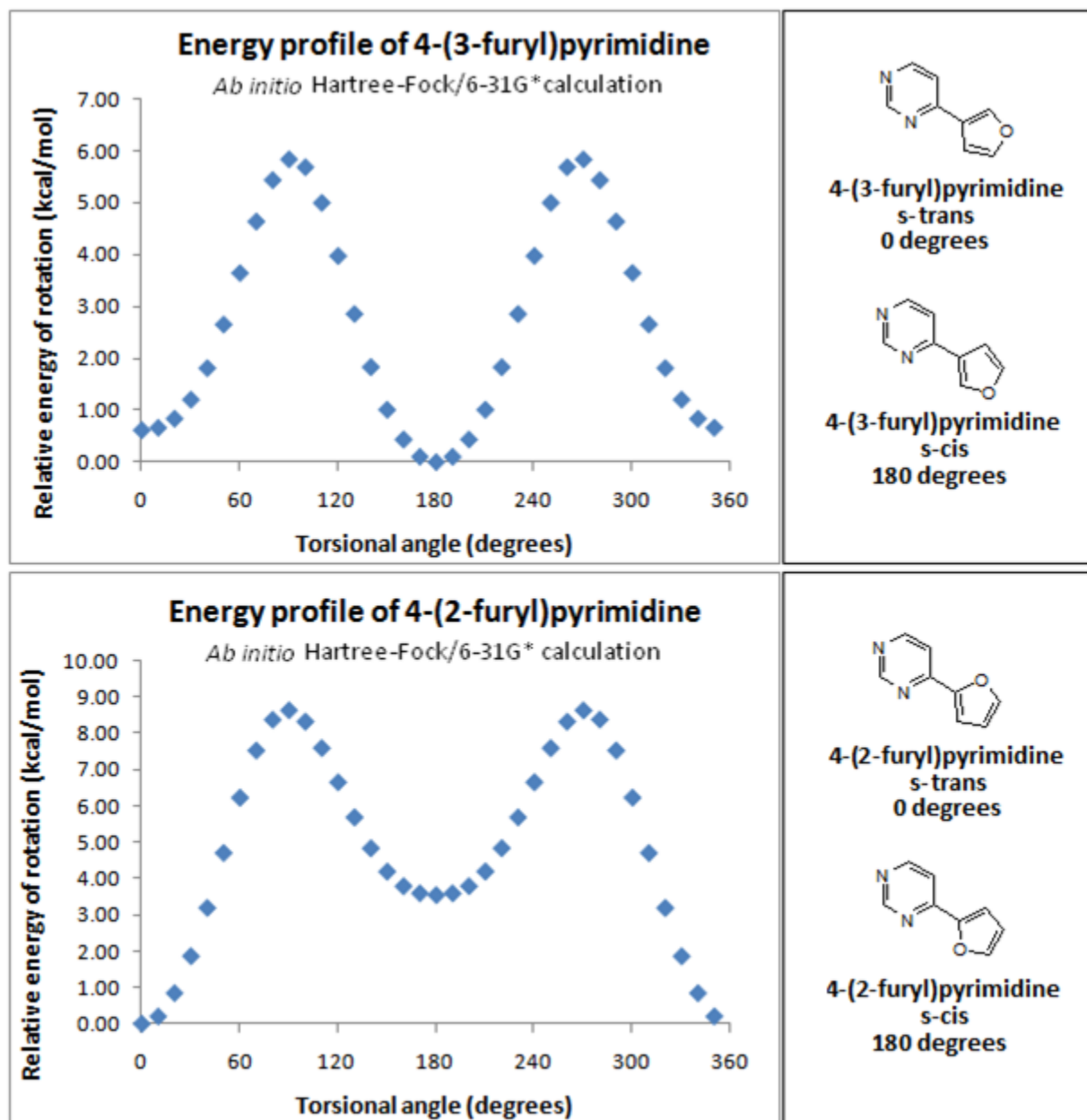


Figure 4-1. Energy profiles for the torsional angle between the aromatic rings of 4-(3-furyl)pyrimidine (top) and 4-(2-furyl)pyrimidine (bottom). Each structure has two local minima corresponding to s-cis and s-trans conformations. The energy difference between the two conformers of 4-(3-furyl)pyrimidine is 0.62 kcal/mol. The energy difference between the two conformers of 4-(2-furyl)pyrimidine is 3.55 kcal/mol.

were calculated in SPARTAN (Wavefunction, Inc). The 2-furyl analogs are shown to prefer the s-trans conformation, while 3-furyl analogs are at a global minimum in the s-cis conformation, albeit by a relatively small margin. The implications of this different lowest energy conformation on the interactions with the binding site and the experimental K_i is discussed later. For the QSAR study, it is prudent to minimize all analogs to the same conformation. Therefore, all furyl and thienyl analogs to

the *s*-cis conformation of the more active 3-furyl analogs resulted in a statistically significant model. Care must be taken in the interpretation of the generated contour maps, specifically with regard to the position of the electrostatic interactions between the receptor and the furyl heteroatom.

In all other instances of arbitrary and minimal disagreement between conformations, efforts were made to minimize the structure to an analogous conformation as that adopted by the highest affinity ligands such as **AR13**. Most compounds were easily adapted to the described conformations, however some compounds were more problematic and required additional attention. These compounds were handled on an individual basis by searching through many local minima to find one that corresponded well to the common alignment of structures. These compounds include those with flexible substituents in the place of piperazine (**SS05**) as well as structures with bulky aromatic substituents to the central aromatic ring.

The overall conformational assignment of the structures is considered to be reasonable. The conformation of **AR13** shown in Figure 4-2 is representative of the general conformation and compares well with previous binding site descriptions. Subsequent CoMSIA models and pharmacophores also support the conformation as a good fit for the proposed binding site structure.

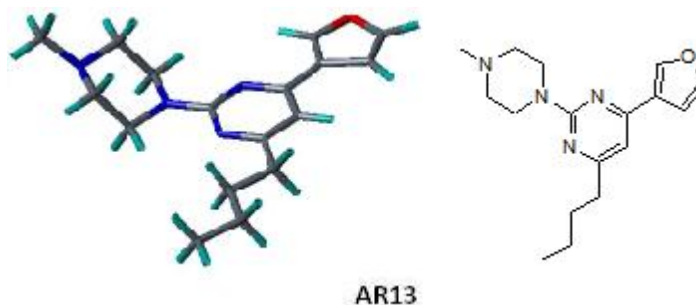


Figure 4-2 AR13 is shown in the conformation used for the calculation of the QSAR models. The alkyl chain extends planar with the central ring, the furyl group is in the *s*-trans conformation, and the piperazine adopts the chair conformation with N-substituents in the equatorial position.

4.1.5 Alignment of structures

Alignment of the structures in a CoMSIA study is the most vital aspect of calculating a predictive model. Without an accurate alignment, structural features cannot be meaningfully correlated. Several methods have been developed in order to achieve this alignment. In the current study, the minimized structure of **AR02** was used as a template for alignment. A root-means squared (RMS) fit of a common set of atoms from this template was used to individually align the structures to the same position. This method has been shown to produce predictive models, especially from models which lack of diversity. The set of structures allowed for reasonable alignments without considering multiple possible binding modes. This final alignment was further supported by a statistically significant model. All structures used to calculate the model are shown as aligned to the template in Figure 4-3.

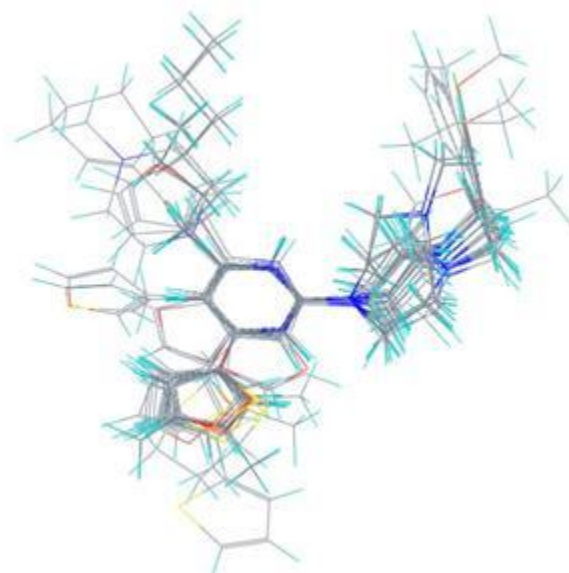


Figure 4-3. All structures used to calculate the CoMSIA model aligned to a common template of atoms.

4.2 Presentation of QSAR models

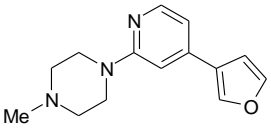
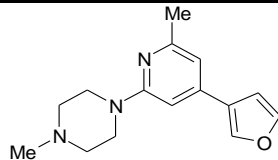
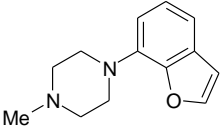
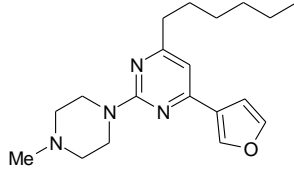
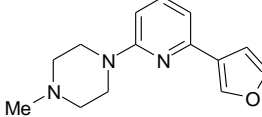
4.2.1 Pharmacophores

There have been several pharmacophore models calculated for affinity [78,80] and selectivity [77,130] of 5HT₇ receptor agonists [81,131] and antagonists [4,79]. The 5-HT₇ receptor pharmacophore has evolved from a single region, a central protonated amine (PA), into a detailed map containing multiple regions. These models for binding the 5-HT₇ receptor have considered a diverse set of ligands and include interactions across the binding site. These models have led to a better understanding of the binding mode for several different classes of 5-HT₇ receptor ligands, including arylpiperazines. The GALAHAD module in SYBYL was employed to analyze several of the most active ligands in the database, shown in Table 4-7. Each structure in the table had been previously aligned to maximize the overlap of similar regions. The standard parameters suggested by SYBYL were not adjusted as each was reasonable for this research. Models to each receptor were calculated and found to be statistically identical. These models were calculated from similar structures, so it was not unexpected that the calculations did not return significantly different models. Therefore, the model for affinity to the 5-HT₇ receptor is used to discuss the binding site interactions exploited by the synthesized ligands. The calculated model (A) is shown in Figure 4-4, along with previously calculated models (B [4] and C [77]) along with an arylpiperazine ligand.

Table 4-7 Compounds used for the calculation of the pharmacophore hypothesis for affinity to 5-HT₇ and 5-HT_{2a} receptors.

5-HT _{2a}		5-HT ₇	
Compound Name	Structure	Compound Name	Structure
AR03		10a	
AR09		AR05	
AR13		10c	
AR30		AR03	
E1712		AR02	
JS41		AR09	
AR02		AR13	
10a		AR30	

Table 4-7, continued.

AB-B51 	E1572 
14d  -	JS41  AB-B68 

Comparisons between these models and the calculated pharmacophore allows for the regions within each synthesized ligand to be associated with a specific binding site interaction. A recent model for 5-HT₇ receptor antagonism (Figure 4-4, C) describes six major binding site interactions. The same naming conventions as in section 2.2.4 are used to describe binding site interactions. Docking experiments²⁸ using homology models of the 5-HT₇ receptor and arylpiperazines have shown that these compounds bind to the 5-HT₇ receptor by forming a salt bridge with Asp 3.32 and participating in interactions with Phe 6.51, Phe 6.52 and Ser 5.42 [77]. Although the size of the synthesized ligands allows for the ability to bind in either of two binding pockets, analysis of the models leads us to conclude that these arylpiperazines must bind in an analogous manner as previous ligands. The problem of multiple binding modes can be addressed by examining the distances between the regions. It is possible that the pyrimidine region of these smaller ligands interacts with either the HYD/AR1 or HYD/AR2 region in the previous models as the distance between these two regions and the central PA is virtually identical (Table 4-8). The synthesized pyrimidines are assumed to bind in a similar manner as previous arylpiperazines. In addition to multiple binding modes, care must be taken not to place unwarranted confidence in absolute positions of calculated regions which are result from the analysis of arbitrary

²⁸ docking – in this case, docking refers to molecular modeling methods which can be used to predict the binding mode of ligands; docking studies find the best fit for known ligands within a binding site, according to their minimized interactions with the receptor

conformations. Examples of this from the database include structures containing *N*-piperazino substituents or alkyl substituents to the central aromatic ring and have been outlined in detail in the previous sections.

The calculated pharmacophore shows the presence of a protonated amine (PA), two hydrophobic or aromatic regions (HYD/AR), and a hydrogen bond acceptor (HBA). Compound **AR13** is shown overlaying the proposed pharmacophore. From the observations above, it is assumed that the protonated amine region seen in each model is represented by the basic nitrogen in the piperazine ring. The pyrimidine ring likely corresponds to the hydrophobic/aromatic region seen in all models at about 5.5 angstroms from the protonated amine. The nitrogen of the pyrimidine ring may interact with Ser 5.42 in the same manner as has been proposed for similar arylpiperazines. Substituents to the pyrimidine ring may affect the interaction with Ser 5.42 (as in furyl substituents) or with Phe 6.51 and Phe 6.52. It is also possible that these substituents interact with a region which has not been previously described. The mechanism by which these substituted pyrimidines affect affinity to the 5-HT₇ receptor is examined in the QSAR study.

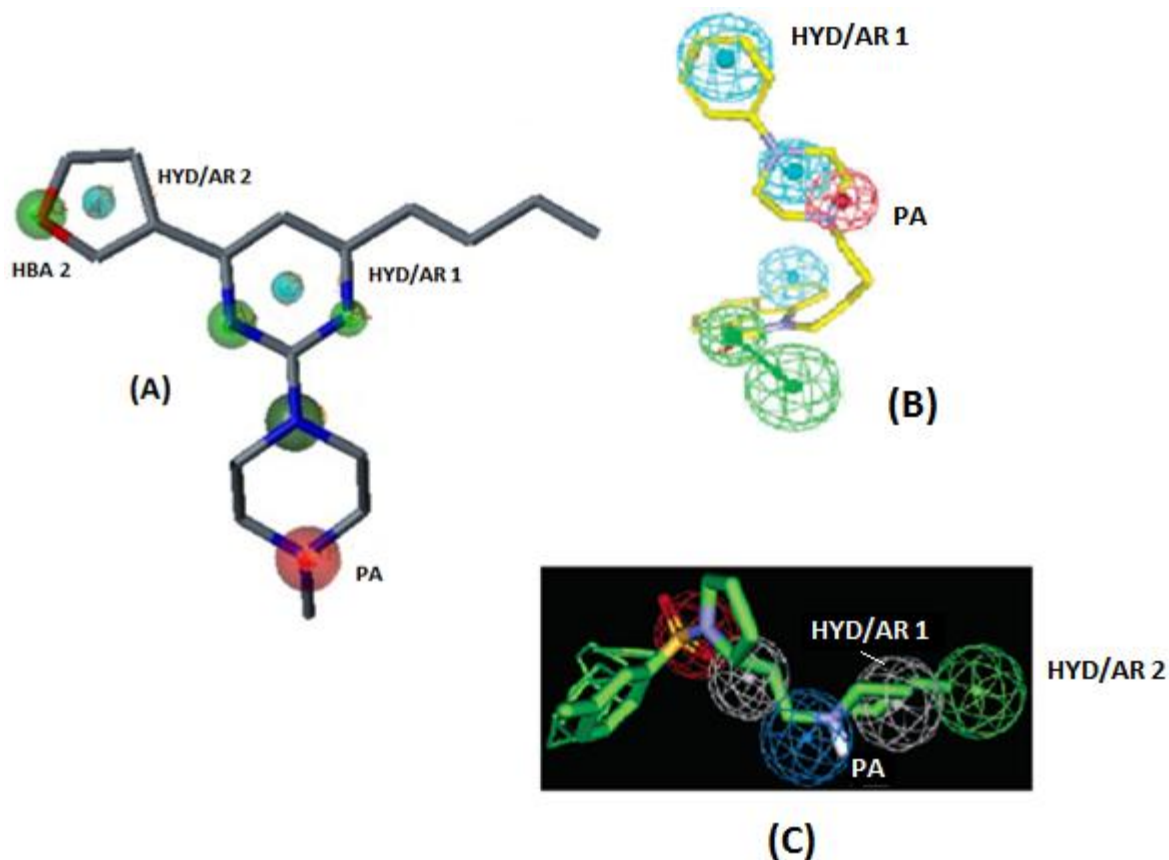


Figure 4-4. Models calculated for antagonism of 5-HT₇ including an arylpiperazine ligand. Model A was calculated from the current set of compounds. Models B [4] and C [77] were calculated in previous studies which considered a diverse set of compounds containing many classes of 5-HT₇ ligands. Regions of favorable interactions are characterized as being hydrogen bond acceptors (HBA), hydrophobic/aromatic (HYD/AR), or protonated amines (PA).

Table 4-8. A list of calculated distances between proposed binding interactions.

Regions	Model A	Model B	Model C
PA – HYD 1	4.6 - 6.2	5.4 - 6.4	4.3 - 7.8
PA – HYD 2	4.3 - 5.9	5.2 – 6.2	3.7 - 6.1
PA – HBA1	N/A	5.6 – 6.6	3.7 - 5.1
HYD 1 – HYD 2	3.5 - 4.7	9.3 – 10.3	4.1 - 4.8

4.2.2 The model for affinity to the 5-HT₇ receptor

A total of 60 compounds had experimental data available to calculate a CoMSIA model for affinity to the 5-HT₇ receptor. These compounds were aligned and loaded into a molecular spreadsheet in SYBYL, as detailed earlier. CoMSIA columns for steric, electrostatic, hydrogen bond acceptor, and hydrophobic characteristics were calculated from within SYBYL's QSAR module. No hydrogen bond donor fields were calculated as no structures in the database exhibited this characteristic and previous research has not described the presence of any hydrogen bond donor regions in previous pharmacophores or QSAR studies. A leave-one-out (LOO) cross-validated PLS was performed and the residuals of the graph of experimental vs. predicted p*K_i* were graphed. The graph revealed four outliers far away from the prediction of the PLS regression. These compounds (**JS06**, **GD02**, **AB-B51**, and **NB45**) were omitted from the calculated model in order to increase the predictivity of the model. These outliers all have similar structural features which make them difficult to be described by the calculated function. **JS06** contains a furyl substituent which cannot adopt a planar arrangement with the central aromatic ring due to a bulky methyl group. This interaction likely disrupts any interaction in the same way as **SB14**, which was also excluded from the analysis. **GD02** showed a high residual despite following general trends seen in the resulting model. This is assumed to be due to the larger than optimal substituents at each position around the central ring. Similarly, compounds **AB-B51** and **NB45** follow the general trends of the calculated model, but are omitted due to high residuals.

In order to externally validate any model, it is common to divide the data set into training and test sets. This helps to ensure a predictive model outside of cross-validated r^2 stats which have been shown to be inconclusive when considered alone. Hierarchical clustering has been shown to produce a more predictive test set. By grouping the structures together according to their structural features, more diverse training and test sets can be constructed. Using the hierarchical clustering feature available in SYBYL, the remaining 56 structures were split into four main groups according to the calculated

dendrogram shown in Fig 4-4. A test set was selected by choosing approximately 25% of the compounds from each group. The training set and test set used to calculate this model is shown in Table 4-9.

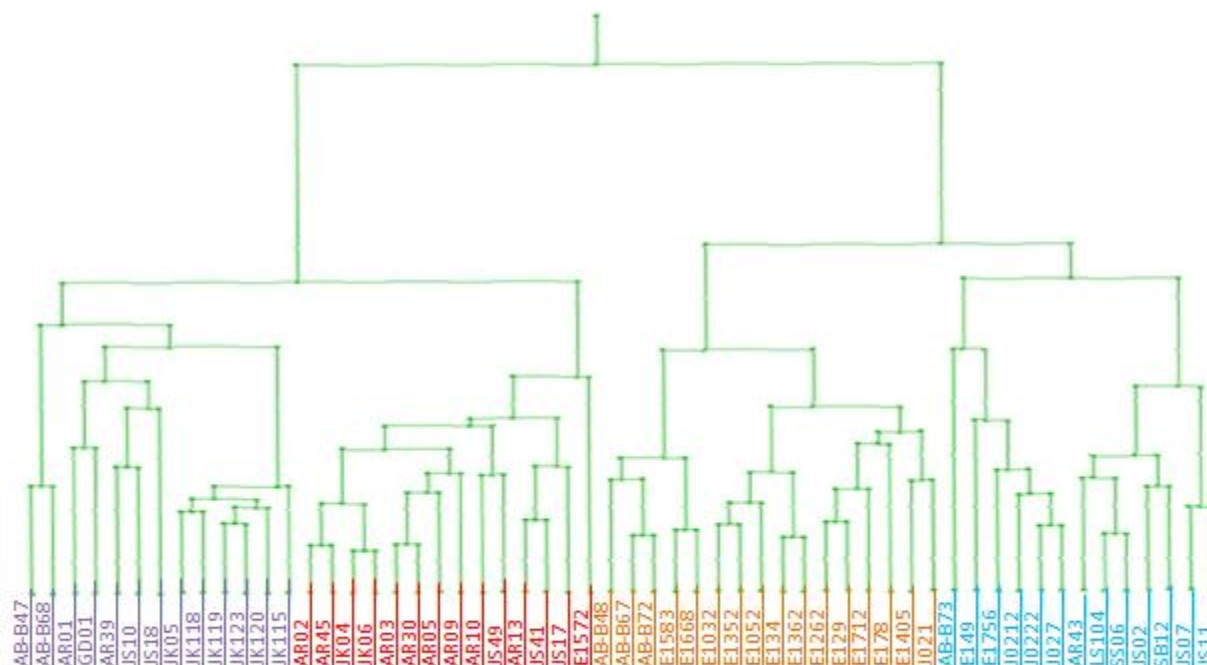
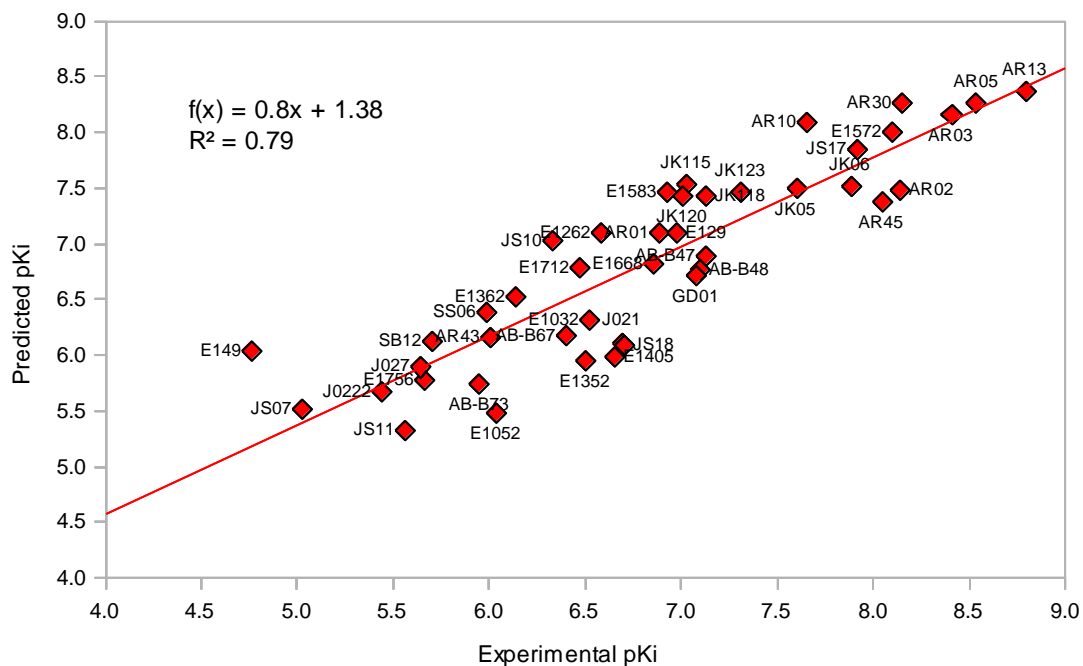


Figure 4-5 Dendrogram of the hierarchial clustering of all 56 structures used to calculate the model for affinity to the 5-HT₇ receptor. The compounds were split into four groups (shown as different colors) based on the similarity of their structural features.

A PLS crossvalidated (LOO) run was performed on the training set of 43 compounds in order to determine the optimal number of principal components (N). It was found that at 3 components, q^2 was at a maximum of 0.530 corresponding to a minimum predicted residual sum of squares (PRESS) of 0.690. The number of principal components was set at three for the following nonvalidated PLS calculation. The resulting calculated model is deemed significantly predictive and is summarized in Table 4-10 below.

Training set affinity for the 5-HT₇ receptor
(predicted vs. experimental)



Test set affinity for the 5-HT₇ receptor
(predicted vs. experimental)

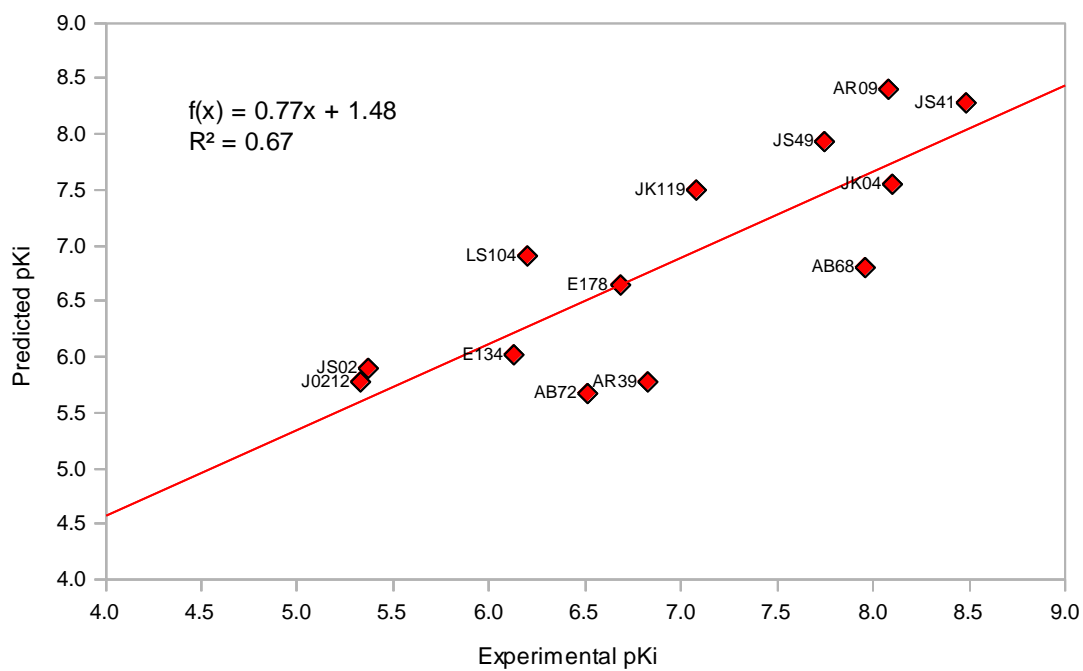


Figure 4-6. These graphs show the correlation between predicted pK_i and experimental pK_i of the training set (top) and test set (bottom). The pK_i of these compounds was predicted by the model calculated for affinity to the 5-HT₇ receptor.

Table 4-9. The tables above list the predicted pK_i and the experimental pK_i to the 5-HT₇ receptor, along with the residual.

Training Set	pKi (Exp.)	pKi (pred.)	Residual	Training Set	pKi (Exp.)	pKi (pred.)	Residual
AB-B47	7.13	6.89	0.24	E1583	6.93	7.47	-0.54
AB-B48	7.10	6.77	0.33	E1668	6.86	6.83	0.03
AB-B67	6.40	6.17	0.23	E1712	6.47	6.78	-0.31
AB-B73	5.95	5.74	0.21	E1756	5.66	5.78	-0.12
AR01	6.89	7.10	-0.22	GD01	7.08	6.72	0.36
AR02	8.14	7.48	0.66	J021	6.69	6.11	0.58
AR03	8.41	8.16	0.25	J0222	5.44	5.68	-0.24
AR05	8.54	8.27	0.27	J027	5.64	5.89	-0.25
AR10	7.66	8.10	-0.44	JK05	7.60	7.50	0.11
AR13	8.80	8.36	0.43	JK06	7.89	7.51	0.38
AR30	8.15	8.27	-0.11	JK115	7.03	7.54	-0.51
AR43	6.00	6.17	-0.16	JK118	7.13	7.43	-0.30
AR45	8.05	7.37	0.67	JK120	7.01	7.43	-0.42
E1032	6.53	6.31	0.21	10j	7.31	7.47	-0.16
E1052	6.04	5.48	0.56	JS07	5.03	5.51	-0.48
E1262	6.58	7.10	-0.52	JS10	6.34	7.03	-0.69
E129	6.97	7.10	-0.13	JS11	5.56	5.32	0.24
E1352	6.51	5.95	0.56	JS17	7.92	7.85	0.08
E1362	6.13	6.52	-0.39	JS18	6.71	6.09	0.61
E1405	6.65	5.99	0.66	SB12	5.71	6.12	-0.42
E149	4.76	6.04	-1.27	SS06	5.99	6.39	-0.40
E1572	8.10	8.00	0.10				
Test Set	pKi (Exp.)	pKi (pred.)	Residual	Test Set	pKi (Exp.)	pKi (pred.)	Residual
AB-B68	7.96	6.80	1.16	JK04	8.10	7.55	0.55
AB-B72	6.51	5.67	0.84	JK119	7.08	7.49	-0.41
AR09	8.08	8.40	-0.32	JS02	5.37	5.90	-0.53
AR39	6.83	5.77	1.06	JS41	8.48	8.29	0.20
E134	6.13	6.02	0.11	JS49	7.74	7.93	-0.19
E178	6.68	6.65	0.03	LS104	6.20	6.90	-0.70
J0212	5.33	5.77	-0.44				

Table 4-10. The statistics relating to the validity and predictivity of the model for affinity to the 5-HT₇ receptor are shown.

5-HT ₇ Model	
q^2	0.530
Size of dataset	43
#/N	19
r^2	0.800
F-value	52.0
Standard Error	0.45

Further validation of the model comes from evaluating the test set predicted pK_i . All compounds fall within a reasonable range of error based on the error in the measurement. Prediction for compounds **AB-B68** and **AR39** are the only compounds that are off by more than a factor of magnitude. In the calculated residuals show that for all structures except **AB-B68** and **AR39**, the predicted pK_i is within 1 of the experimental value. This suggests that most error in the model comes from the artificial tilt of the piperazine ring present in the minimized structures of benzenes and pyridines, as well as homopiperazines such as **AR39**.

4.2.3 Calculation of a model for affinity to the 5-HT_{2a} receptor

The model for affinity to the 5-HT_{2a} receptor was calculated by the same procedures as for the 5-HT₇ receptor. Less experimental data was available for the 5-HT_{2a} receptor, so only 50 compounds were able to be analyzed initially. After a PLS analysis which showed reasonable predictivity, the residuals of this group were plotted and the compounds that deviated the most were excluded from the subsequent model calculation. These 5 compounds were **JS41**, **E178**, **E149**, **10j**, and **JS17**. Compounds **10j** and **E149** did not align well to the common template with respect to large substituents. While these compounds

provided increased diversity to the calculated model, the inconsistencies with alignment of the side chains led to large residuals in the non-crossvalidated analysis.

The remaining 45 compounds were analyzed by hierarchical clustering as outlined in the previous section and split into four groups according to their structural features. The dendrogram is shown below. These structures were split into a training set and a test set as before.

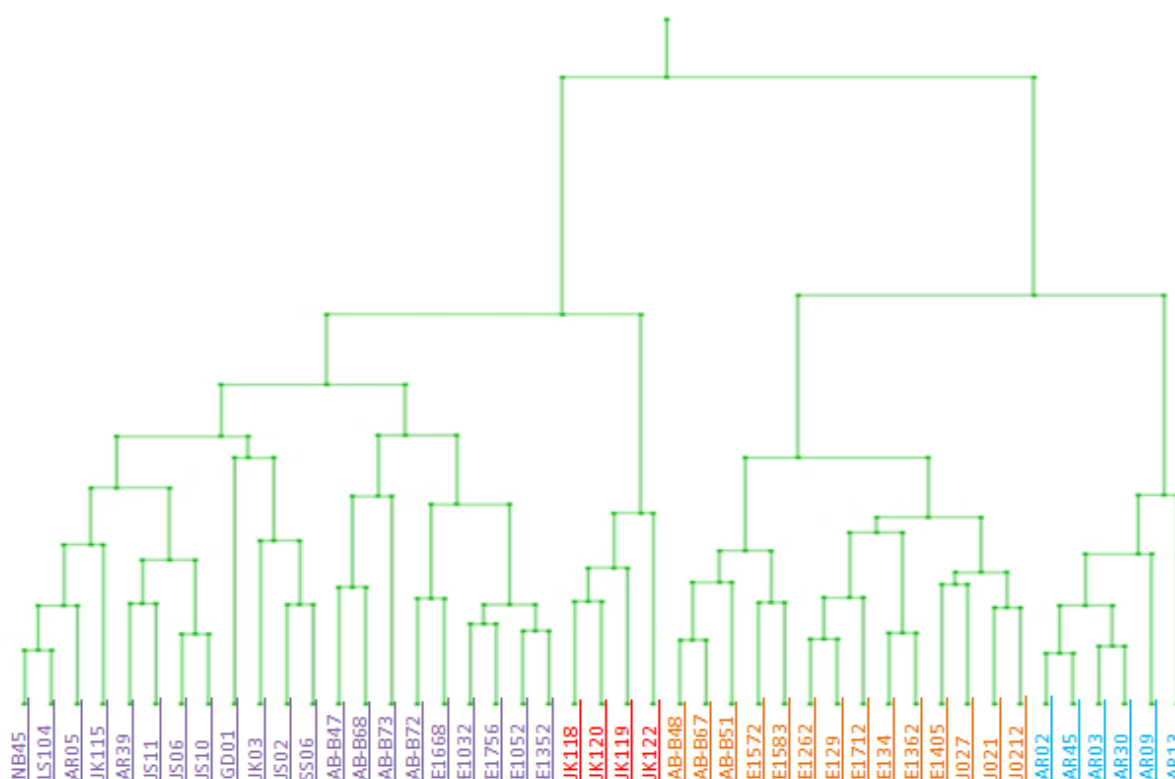
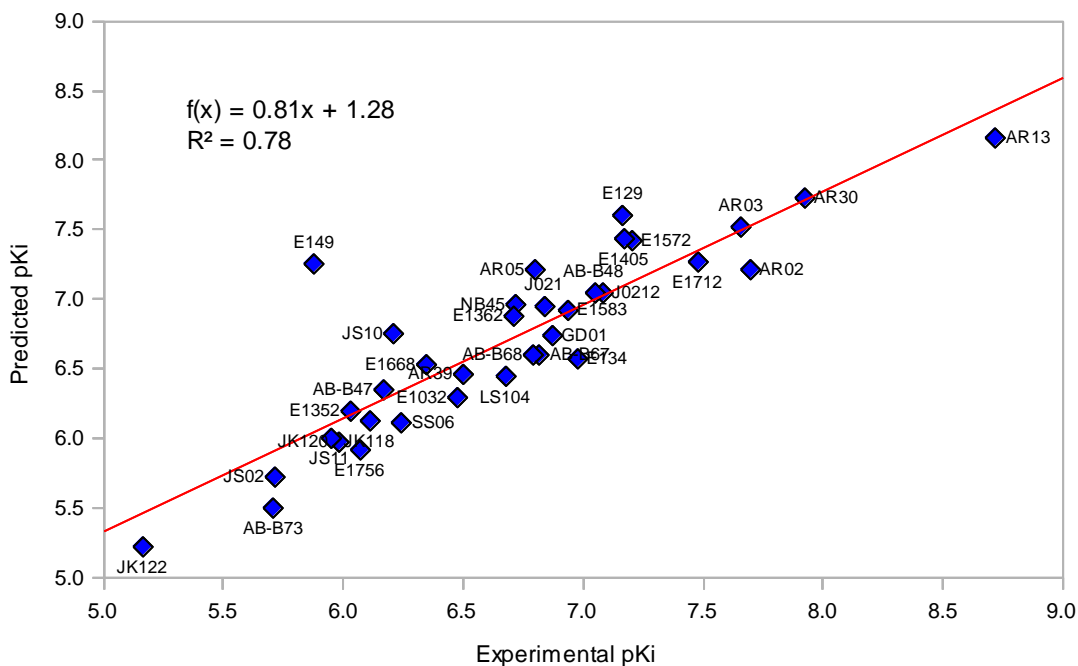


Figure 4-7. Dendrogram of the hierarchical clustering of all 45 structures used to calculate the model for affinity to the 5-HT_{2a} receptor. The compounds were split into four groups (shown as different colors) based on the similarity of their structural features.

A PLS crossvalidated (LOO) run was performed on the training set of 35 compounds and the optimum number of components was determined to be 4 which corresponds to a minimum PRESS and a q^2 of 0.683. The subsequent PLS analysis yielded a statistically significant model and is summarized in Table

4-. The model is further supported by a strong correlation between the test set experimental and predicted pK_i .

Training set affinity for the 5-HT_{2a} receptor
(predicted vs. experimental)



Test set affinity for the 5-HT_{2a} receptor
(predicted vs. experimental)

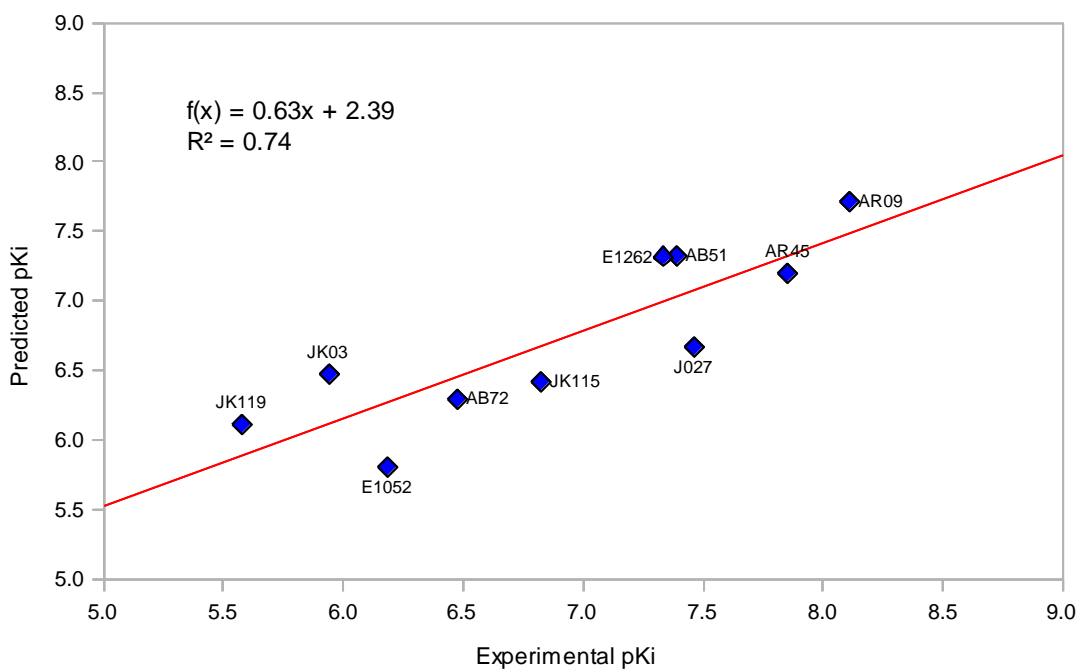


Figure 4-8. These graphs show the correlation between predicted pK_i and experimental pK_i of the training set (top) and test set (bottom). The pK_i of these compounds was predicted by the model calculated for affinity to the 5-HT_{2a} receptor.

Table 4-11. The tables above list the predicted pK_i and the experimental pK_i to the 5-HT_{2a} receptor, along with the residual.

Training Set	pKi (Exp.)	pKi (pred.)	Residual	Training Set	pKi (Exp.)	pKi (pred.)	Residual
AR13	8.72	8.16	0.57	E1362	6.71	6.88	-0.18
AR30	7.92	7.73	0.19	LS104	6.68	6.45	0.23
AR02	7.70	7.22	0.48	AR39	6.50	6.46	0.04
AR03	7.66	7.51	0.14	E1032	6.48	6.29	0.19
E1712	7.48	7.27	0.22	E1668	6.35	6.53	-0.18
E1572	7.21	7.43	-0.22	SS06	6.25	6.11	0.14
E1405	7.17	7.43	-0.26	JS10	6.21	6.76	-0.55
E129	7.17	7.60	-0.43	AB-B47	6.17	6.36	-0.19
J0212	7.08	7.05	0.03	JK118	6.11	6.13	-0.02
AB-B48	7.05	7.04	0.01	E1756	6.07	5.92	0.15
E134	6.97	6.57	0.40	E1352	6.04	6.20	-0.16
E1583	6.94	6.92	0.02	JK120	5.99	5.98	0.01
GD01	6.87	6.74	0.13	JS11	5.95	6.01	-0.06
J021	6.84	6.94	-0.10				
AB-B67	6.82	6.61	0.21	JS02	5.72	5.72	-0.01
AR05	6.80	7.22	-0.42	AB-B73	5.71	5.51	0.20
AB-B68	6.79	6.60	0.19	JK122	5.16	5.23	-0.07
NB45	6.72	6.97	-0.25				
Test Set	pKi (Exp.)	pKi (pred.)	Residual	Test Set	pKi (Exp.)	pKi (pred.)	Residual
AB-B51	7.39	7.33	0.06	E1262	7.34	7.32	0.02
AB-B72	6.48	6.30	0.19	J027	7.46	6.67	0.79
AR09	8.11	7.71	0.40	JK03	5.94	6.47	-0.53
AR45	7.85	7.20	0.65	JK115	6.82	6.42	0.41
E1052	6.19	5.80	0.38	JK119	5.58	6.12	-0.54

Table 4-12. The statistics relating to the validity and predictivity of the model for affinity to the 5-HT_{2a} receptor are shown.

5-HT _{2a} Model	
q ²	0.683
Size of dataset	35
#/N	4
r ²	0.864
F-value	47.8
Standard Error	0.28

4.3 Analysis of each set of compounds according to the calculated models

As was outlined in the introduction, it is the goal of this research to synthesize novel, selective 5-HT₇ receptor ligands. A large library of compounds which show high affinity to the receptor has been synthesized and QSAR models have been calculated which detail the requirements for binding to the 5-HT₇ receptor and to the receptor which has the most similar binding profile, the 5-HT_{2a} receptor. By examining the differences between these two models, information pertaining to increasing the selectivity of ligands over the 5-HT_{2a} receptor can be gained. Each subset of synthesized ligands has been analyzed using the QSAR models to provide ways of increasing affinity and selectivity. These models are shown below in Figure 4-9 through 4-13.

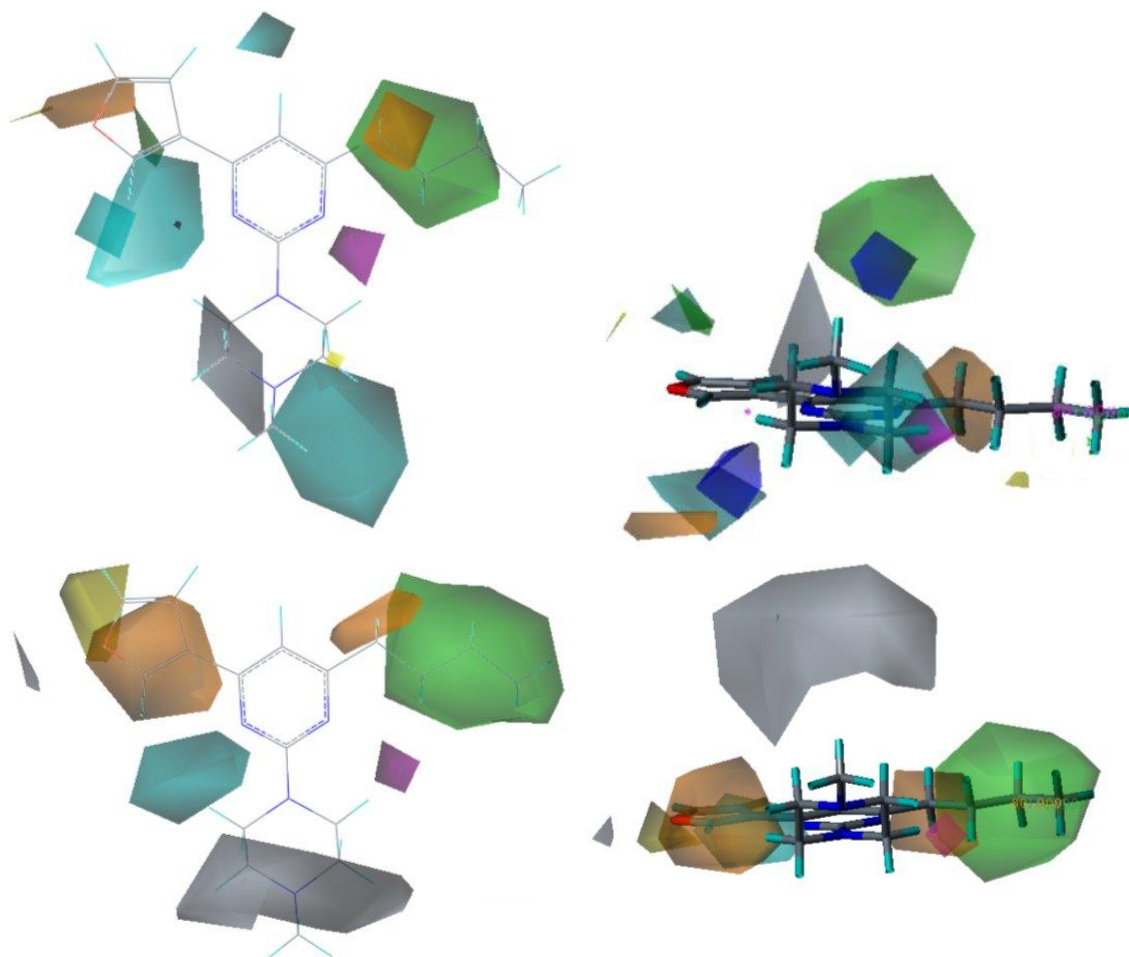


Figure 4-9. The calculated CoMSIA models for binding affinity to 5-HT₇ (top) and 5-HT_{2a} (bottom). Favored and disfavored regions of steric bulk (green/yellow), electrostatic charge (red/blue), hydrophobicity (orange/grey), and hydrogen bond acceptors (magenta/cyan) describe the binding site interactions with these ligands.

4.3.1 Steric interactions

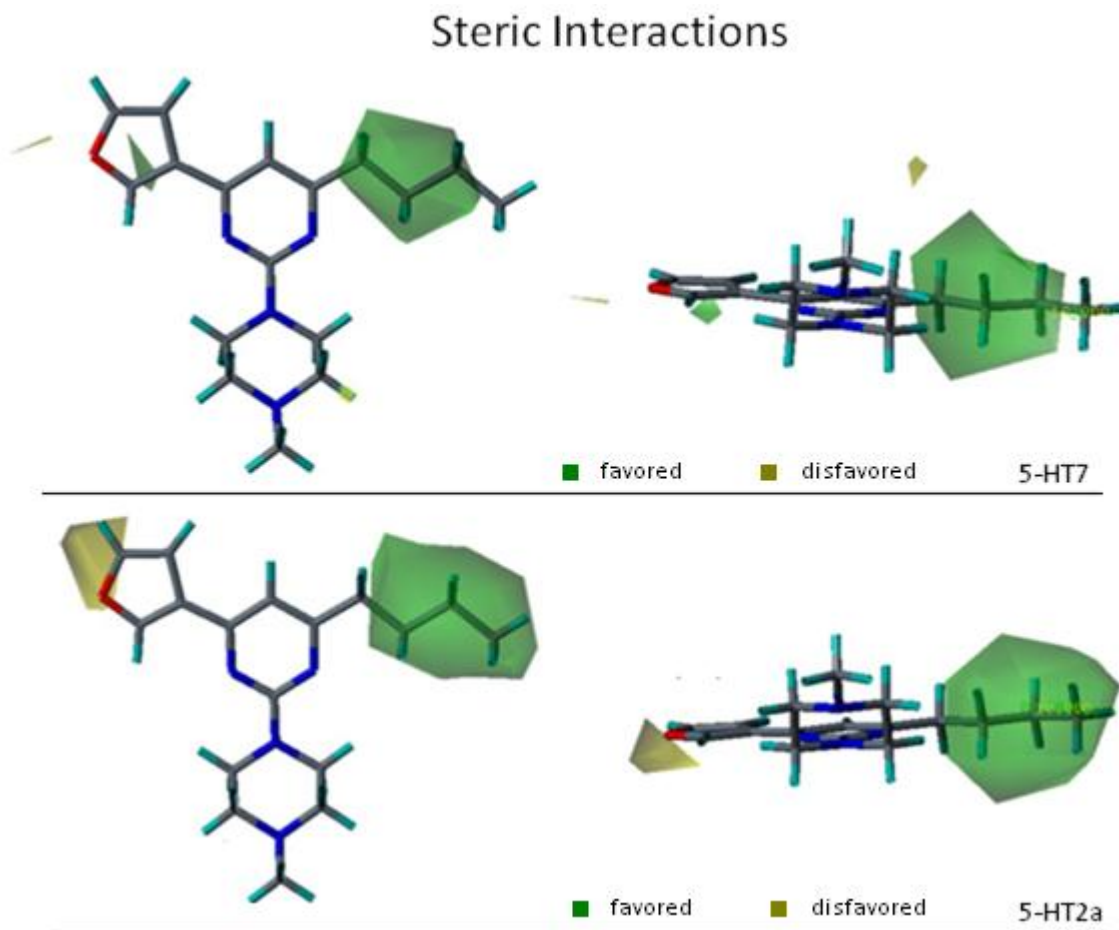


Figure 4-10. Contours of favored and disfavored steric interactions to both the 5-HT₇ and 5-HT_{2a} receptors.

The steric interactions as calculated are shown in Figure 4-10 above. The major region of interest surrounds the alkyl substituents to the pyrimidine ring. This region of favorable interaction is larger in the model for affinity to the 5-HT_{2a} receptor. This difference is likely due to the drastic increase in affinity exhibited by compounds with an *n*-hexyl substituent at this position, such as JS41. This region of the ligands likely binds with the alkyl group near the hydrogen bond acceptor Ser 5.42. Due to the diversity of the synthesized compounds with respect to steric properties of substituents in this region, this interaction does not appear to offer any selectivity advantages by further optimization. Also seen are disfavored regions surrounding furyl substituents in both models. This leads to the conclusion that

this region will also not allow for any further optimizations, as the furyl substituent is a relatively small aromatic substituent and increases in size are not advantageous.

4.3.2 Electrostatic Interactions

The electrostatic interactions, displayed in Figure 4-11 show two areas of interest, corresponding with the furyl substituents and the protonated amine of piperazine substituents. The fields surrounding furyl substituents are likely a result of the large difference in affinity observed between 4-(2-furyl)pyrimidines and 4-(3-furyl)-pyrimidines, as discussed earlier. This difference (two orders of magnitude) results in sharply defined fields in both models which result in favored electrostatic interactions corresponding with the 2-furyl analogs and regions of disfavored interactions corresponding with 3-furyl analogs. In the model for affinity to the 5-HT₇ receptor, there is an additional region near the protonated amine. This disfavored interaction results from the decreased affinity of homopiperazine compounds which were aligned with the protonated amine centered over this disfavored region. The decrease in affinity also results in disfavored hydrophobic interactions as is discussed later.

The calculated models show limited opportunities for further optimizations with regard to electrostatic modifications. The calculated regions in each model are largely identical, although the homopiperazine moiety seems to be tolerated better by the 5-HT₇ receptor. Shortening the distance between the central aromatic ring and the protonated amine, or constraining the amine to one side of the central ring are possible ways to increase the selectivity of future ligands.

Electrostatic Interactions

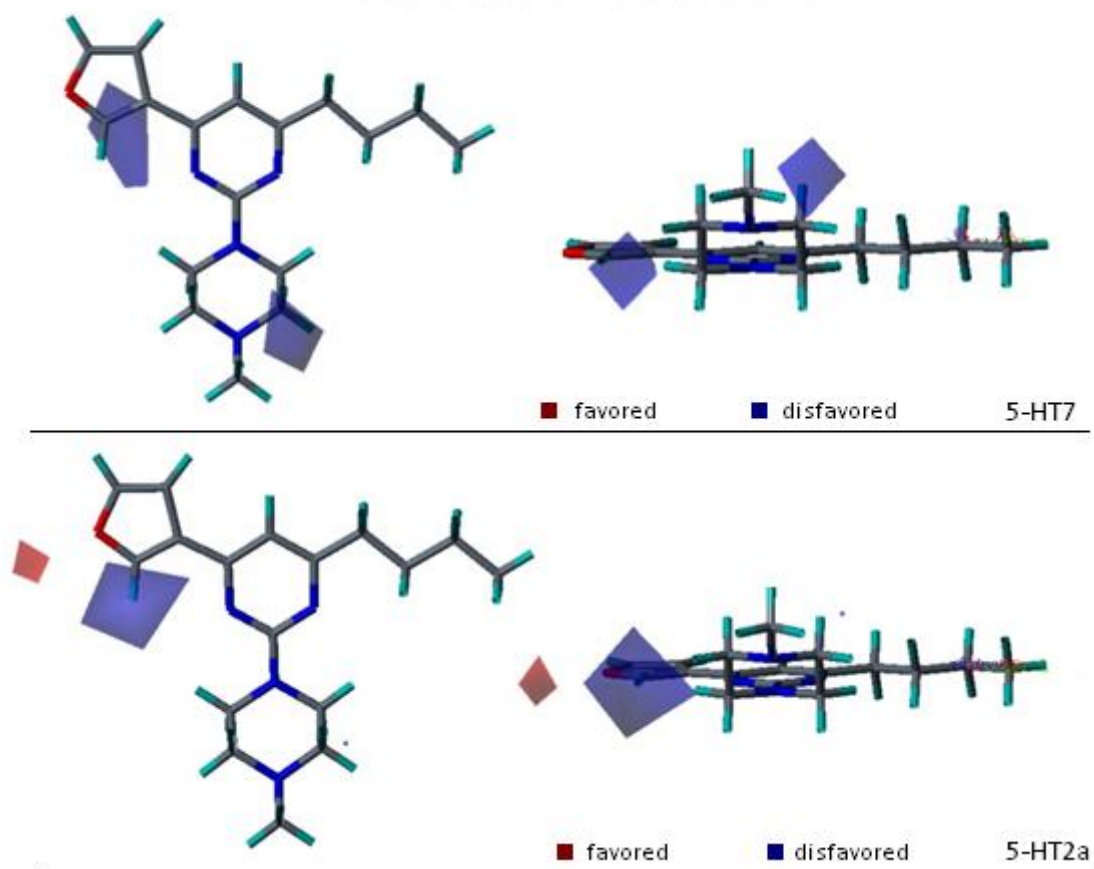


Figure 4-1. Contours of favored and disfavored electrostatic interactions to both the 5-HT₇ and 5-HT_{2a} receptors.

4.3.3 Hydrophobic interactions

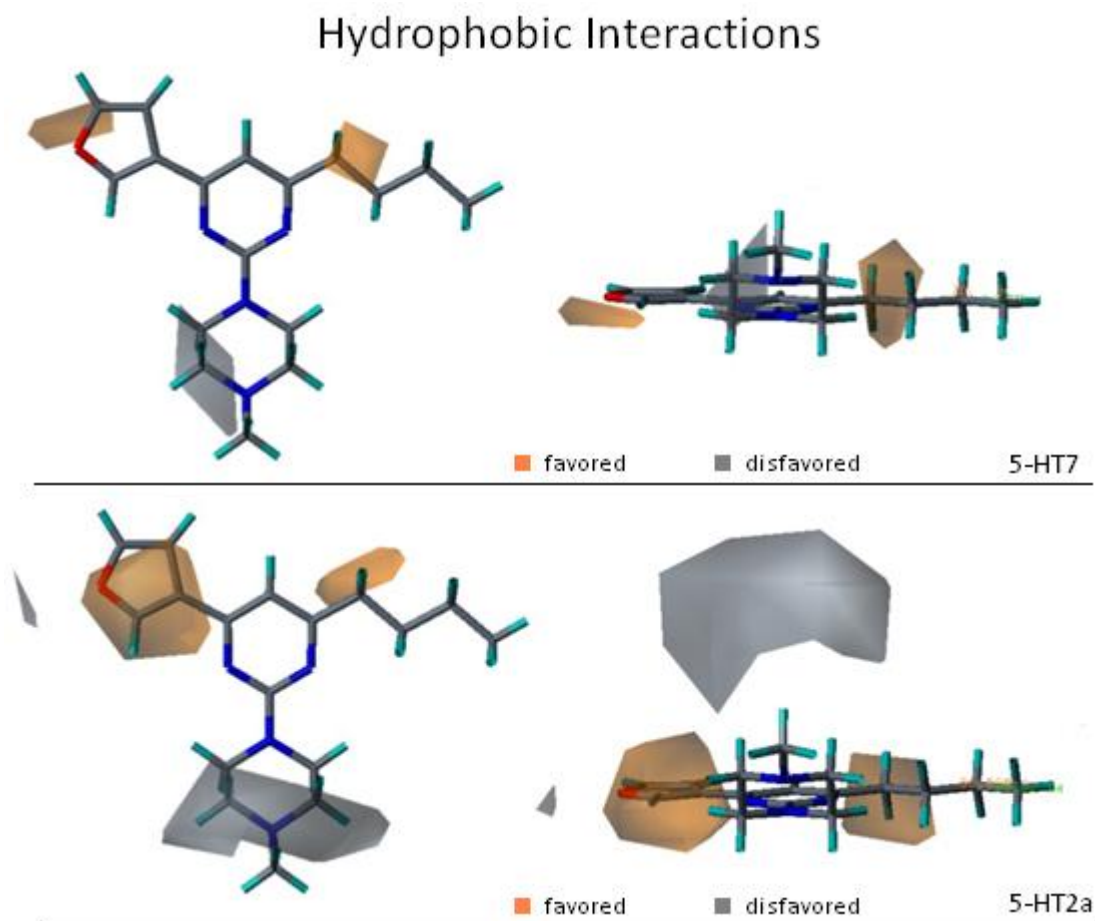


Figure 4-2. Contours of favored and disfavored hydrophobic interactions to both the 5-HT₇ and 5-HT_{2a} receptors.

Hydrophobic interactions were the most prevalent CoMSIA field calculated in both models. The most interesting of these hydrophobic regions is the large disfavored region surrounding *N*-substituents of piperazine compounds. This large grey region is seen only in the model for affinity to 5-HT_{2a}. Compounds such as JK118 which exploit this region by including a benzyl moiety show higher affinity to the 5-HT₇ receptor, although within the experimental error. This disfavored region provides an excellent lead for further modifications in this region.

Also shown is the disfavored region corresponding to the homopiperazine moiety mentioned earlier, in the model for affinity to the 5-HT₇ receptor. This region supports the presence of the disfavored electrostatic region observed previously. Regions of favored hydrophobic interactions correspond with

the furyl ring which supports the qualitative assumptions made previously about the interaction with this group and phenylalanine residues of the binding site. Other small favored regions exist around the alkyl substituents, but no differences are observed that can be exploited for increasing affinity or selectivity of ligands to either receptor.

4.3.4 Hydrogen bond donor interactions

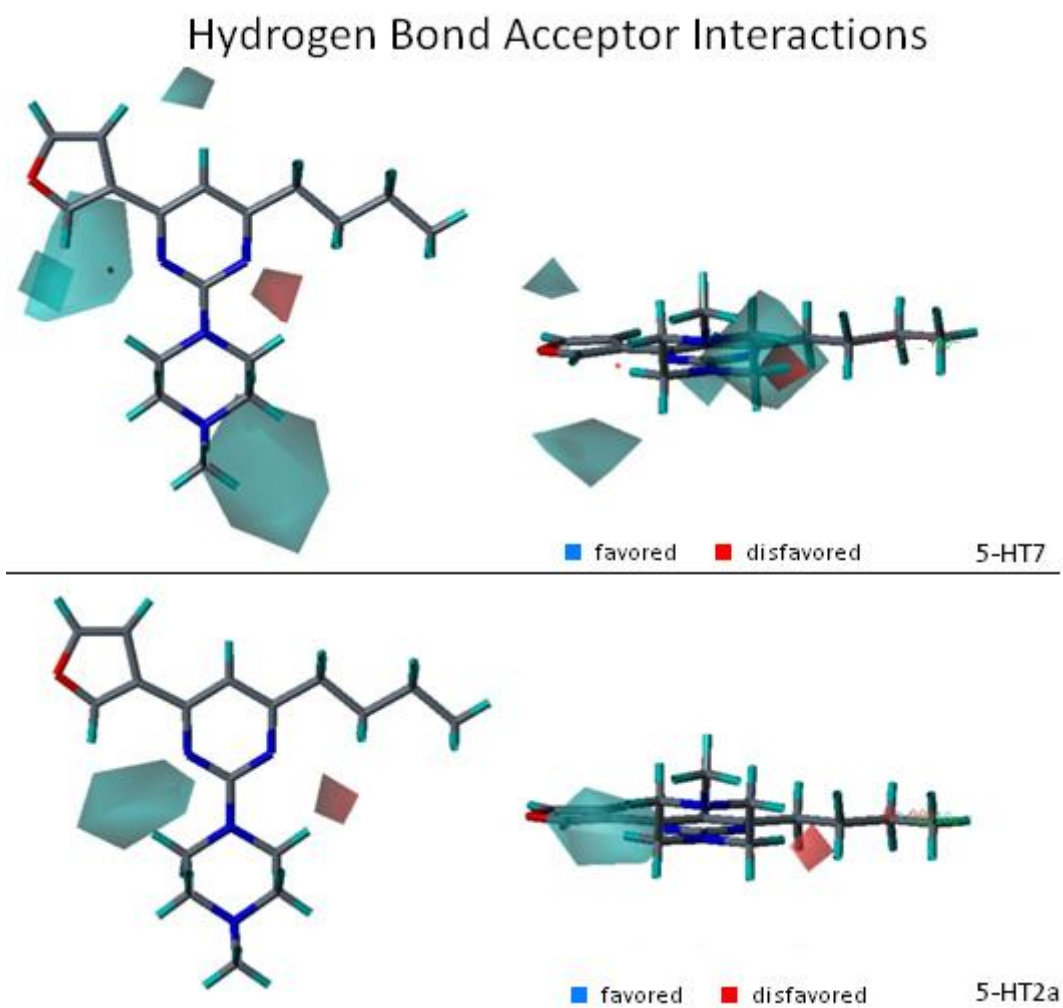


Figure 4-3. Contours of favored and disfavored hydrogen bond acceptor interactions to both the 5-HT₇ and 5-HT_{2a} receptors.

There are typically regions in each compound which contain a hydrogen bond acceptor. These correspond to the oxygen in furyl substituents, each nitrogen in pyrimidine (or pyridine), and each nitrogen in piperazine. The most crucial of these hydrogen bond acceptors is the protonated amine, which has been shown to form a salt bridge with Asp 3.32 in the central binding site region. The models do not represent this well, although the database of structures were not protonated. A large disfavored region is observed in the model for affinity to the 5-HT₇ receptor, which again may be representative of the disfavored interaction of the homopiperazine moiety. Regions also exist around the the furyl substituent of the compound shown, also likely due to disfavored interactions of 4-(2-furyl)pyrimidines. These interactions have already been attributed to the enhanced ability of 4-(3-furyl)pyrimidines to rotate with respect to the torsion angle between the aromatic rings.

The most interesting regions described by hydrogen bond acceptor interactions are those surrounding the central aromatic ring. A series of pyridines and benzenes allows for the comparison of the necessity of each nitrogen in pyrimidine ligands. It is observed that a favored hydrogen bond acceptor interaction is calculated at the nitrogen near alkyl substituents, or away from aromatic substituents. This observation provides additional support for the interaction between substituents to the opposite side of the pyrimidine ring and phenylalanine residues in the binding site. This favored interaction may therefore correspond to Ser 5.42 in the binding site. This would allow for further optimization of this region of the 5-HT₇ pharmacophore with respect to affinity and selectivity over 5-HT_{2a}.

5 CONCLUSIONS

Several potential therapeutic applications exist for selective 5-HT ligands. This potential has not been completely defined or exploited. This is partially due to the unavailability of potent and selective 5-HT ligands. This is particularly true with the 5-HT₇ receptor, as it is the most recently characterized of the 5-HT receptor subtypes. Hundreds of novel 5-HT₇ ligands have been synthesized at Georgia State University in order to address this need. These compounds were optimized based on previous research and have yielded ligands with greater potency and selectivity to the 5-HT₇ receptor, with respect to 5-HT_{2a}. The 5-HT₇ binding site has been explored with analogs by both qualitative and quantitative means, resulting in a better understanding of the receptor structure.

In synthesizing new 5-HT₇ receptor ligands, systematic substitutions of pyrimidines were examined. The substituents of pyrimidine ligands were optimized by adding diverse substituents to the aromatic ring. Several different synthetic pathways were described to yield novel substituted pyrimidines. These include the nucleophilic addition to pyrimidine as previously described. These additions included highly functionalizable groups which underwent subsequent modifications allowing more many diverse substitutions. This was the case for 1,4 addition to 4-vinylpyrimidines as well as hydrolysis of 1-ethoxy-1-ethenyl substituents. These compounds were used as starting material for the synthesis of several diverse 5-HT₇ receptor ligands. Evaluation of these ligands revealed a ligand with high potency and selectivity to the 5-HT₇ receptor, **AR13**. This ligand was used as a scaffold to investigate other proposed binding site interactions.

The region corresponding to the linker between the two binding pockets of the receptor was explored by altering the piperazino substituents. The presence of a steric group extending past the piperazino protonated amine was shown to be well tolerated by the 5-HT₇ receptor. Bulky groups, such as the

benzyl analogs synthesized, were not well tolerated by the 5-HT_{2a} receptor which led to a significant selectivity advantages.

The synthesized pyrimidines and benzofurans, along with other pyridines and benzenes were analyzed by 3D-QSAR methods to yield models for affinity to 5-HT₇ and 5-HT_{2a}. These models clearly describe the observations noted above and detail pharmacophore regions of these receptors. These two models have been compared to find that two significant regions of steric interactions differ significantly between the two models. These relationships have not been previously described and will lead to more potent and selective ligands. These ligands will allow for further physiological studies and possibly lead to therapeutics.

6 EXPERIMENTAL

Equipment:

All reagents were purchased from Aldrich Chemical Company or prepared according to the literature. Compounds prepared by others under the direction of Dr. Strekowski include **3b**, **6d-k**, **6m-n**, **10a**, and **10l**. Reactions were monitored by TLC (EMD Chemicals, TLC Silica Gel 60 F₂₅₄) or GCMS (Shimadzu GC-17A, QP-5000 MS). All purifications were performed on a Chromatotron (Harrison Research, Model 7924T). Solid samples were subjected to melting point analysis (Barnstead International, Mel-Temp 1201D). All samples sent for biological testing were converted to salts by the procedure outlined below and analyzed for elemental composition (Perkin Elmer, 2400 Series II) to ensure purity. NMR data was acquired using the Bruker Avance 400 MHz NMR spectrometer. NMR data was processed using TOPSPIN v.3.0.b.8 software (Bruker). All NMR spectra were obtained in deuterated chloroform at room temperature. Experimental affinity to 5-HT receptors was determined in a separate lab by the procedure outlined by below. All samples sent for biological testing were converted to salts and analyzed for elemental composition (Perkin Elmer, 2400 Series II) to ensure purity.

Biological evaluation:

All biological evaluation was determined through collaboration with Dr. Andrzej Bojarski in The Institute of Pharmacology at the Polish Academy of Sciences. Below are details of the analyses as described by Dr. Bojarski.

***In vitro* radioligand binding assays:** Inhibition constants (K_i) were determined from at least three separate experiments in which 7–9 drug concentrations, run in triplicate, were used (SEM \pm 20%). The binding reaction was terminated by rapid filtration through Whatman GF/B filters followed by three 4-ml washes with ice-cold incubation buffer.

The radioactivity retained on the filters was measured by liquid scintillation counting (Beckman LS 6500 apparatus) in 4 ml scintillation fluid (Akwascynt, BioCare). Binding isotherms of the tested compounds were analyzed by non-linear regression (Prism, GrafPad Software Inc., San Diego), using the Cheng-Prusoff equation [132] to calculate K_i values.

5-HT_{1A}, 5-HT_{2A}, dopamine D₂ and α_1 -adrenergic receptor binding assay: Radioligand studies with native 5-HT_{1A}, 5-HT_{2A}, D₂ and α_1 -adrenergic receptors were conducted according to the methods previously described [116,133,134]. Briefly: 5-HT_{1A} assays used rat hippocampal membranes, [³H]-8-OH-DPAT (106 Ci/mmol, Perkin-Elmer) and 5-HT for nonspecific binding; 5-HT_{2A} assays used rat cortical membranes, [³H]-ketanserin (67 Ci/mmol, Perkin-Elmer) and methysergide for nonspecific binding; dopamine D₂ assays used rat striatal membranes, [³H]-spiperone (15.0 Ci/mmol, Perkin-Elmer) and butaclamol for nonspecific binding; α_1 assays used rat cortical membranes, [³H]-Prazosine (25.0 Ci/mmol, Amersham) and phentolamine for non-specific binding.

Expression of the gene for the human 5-HT_{7(b)} receptor: The full length human 5-HTR_{7(b)} cDNA cloned into mammalian expression vector pcDNA3.1(+) was purchased from UMR cDNA Resource Center (www.cdna.org). The receptor cDNA was stably transfected into human embryonic kidney cells (HEK293, ATCC) with use of Lipofectamine 2000 (Invitrogen). A clone yielding high expression level of 5-HTR_{7(b)} was selected during preliminary experiments including Western Blot analysis, [³H]-CT saturation binding studies as well as cAMP accumulation assays.

Cell culture and preparation of cell membranes: HEK293 cells with stable expression of 5-HTR_{7(b)} were maintained at 37 °C in a humidified atmosphere with 5% CO₂ and were grown in Dulbecco's Modified Eagle Medium (Gibco BRL) containing 5% dialysed foetal bovine serum (Gibco BRL) and 500 µg/ml G418 sulphate (Sigma-Aldrich). For membranes preparations, cells were subcultured in 10 cm diameter dishes, grown to 90% confluence, washed twice with prewarmed to 37 °C phosphate buffered saline and

pelleted by centrifugation (1000 g) in phosphate buffered saline containing 0.1 mM EDTA and 1 mM dithiothreitol. Prior to membrane preparations pellets were stored at -80°C .

Membranes were prepared from frozen cell pellets by homogenization (Polytron, setting 5 for 15 s) and centrifugation (50,000 g, 15 min., 4°C) in 20 volumes of Tris HCl buffer (50 mM, pH 7.4) containing EDTA (0.1 mM). The pellets were then re-suspended in buffer, incubated 20 min. in 37°C and once again centrifuged as described above. The membranes were stored in aliquots at -80°C until use for binding assays.

The protein concentration was determined with bicinchoninic acid protein assay kit (Pierce, USA).

5-HT₇ receptor binding assay: Binding assays on membranes from HEK 293 cells stably expressing human 5-HT_{7(b)} receptor were performed according to procedure described by Thomas et al. [135]. Briefly, the membranes (10 μg protein per tube) were incubated in 50 mM Tris HCl buffer (pH 7.4) containing 4 mM MgCl_2 , 0.1 mM pargyline and 0.1% ascorbic acid, in the presence of 7–9 concentrations of test drug and 0.5 nM [³H]-5-CT (93.0 Ci/mmol, Amersham). Nonspecific binding was defined in the presence of 10 μM of 5-HT. After a 1-h incubation at 37°C , the assay samples were rapidly filtered through Whatman GF/B filters and subsequently washed with ice-cold 50 mM Tris buffer (pH 7.4) using a Brandel harvester.

Computer methods:

Conformational analysis: Structures were drawn in their *s*-cis conformation using HyperChem 8.0 (Hypercube, Inc.). Each structure was imported into Spartan '04 (Wavefunction, Inc.) and minimized using the MMFF force field. The torsion angle consisting of N3-C4-C7-C8 was set to 0 degrees. A dynamic constraint was applied to this torsion angle ranging from 0 to 350 degrees in 36 steps, resulting in a stepwise rotation of 10 degrees. An *ab initio* Hartree-Fock calculation was performed using the 6-

31G* basis set. The calculated energy of the structure corresponding to a global minimum was set to 0 kcal/mol and energies for all other torsions were reported relative to the global minimum.

Calculation of pharmacophore model: Structures exhibiting high affinity (top 20%, by pK_i) to the receptor in question were chosen from the database of aligned structures to each receptor. The highest affinity compound was conformed analogous to the total set of structures. All structures were then aligned by features to the template using the GALAHAD module in Sybyl (Tripos, Inc.), using the parameters suggested. The best calculated model was chosen as the model which fit the highest percentage of compounds from the original dataset.

Calculation of 3D-QSAR models: A database of aligned structures with corresponding experimental data was loaded into a Sybyl molecular spreadsheet. The structures were represented in the molecular spreadsheet by calculating CoMSIA fields for steric, electrostatic, hydrophobic, and hydrogen bond acceptor interactions. Internal validation was conducted by leave-one-out crossvalidation. The SAMPLS method (Merck & Co., Inc.) was used in order to minimize computational time. A non-crossvalidated partial least squares analysis was calculated using the optimal number of components (least number of components which did not observe > 5% decrease in predicted error). The QSAR model was presented with favorable contours at 80% of the total contribution and unfavorable contours at 10% of the contribution.

Synthesis:

Conversion to salts: The appropriate compound was dissolved in diethyl ether:methanol (3 mL, 10:1) before the addition of HBr (0.2 mL, 48%) or HCl (0.2 mL, 38%). The solution showed evidence of precipitant before the addition of more diethyl ether (20 mL). The additional ether precipitated the compound as the corresponding salt.

Preparation of organolithium reagents. Alkylolithium reagents *n*-butyllithium (2.5 M in hexanes), *tert*-butyllithium (1.7 M in pentane), and *sec*-butyllithium (1.4 M in cyclohexane) were commercial reagents. All other organolithium reagents were generated *in situ* and used without characterization.

3-lithio furan was generated as described in the literature [136]. In summary, a solution of 3-bromofuran (0.33 mL, 3.7 mmol) in tetrahydrofuran (3 mL) was treated dropwise at -78°C with *n*-butyllithium (1.5 mL, 3.7 mmol). The solution was stirred for an additional 10 min at -78°C before use. 2-lithiofuran was prepared in a similar manner by treatment of a solution of furan (2.18 mL, 24.7 mmol) with *n*-butyllithium (4.0 mL, 10.0 mmol). 2-lithio-4,5-dihydrofuran was also generated in this manner by treating a solution of 2,3-dihydrofuran (0.23 mL, 3.0 mmol) in tetrahydrofuran (3 mL) with *tert*-butyllithium (1.8 mL, 3.0 mmol). Ethoxyvinyl lithium was prepared according to the literature [137], by treating a solution of ethyl vinyl ether (0.49 g, 6.8 mmol) in tetrahydrofuran (3 mL) with *tert*-butyllithium (2.0 mL, 3.4 mmol) at -78°C . The bright yellow solution was stirred at 0°C for 10 min. The reagent was cooled to -78°C after the solution had become colorless for immediate use. Vinylolithium was generated as described [94,138], by treatment of a solution of tetravinyltin (0.98 mL, 5.1 mmol) in tetrahydrofuran (3 mL) with *tert*-butyllithium (2.4 mL, 4.1 mmol) at -78°C . The solution was stirred for 10 min until the formation of a white precipitant was evident. α -lithiostyrene was generated by dropwise addition of *n*-butyllithium (1.2 mL, 3.0 mmol) to a solution of α -bromostyrene (0.43 mL, 3.0 mmol) in tetrahydrofuran (3 mL) at -78°C . The resulting deep red mixture was used immediately.

General procedures for 3a-f, and 4a-g [13]. 2-chloropyrimidine (**1a**), 2-chloro-5-fluoropyrimidine (**1b**) and 2,4-dichloropyrimidine (**1c**) were purchased from Aldrich Chemical Company. A solution of the appropriate organolithium reagent (3.0 mmol) was generated as described above. Dropwise addition of 2-chloropyrimidine **1** (3.0 mmol) dissolved in a minimum amount of anhydrous THF caused the solution to darken to black with a green tint over the course of the addition. The flask was slowly warmed to -

40°C over a period of 1 hour, and then stirred at -40°C for an additional three hours. The reaction was then quenched by the dropwise addition of deionized water (0.1 ml, 6 mmol) dissolved in THF (5 ml). The mixture was stirred at 20°C for 10 min, resulting in a pale orange solution with white precipitate (LiOH). To this mixture was added 2,3-dichloro-2,3-dicyanoquinone (DDQ, 0.68 g, 3.0 mmol) dissolved in THF (5 ml). The solution was stirred for 2 min before the addition of 3M NaOH (20 ml). The solution was extracted with hexanes (20 ml) and hexanes:THF (20 ml, 1:1) and the extract was dried over magnesium sulfate, filtered and concentrated under reduced pressure. The resulting residue was purified qualitatively to yield the 4-substituted 2-chloropyrimidines **4**, which were subsequently used in the reaction with *N*-methylpiperazine. A flask dried as before was charged with **3** (1.0 mmol) and dry toluene (3 ml). To the solution was added an excess of an appropriate piperazine (3.0 mmol) and the solution was heated at 110°C for 1 day. The reaction was monitored by TLC, and after the reaction had gone to completion (by absence of starting material), the solution was made basic with 2M sodium carbonate (10 ml). The resulting solution was extracted with diethyl ether (3 X 20 ml). The organic layers were combined, dried over magnesium sulfate, filtered and concentrated under reduced pressure before purification by chromatography (dichloromethane:methanol, 10:1) yielded the piperazine derivatives **4** as yellow oil.

4-*tert*-Butyl-2-chloropyrimidine (3a). This compound was prepared using minor variations to the general procedure. The addition of *tert*-butyllithium occurred at -40°C, and was then allowed to reach 0°C over 1 hour. Purification using a mobile phase of hexanes:dichloromethane (2:1) yielded **3a** (0.223 g, 1.3 mmol, 44%) as a white solid. Characterization matches that previously reported. ¹H NMR (400 MHz, CDCl₃) δ 8.51 (d, *J* = 5.1 Hz, 1H), 7.26 (d, *J* = 5.1 Hz, 1H), 1.35 (s, 9H). ¹³C NMR (100 MHz, CDCl₃) δ 181.8, 161.1, 159.4, 115.3, 37.9, 29.2.

2-Chloro-4-(3-furyl)pyrimidine (3b). This compound was obtained in 57% yield as a white solid: mp 88-89°C. Characterization correlated with that previously recorded (publication in writing). ^1H NMR (400 MHz, CDCl_3) δ 8.55 (d, $J = 5.1$ Hz, 1H), 8.22 (m, 1H), 7.54 (m, 1H), 7.31 (d, $J = 5.1$ Hz, 1H), 6.91 (m, 1H).

2-Chloro-4-(1-ethoxy-1-ethenyl)pyrimidine (3c). This compound was obtained in 40% yield as a white solid. Characterization correlated with that previously recorded (publication in writing). ^1H NMR (400 MHz, CDCl_3) δ 8.61 (d, $J = 5.1$ Hz, 1H), 7.57 (d, $J = 5.1$ Hz, 1H), 5.73 (d, $J = 2.4$ Hz, 1H), 4.57 (d, $J = 2.4$ Hz, 1H), 3.97 (q, $J = 7.0$ Hz, 2H), 1.44 (t, $J = 7.0$ Hz, 3H).

2-Chloro-4-vinylpyrimidine (3d). This compound was synthesized using a modification of the general procedure. Addition of 2-chloropyrimidine to a mixture of vinyl lithium at -78 °C caused the solution to darken, eventually turning black. The reaction was allowed to reach -60 °C over 1 hour before quenching. Workup and purification using a mobile phase of hexanes:dichloromethane (1:1) yielded **3d** in 59% yield as a faintly yellow oil. Characterization correlated with that previously reported [138]. ^1H NMR (400 MHz, CDCl_3) δ 5.79 (d, 1H, $-\text{CH}_2$, $J=10.8$ Hz), 6.54 (d, 1H, $-\text{CH}_2$, $J=17.4$ Hz), 6.71 (dd, 1H, $-\text{CH}$, $J=10.8, 17.4$ Hz), 7.24 (d, 1H, $-\text{CH}$, $J=5.0$ Hz), 8.57 (d, 1H, $-\text{CH}$, $J=5.0$ Hz).

2-Chloro-4-(1-phenylethenyl)pyrimidine (3e). This compound was obtained in 58% yield as a colorless oil. ^1H NMR (400 MHz, CDCl_3) δ 8.53 (d, $J = 5.1$ Hz, 1H), 7.40 (m, 3H), 7.31 (m, 2H), 7.09 (d, $J = 5.1$ Hz, 1H), 6.48 (m, 1H), 5.77 (m, 1H) ^{13}C NMR (CDCl_3): δ 167.7, 161.5, 159.8, 145.9, 138.1, 128.6, 128.5, 128.4, 123.1, 117.5. *High-resolution ms* (ESI, positive ion mode): calcd. for $\text{C}_{12}\text{H}_9^{35}\text{ClN}_2$ ($\text{M}^+ + 1$), m/z 217.0533; found m/z 217.0526.

2-Chloro-4-(3-furyl)-5-propylpyrimidine (3f). This compound was obtained in 17% as a crude, colorless oil. The oil was used without further purification. ^1H NMR (400 MHz, CDCl_3) δ 8.41 (s, 1H, $-\text{CH}$), 8.03 (s, 1H), 7.54 (m, 1H), 7.00 (m, 1H), 2.74 (t, $J = 7.4$ Hz, 2H), 1.70 (sxt, $J = 7.4$ Hz, 2H), 1.05 (t, $J = 7.4$ Hz, 3H).

4-sec-Butyl-2-(4-methylpiperazino)pyrimidine hydrobromide (4a). The free base was obtained in 32% yield. ^1H NMR for the free base (400 MHz, CDCl_3) δ 8.18 (d, $J = 5.1$ Hz, 1H), 6.34 (d, $J = 5.1$ Hz, 1H), 3.85 (m, 4H), 2.53 (m, 2H), 2.46 (m, 4H), 2.33 (s, 3H), 1.62 (m, 1H), 1.20 (d, $J = 6.8$ Hz, 3H), 0.85 (t, $J = 7.4$ Hz, 3H). A hydrobromide salt: mp 177 - 179 °C. *Anal.* Calcd for $\text{C}_{13}\text{H}_{22}\text{N}_4 \cdot \text{HBr}$: C, 49.53; H, 7.35; N, 17.77. Found: C, 49.41; H, 7.47; N, 17.47.

4-tert-Butyl-2-(4-methylpiperazino)pyrimidine hydrobromide(4b). The free base was obtained in 52% yield. ^1H NMR for the free base (400 MHz, CDCl_3) δ 8.22 (d, $J = 5.1$ Hz, 1H), 6.51 (d, $J = 5.1$ Hz, 1H), 3.86 (m, 4H), 2.47 (m, 4H), 2.34 (s, 3H), 1.27 (s, 9H). ^{13}C NMR for the free base (100 MHz, CDCl_3) δ 178.2, 161.5, 157.5, 105.5, 55.1 (2 signals), 46.3, 43.7 (2 signals), 37.5, 29.3. A hydrobromide salt: mp 221 °C. *Anal.* Calcd for $\text{C}_{13}\text{H}_{22}\text{N}_4 \cdot \text{HBr}, \frac{1}{2} \text{H}_2\text{O}$: C, 48.15; H, 7.46; N, 17.28. Found: C, 47.82; H, 6.92; N, 16.93.

4-(4,5-Dihydro-2-furyl)-2-(4-methylpiperazino)pyrimidine (4c). This compound was obtained in 53% yield. ^1H NMR (400 MHz, CDCl_3) δ 8.32 (d, $J = 5.1$ Hz, 1H), 6.66 (d, $J = 5.1$ Hz, 1H), 5.97 (t, $J = 3.0$ Hz, 1H), 4.53 (t, $J = 9.7$ Hz, 2H), 3.86 (m, 4H), 2.83 (dt, $J = 3.0, 9.7$ Hz, 2H), 2.47 (m, 4H), 2.34 (s, 3H). ^{13}C NMR (100 MHz, CDCl_3) δ 164.7, 158.6, 156.7, 155.5, 105.4, 103.0, 70.5, 55.0, 46.2, 43.6, 30.6. *High-resolution ms* (ESI, positive ion mode): calcd for $\text{C}_{13}\text{H}_{18}\text{N}_4\text{O}$, ($\text{M}^+ + 1$), m/z 247.1559; found m/z 247.1562.

2-(4-Methylpiperazino)-5-propylpyrimidine dihydrobromide (4d). The free base was obtained in 82% yield as an oil. ^1H NMR for the free base (400 MHz, CDCl_3) δ 8.16 (s, 2H), 3.81 (t, $J = 4.8$ Hz, 4H), 2.47 (t, $J = 4.8$ Hz, 4H), 2.40 (t, $J = 7.6$ Hz, 2H), 2.34 (s, 3H), 1.56 (sxt, $J = 7.6$ Hz, 2H), 0.93 (t, $J = 7.6$ Hz, 3H). A hydrobromide salt: mp 251 °C (dec.). *Anal.* Calcd. for $\text{C}_{12}\text{H}_{20}\text{N}_4 \cdot 2 \text{HBr}$: C, 37.72; H, 5.80; N, 14.66. Found: C, 37.87; H, 5.75; N, 14.52.

4-(3-Furyl)-2-(4-methylpiperazino)-5-propylpyrimidine hydrobromide (4e). The free base was obtained in 44% yield as an oil. ^1H NMR for the free base (400 MHz, CDCl_3) δ 8.17 (s, 1H), 7.91 (s, 1H), 7.48 (s, 1H), 6.95 (s, 1H), 3.85 (m, 4H), 2.59 (t, $J = 7.6$ Hz, 2H), 2.49 (m, 4H), 2.35 (s, 3H), 1.59 (sxt, $J = 7.6$ Hz, 2H),

0.99 (t, $J = 7.6$ Hz, 3H). A hydrobromide salt: mp 206 - 208 °C. *Anal.* Calcd. for $C_{16}H_{22}N_4O \cdot HBr$: C, 52.32; H, 6.31; N, 15.25. Found: C, 52.34; H, 6.11; N, 15.12.

4-Butyl-6-(3-furyl)-2-(4-methylpiperazino)-5-propylpyrimidine dihydrobromide (4f). The free base was obtained in 73% yield as an oil. 1H NMR for the free base (400 MHz, $CDCl_3$) δ 7.80 (m, 1H), 7.47 (m, 1H), 6.86 (m, 1H), 3.84 (m, 4H), 2.66 (m, 2H), 2.59 (m, 2H), 2.47 (m, 4H), 2.34 (s, 3H), 1.69 (m, 2H), 1.47 (m, 4H), 1.01 (t, $J = 7.6$ Hz, 3H), 0.96 (t, $J = 7.6$ Hz, 3H). A hydrobromide salt: mp 203 °C (dec.). *Anal.* Calcd. for $C_{20}H_{30}N_4O \cdot 2 HBr$: C, 47.63; H, 6.40; N, 11.11. Found: C, 47.34; H, 6.65; N, 11.08.

4-(2-Furyl)-2,4-bis-(4-methylpiperazino)pyrimidine trihydrobromide (4g). The free base was obtained in 37% yield as a colorless oil. 1H NMR for the free base (400 MHz, $CDCl_3$) δ 7.47 (m, 1H), 7.05 (m, 1H), 6.48 (m, 1H), 6.31 (s, 1H), 3.86 (m, 4H), 3.67 (m, 4H), 2.47 (m, 8H), 2.34 (s, 6H). ^{13}C NMR for the free base (100 MHz, $CDCl_3$) δ 163.4, 161.7, 155.4, 153.8, 143.2, 111.8, 109.7, 86.9, 55.2, 54.8, 46.3, 46.2, 43.9, 43.8. A hydrobromide salt: mp 222 °C (dec.). *Anal.* Calcd. for $C_{18}H_{26}N_6O \cdot 3 HBr$: C, 36.95; H, 5.00; N, 14.36. Found: C, 37.14; H, 5.29; N, 14.62.

General procedure for 5a-b and 6a-c, and 6l. A procedure and characterization for compounds **5** and **6** has been submitted for publication. In summary, a solution of **3d** or **3e** (0.4 mmol) is treated with a prepared nucleophile (0.4 mmol). Unless using a Grignard reagent as a nucleophile, the reaction was heated for 2 hours near reflux. Grignard reagents were prepared as reported [139]. Briefly, a suspension of copper (I) iodide was treated with two equivalents of a carbon nucleophile at -78 °C and stirred for 10 min. The Grignard reagents were then treated with **3d** or **3e** (0.4 mmol) at -40 °C. After the addition of the pyrimidine to the nucleophile, the solution was stirred for 2 hours at -40 °C and quenched. Workup and purification on a chromatotron (hexanes:dichloromethane, 4:1) yielded the 1,4-addition products **5**. A solution of **5** (1.0 mmol) in toluene (5 mL) was then treated with *N*-methylpiperazine (1.2 mmol) and stirred at reflux until the presence of **5** was no longer detectable by

TLC. Purification by chromatography (dichloromethane:methanol, 10:1) yielded the substituted arylpiperazines **6**. Examples of **5** synthesized from nucleophiles and by Grignard reagents were characterized and are shown below.

2-Chloro-4-(2-methoxy-1-phenylethyl)pyrimidine (5a). This compound was obtained as an oil in 25% yield. ^1H NMR (CDCl_3): δ 8.47 (d, $J = 5.2$ Hz, 1H), 7.29 (m, 4H), 7.26 (m, 1H), 7.12 (d, $J = 5.2$ Hz, 1H), 4.31 (dd, $J = 8.8, 5.6$ Hz, 1H), 4.20 (t, $J = 8.8$ Hz, 1H), 3.88 (dd, $J = 8.8, 5.6$ Hz, 1H), 3.35 (s, 3H); ^{13}C NMR (CDCl_3): δ 173.6, 161.3, 159.3, 138.4, 128.9, 128.3, 127.6, 119.5, 74.5, 59.1, 53.2. *High-resolution MS* (ESI, positive ion mode): calcd. for $\text{C}_{13}\text{H}_{13}^{35}\text{ClN}_2\text{O}$ ($\text{M}^+ + 1$), m/z 249.0795; found m/z 249.0784.

2-Chloro-4-(1,2-diphenylethyl)pyrimidine (5b). This compound was obtained in 61% yield. ^1H NMR (CDCl_3) δ 8.38 (d, $J = 5.2$ Hz, 1H), 7.22 (m, 9H), 7.05 (m, 2H), 7.00 (d, $J = 5.2$ Hz, 1H), 4.28 (dd, $J = 7.4, 7.8$ Hz, 1H), 3.64 (dd, $J = 7.8, 13.6$ Hz, 1H), 3.30 (dd, $J = 7.4, 13.6$ Hz, 1H). ^{13}C NMR (CDCl_3) δ 175.0, 161.3, 159.2, 140.7, 139.1, 129.0, 128.8, 128.3, 128.2, 127.4, 126.3, 119.1, 55.1, 40.5. *High-resolution ms* (ESI, positive ion mode): calcd. for $\text{C}_{18}\text{H}_{15}^{35}\text{ClN}_2$, ($\text{M}^+ + 1$), m/z 295.1002; found m/z 295.1013.

2-(4-Methylpiperazino)-4-(2-(4-methylpiperazino)ethyl)pyrimidine tetrahydrochloride (6a). The free base was obtained as an oil in 22% yield; ^1H NMR for the free base (CDCl_3): δ 8.17 (d, $J = 5.1$ Hz, 1H), 6.38 (d, $J = 5.1$ Hz, 1H), 3.83 (m, 4H), 2.75 (s, 4H), 2.46 (m, 10H), 2.33 (s, 3H), 2.28 (s, 3H), 1.92 (m, 2H). A hydrochloride salt. *Anal.* Calcd for $\text{C}_{16}\text{H}_{28}\text{N}_6 \cdot 4\text{HCl} \cdot \frac{1}{2} \text{H}_2\text{O}$: C, 41.84; H, 7.24; N, 18.30. Found: C, 41.76; H, 7.10; N, 18.06.

N-benzyl-2-(2-(4-methylpiperazino)-4-pyrimidinyl)-2-phenylethanamine (6b). This compound was obtained as an oil in 57% yield; ^1H NMR (400 MHz, CDCl_3) δ 8.13 (d, $J = 5.1$ Hz, 1H), 7.25 (m, 10H), 6.29 (d, $J = 5.1$ Hz, 1H), 4.11 (dd, $J = 6.4, 8.4$ Hz, 1H), 3.82 (m, 6H), 3.49 (dd, $J = 8.4, 11.8$ Hz, 1H), 3.07 (dd, $J = 6.4, 11.8$ Hz, 1H), 2.45 (m, 4H), 2.34 (s, 3H); ^{13}C NMR (100 MHz, CDCl_3) δ 170.8, 161.6, 157.7, 141.1,

140.3, 128.6, 128.4, 128.3, 128.1, 127.0, 126.9, 109.7, 55.0, 53.9, 53.1, 53.0, 46.3, 43.7. *High resolution ms* (ESI, positive ion mode): calc'd for $C_{24}H_{29}N_5$, ($M^+ + 1$), m/z 388.2501, found m/z 388.2491.

4-(2-Ethylthio)-1-phenylethyl)-2-(4-methylpiperazino)pyrimidine (6c). This compound was obtained as an oil in 37% yield; 1H NMR ($CDCl_3$) δ 8.15 (d, $J = 5.2$ Hz, 1H), 7.29 (m, 5H), 6.34 (d, $J = 5.2$ Hz, 1H), 4.01 (m, 1H), 3.88 (m, 4H), 3.48 (m, 1H), 3.06 (m, 1H), 2.48 (m, 6H), 2.35 (s, 3H), 1.22 (t, $J = 7.2$ Hz, 3H); ^{13}C NMR ($CDCl_3$): δ 170.7, 161.6, 157.7, 141.7, 128.5, 128.1, 127.1, 109.4, 55.0, 53.8, 46.3, 43.7, 36.1, 26.7, 14.8. *High-resolution ms* (ESI, positive ion mode): calcd. for $C_{19}H_{26}N_4S$ ($M^+ + 1$), m/z 343.1956; found m/z 343.1947.

2-(4-Methylpiperazino)-4-(1-phenylpropyl)pyrimidine (6l). This compound was obtained as an oil in 39% yield. 1H NMR ($CDCl_3$) δ 8.13 (d, $J = 5.2$ Hz, 1H), 7.30 (m, 4H), 7.20 (m, 1H), 6.32 (d, $J = 5.2$ Hz, 1H), 3.86 (t, $J = 5.2$ Hz, 4H), 3.66 (t, $J = 7.6$ Hz, 1H), 2.46 (t, $J = 5.2$ Hz, 4H), 2.34 (s, 3H), 2.23 (m, 1H), 1.99 (m, 1H), 0.88 (t, $J = 7.6$ Hz, 3H); ^{13}C NMR ($CDCl_3$) δ 172.5, 161.7, 157.4, 142.8, 128.3, 128.2, 126.5, 109.0, 55.4, 55.0, 46.3, 43.7, 27.5, 12.5. *High-resolution ms* (ESI, positive ion mode): calcd. for $C_{18}H_{24}N_4$ ($M + 1$)⁺, m/z 297.2079; found m/z 297.2089.

4-Acetyl-2-chloropyrimidine (7). To **3c** (0.230 g, 0.125 mmol) was added ethanol (6 mL), methanol (6 mL), water (6 mL), and conc. HCl (2 mL). The solution was stirred for 12 hours at 20 °C until starting material was no longer detected by TLC. The solution was made basic with sodium carbonate (2M, 5 mL) and separated with diethyl ether:hexanes (1:1, 3 X 20 mL), dried over magnesium sulfate, filtered and concentrated under reduced pressure. Purification by chromatography using an eluent of hexanes:dichloromethane (1:1) yielded **7** (0.116 g, 0.740 mmol, 59%) as a yellow crystalline solid. Characterization agrees with that reported elsewhere (publication in writing). 1H NMR (400 MHz, $CDCl_3$) δ 8.86 (d, $J = 5.1$ Hz, 1H), 7.84 (d, $J = 5.1$ Hz, 1H), 2.72 (s, 3H).

Di-(4-acetyl-2-(4-methylpiperazino)pyrimidine) trihydrobromide (8). A solution of **7** (0.18 g, 1.0 mmol) in toluene (3 ml) was treated with *N*-methylpiperazine (0.55 mL, 5.0 mmol). The solution was heated to 70°C and stirred for 1 day until starting material was no longer detected by TLC. The solution was then evaporated to dryness under reduced pressure and purified by chromatography (dichloromethane:methanol, 10:1) yielded the free base (0.170 g, 0.69 mmol, 70%) as a yellow oil. ¹H NMR for the free base (400 MHz, CDCl₃) δ 8.50 (d, *J* = 5.1 Hz, 1H) 7.03 (d, *J* = 5.1 Hz, 1H), 3.91 (m, 4H), 2.62 (s, 3H), 2.50 (m, 4H), 2.36 (s, 3H). A hydrobromide salt. *Anal.* Calcd. for (C₁₁H₁₆N₄O)₂•3 HBr: C, 38.67; H, 5.16; N, 16.40. Found: C, 38.82; H, 5.05; N, 16.41.

General procedure for compounds 9a-c[14]. A solution of **8** (0.12 g, 0.5 mmol) and sodium hydroxide (0.12 g, 3.0 mmol) dissolved in ethanol (10 mL) was treated with the appropriate hydroxylamine or hydrazine (5 mmol). The solution was stirred for two hours then extracted into diethyl ether (3 X 20 mL). Purification by chromatography (dichloromethane:methanol, 6:1) yielded pyrimidine derivatives **9a-c** as yellow oils.

Di-(1-(2-(4-methylpiperazino)-4-pyrimidinyl)ethanone oxime) trihydrobromide (9a). The free base was obtained in 76% yield. ¹H NMR of the free base (400 MHz, CDCl₃) δ 8.50 (d, *J* = 5.1 Hz, 1H) 7.03 (d, *J* = 5.1 Hz, 1H), 3.91 (m, 4H), 2.62 (s, 3H), 2.50 (m, 4H), 2.36 (s, 3H); NOESY correlations observed between hydrogens bonded to adjacent piperazine carbons. A hydrobromide salt: mp 249 °C (dec.). *Anal.* Calcd. for C₁₁H₁₇N₅O • 2 HBr, ½ H₂O: C, 32.53; H, 4.96; N, 17.24. Found: C, 32.55; H, 4.77; N, 17.07.

4-(1-Hydrazonoethyl)-2-(4-methylpiperazino)pyrimidine dihydrobromide (9b). The free base was obtained in 76% yield. ¹H NMR of the free base (400 MHz, CDCl₃) δ 8.23 (d, *J* = 5.1 Hz, 1H) 7.07 (d, *J* = 5.1 Hz, 1H), 5.71 (s, 2H, -NH₂), 3.88 (m, 4H), 2.49 (m, 4H), 2.35 (s, 3H), 2.15 (s, 3H). A hydrobromide salt: mp 207 °C (dec.). *Anal.* Calcd. for C₁₁H₁₈N₆O • 1.5 HBr, 1.5 H₂O: C, 34.52; H, 5.93; N, 21.96. Found: C, 34.64; H, 5.48; N, 21.51.

1-(2-(4-Methylpiperazino)-4-pyrimidinyl)ethanone O-ethyl oxime dihydrobromide (9c). The free base was obtained in 29% yield. ^1H NMR of the free base (400 MHz, CDCl_3) δ 8.26 (d, $J = 5.1$ Hz, 1H), 7.04 (d, $J = 5.1$ Hz, 1H), 4.27 (q, $J = 7.0$ Hz, 2H), 3.87 (m, 4H), 2.48 (m, 4H), 2.34 (s, 3H), 2.21 (s, 3H), 1.33 (t, $J = 7.0$ Hz, 3H). A hydrobromide salt. *Anal.* Calcd for $\text{C}_{13}\text{H}_{21}\text{N}_5\text{O} \cdot 2 \text{HBr}, \text{H}_2\text{O}$: C, 35.23; H, 5.69; N, 15.80. Found: C, 35.50; H, 5.52; N, 15.39.

General procedure for compounds 10b-l. A solution of **3b** (0.18 g, 1.0 mmol) and potassium carbonate (0.27 g, 2.0 mmol) in acetonitrile (5 mL) was treated with the appropriate 4-substituted piperazine (1.1 mmol). The solution was heated to 100 °C until starting material was no longer detected by TLC (5-24 hours). The solution was diluted with water (10 mL) and the product was extracted into diethyl ether (3 X 20 mL). The organic phase was dried over magnesium sulfate and concentrated before purification by chromatography (dichloromethane:methanol, 10:1).

2-(4-Ethylpiperazino)-4-(3-furyl)pyrimidine dihydrobromide (10b). The free base was obtained in 61% yield as an oil. ^1H NMR of the free base (400 MHz, CDCl_3) δ 8.29 (d, $J = 5.1$ Hz, 1H), 8.07 (m, 1H), 7.48 (m, 1H), 6.86 (m, 1H), 6.63 (d, $J = 5.1$ Hz, 1H), 3.91 (m, 4H), 2.53 (m, 4H), 2.49 (q, $J = 7.2$ Hz, 2H), 1.14 (t, $J = 7.2$ Hz, 3H). A hydrobromide salt. *Anal.* Calcd for $\text{C}_{14}\text{H}_{18}\text{N}_4\text{O} \cdot 2 \text{HBr}, \frac{1}{2} \text{H}_2\text{O}$: C, 39.18; H, 4.93; N, 13.06. Found: C, 39.29; H, 4.36; N, 12.81.

4-(3-Furyl)-2-(4-propylpiperazino)pyrimidine dihydrobromide (10c). The free base was obtained in 39% yield as an oil. ^1H NMR of the free base (400 MHz, CDCl_3) δ 8.29 (d, $J = 5.1$ Hz, 1H), 8.06 (s, 1H), 7.48 (s, 1H), 6.86 (s, 1H), 6.63 (d, $J = 5.1$ Hz, 1H), 3.90 (t, 4H), 2.52 (m, 4H), 2.36 (t, $J = 7.4$ Hz, 2H), 1.57 (m, 2H), 0.94 (t, $J = 7.4$ Hz, 3H). A hydrobromide salt: mp 274 - 277 °C. *Anal.* Calcd for $\text{C}_{15}\text{H}_{20}\text{N}_4\text{O} \cdot 2 \text{HBr}, \text{H}_2\text{O}$: C, 39.84; H, 5.35; N, 12.39. Found: C, 40.39; H, 4.84; N, 12.45.

2-(4-Benzylpiperazino)-4-(3-furyl)pyrimidine dihydrobromide (10d). The free base was obtained in 73% yield as an oil. ^1H NMR of the free base (400 MHz, CDCl_3) δ 8.28 (d, $J = 5.1$ Hz, 1H), 8.05 (m, 1H), 7.47 (m,

1H), 7.31 (m, 5H), 6.85 (s, 1H), 6.62 (d, $J = 5.1$ Hz, 1H), 3.89 (m, 4H), 3.57 (s, 2H), 2.53 (m, 4H). A

hydrobromide salt. *Anal.* Calcd for $C_{19}H_{20}N_4O \cdot 2$ HBr, H_2O : C, 45.62; H, 4.84; N, 11.20. Found: C, 45.93; H, 4.67; N, 11.11.

Di-(4-(3-furyl)-2-(4-(4-methoxybenzyl)piperazino)pyrimidine) trihydrobromide (10e). The free base was obtained in 87% yield as a colorless oil. 1H NMR of the free base (400 MHz, $CDCl_3$) δ 8.27 (d, $J = 5.1$ Hz, 1H), 8.04 (m, 1H), 7.47 (m, 1H), 7.26 (m, 2H), 6.87 (m, 2H), 6.84 (m, 1H), 6.61 (d, $J = 5.1$ Hz, 1H), 3.87 (m, 4H), 3.81 (s, 3H), 3.50 (s, 2H), 2.50 (m, 4H). ^{13}C NMR of the free base (100 MHz, $CDCl_3$) δ 161.8, 159.0, 158.8, 158.0, 143.9, 143.0, 130.4, 130.0, 126.2, 113.7, 108.5, 105.6, 62.6, 55.3, 53.0, 43.7. A hydrobromide salt: mp 195 °C (dec.). *Anal.* Calcd for $C_{20}H_{22}N_4O_2 \cdot 1\frac{1}{2}$ HBr: C, 50.92; H, 5.02; N, 11.88. Found: C, 50.82; H, 4.56; N, 11.89.

4-(3-Furyl)-2-(4-(3-methoxybenzyl)piperazino)pyrimidine hydrobromide (10f). The free base was obtained in 40% yield. 1H NMR (400 MHz, $CDCl_3$) δ 8.27 (d, $J = 5.1$ Hz, 1H), 8.04 (m, 1H), 7.46 (t, $J = 1.8$ Hz, 1H), 7.25 (m, 1H), 6.93 (m, 2H), 6.84 (m, 1H), 6.81 (m, 1H), 6.60 (d, $J = 5.1$ Hz, 1H), 3.88 (m, 4H), 3.81 (s, 3H), 3.53 (s, 2H), 2.52 (m, 4H). A hydrobromide salt: mp 245 - 247 °C (dec.). *Anal.* Calcd for $C_{20}H_{22}N_4O_2 \cdot HBr, \frac{1}{2} H_2O$: C, 54.55; H, 5.49; N, 12.72. Found: C, 54.87; H, 5.04; N, 12.89.

2-(4-(4-Chlorobenzyl)piperazino)-4-(3-furyl)pyrimidine dihydrobromide (10g). The free base was obtained in 36% yield as a colorless oil. 1H NMR of the free base (400 MHz, $CDCl_3$) δ 8.28 (d, $J = 5.1$ Hz, 1H), 8.05 (m, 1H), 7.47 (m, 1H), 7.28 (m, 4H), 6.84 (m, 1H), 6.62 (d, $J = 5.1$ Hz, 1H), 3.88 (m, 4H), 3.51 (s, 2H), 2.50 (m, 4H). ^{13}C NMR of the free base (100 MHz, $CDCl_3$) δ 161.8, 159.0, 158.0, 143.9, 143.0, 136.6, 132.8, 130.4, 128.4, 126.2, 108.5, 105.7, 62.4, 53.0, 43.7. *Mass spectroscopy* (EI); calcd for $C_{19}H_{19}^{35}ClN_4O$: 354, found: 354. A hydrobromide salt: mp 231 °C (dec.). *Anal.* Calcd for $C_{19}H_{19}ClN_4O \cdot 2$ HBr: C, 44.17; H, 4.10; N, 10.84. Found: C, 44.24; H, 3.80; N, 10.84.

2-(4-(3-Chlorobenzyl)piperazino)-4-(3-furyl)pyrimidine dihydrobromide (10h). The free base was obtained in 60% yield as a colorless oil. ^1H NMR of the free base (400 MHz, CDCl_3) δ 8.28 (d, $J = 5.1$ Hz, 1H), 8.05 (m, 1H), 7.47 (t, $J = 1.8$ Hz, 1H), 7.38 (s, 1H), 7.25 (m, 3H), 6.85 (m, 1H), 6.62 (d, $J = 5.1$ Hz, 1H), 3.89 (m, 4H), 3.53 (s, 2H), 2.52 (m, 4H). ^{13}C NMR of the free base (100 MHz, CDCl_3) δ 161.8, 159.0, 158.0, 143.9, 143.0, 140.3, 134.2, 129.5, 129.1, 127.3, 127.2, 126.2, 108.5, 105.7, 62.6, 53.1, 43.7. A hydrobromide salt: mp 257-259 °C. *Anal.* Calcd for $\text{C}_{19}\text{H}_{19}\text{ClN}_4\text{O}\cdot 2 \text{HBr}$: C, 44.17; H, 4.10; N, 10.84. Found: C, 44.39; H, 3.83; N, 10.77.

2-(4-Benzoylpiperazino)-4-(3-furyl)pyrimidine hydrobromide (10i). The free base was obtained in 33% yield as a yellow oil. ^1H NMR of the free base (400 MHz, CDCl_3) δ 8.31 (d, $J = 5.1$ Hz, 1H), 8.06 (m, 1H), 7.48 (m, 1H), 7.44 (m, 5H), 6.85 (m, 1H), 6.69 (d, $J = 5.1$ Hz, 1H), 3.48-4.05 (broad m, 8H). ^{13}C NMR of the free base (100 MHz, CDCl_3) δ 170.6, 161.7, 159.2, 158.13, 144.0, 143.1, 135.8, 129.8, 128.6, 127.1, 126.0, 108.5, 106.3, 44.0, 42.3. A hydrobromide salt: mp 221 °C (dec.). *Anal.* Calcd for $\text{C}_{19}\text{H}_{18}\text{N}_4\text{O}_2\cdot \text{HBr}, \frac{1}{2} \text{H}_2\text{O}$: C, 53.79; H, 4.75; N, 13.20. Found: C, 53.97; H, 4.32; N, 13.15.

2-(4-(4-tert-Butylbenzyl)piperazino)-4-(3-furyl)pyrimidine dihydrobromide (10j). The free base was obtained in 45% yield as an oil. ^1H NMR of the free base (400 MHz, CDCl_3) δ 8.27 (d, $J = 5.1$ Hz, 1H), 8.04 (m, 1H), 7.46 (m, 1H), 7.38 (d, $J = 8.0$ Hz, 2H), 7.30 (d, $J = 8.0$ Hz, 2H), 6.84 (m, 1H), 6.61 (d, $J = 5.1$ Hz, 1H), 3.88 (m, 4H), 3.53 (s, 2H), 2.52 (m, 4H), 1.33 (s, 9H). ^{13}C NMR of the free base (100 MHz, CDCl_3) δ 161.8, 159.0, 158.0, 150.0, 143.9, 143.0, 134.9, 129.0, 126.3, 125.2, 108.5, 105.5, 62.9, 53.1, 43.8, 34.5, 31.4. A hydrobromide salt: mp 235 - 237 °C (dec.). *Anal.* Calcd for $\text{C}_{23}\text{H}_{28}\text{N}_4\text{O}\cdot 2 \text{HBr}, \text{H}_2\text{O}$: C, 49.66; H, 5.80; N, 10.07. Found: C, 49.48; H, 5.23; N, 10.01.

4-(3-Furyl)-2-(4-naphthylmethylpiperazino)pyrimidine dihydrobromide (10k). The free base was obtained in 22% yield. ^1H NMR of the free base (400 MHz, CDCl_3) δ 8.35 (d, $J = 7.6$ Hz, 1H), 8.27 (d, $J = 5.1$ Hz, 1H), 8.04 (s, 1H), 7.86 (d, $J = 7.6$ Hz, 1H), 7.79 (d, $J = 7.6$ Hz, 1H), 7.40-7.55 (m, 5H), 6.84 (s, 1H), 6.61

(d, $J = 5.1$ Hz, 1H), 3.95 (s, 2H), 3.87 (m, 4H), 2.59 (m, 4H). ^{13}C NMR of the free base (100 MHz, CDCl_3) δ 161.8, 159.0, 158.0, 143.9, 143.0, 133.9 (2 signals), 132.6, 128.4, 128.0, 127.5, 126.2, 125.8, 125.7, 125.1, 124.8, 105.5, 61.3, 53.3, 43.8. A hydrobromide salt. *Anal.* Calcd for $\text{C}_{23}\text{H}_{22}\text{N}_4\text{O} \cdot 2 \text{HBr}, \text{H}_2\text{O}$: C, 50.20; H, 4.76; N, 10.18. Found: C, 49.79; H, 4.47; N, 9.93.

1,4-Bis(4-(3-furyl)-2-pyrimidinyl)piperazine dihydrobromide (10I). The free base was obtained in 16% yield as an oil. ^1H NMR of the free base (400 MHz, CDCl_3) δ 8.32 (d, $J = 5.1$ Hz, 2H), 8.10 (m, 2H), 7.50 (m, 2H), 6.89 (m, 2H), 6.68 (d, $J = 5.1$ Hz, 2H), 3.98 (s, 8H). ^{13}C NMR of the free base (100 MHz, CDCl_3) δ 161.9, 159.1, 158.1, 143.9, 143.1, 126.2, 108.5, 105.9, 43.7. A hydrobromide salt: mp: 270 °C (dec.). *Anal.* Calcd for $\text{C}_{20}\text{H}_{18}\text{N}_6\text{O}_2 \cdot 2 \text{HBr}, 3 \text{H}_2\text{O}$: C, 40.70; H, 4.44; N, 14.24. Found: C, 40.58; H, 4.23; N, 14.07.

General procedure for compounds 12a-f and 13a-f. Bromophenols **11a-e** were commercially available. The established procedure was followed [11]. In summary, potassium hydroxide (0.7 g, 10 mmol) was dissolved in H_2O (4 mL). The solution was stirred during the sequential addition of DMSO (20 mL), the appropriate bromophenol **11** (8.6 mmol), and 2-bromo-1,1-diethoxyethane (1.4 mL, 9.3 mmol). After complete addition, the mixture was heated under reflux for 1 day. After cooling, the product was extracted into diethyl ether and washed with H_2O and 5% NaOH. The organic solution was then dried over MgSO_4 , filtered, and concentrated to yield **12a-e** as colorless oils. Compounds **12a-e** were used without purification. A solution of polyphosphonic acid (20 g) in chlorobenzene (50 mL) was heated to reflux before the dropwise addition of **12a-e** (33 mmol). The solution was kept at reflux for 24 hours, resulting in a black solution containing a large amount of tar. The product was decanted from the remaining solid, which was then washed with diethyl ether (2 X 20 mL). The organic layer was then washed with aqueous sodium hydroxide (5%, 100 mL). The organic layer was dried over magnesium sulfate and concentrated before purification by chromatography (hexanes) yielded benzofurans **13a-e** as

colorless oils. Compounds **12c**, **12d** and **13a** were used in subsequent steps without isolation.

Compounds which were isolated are characterized below.

1-Bromo-3-(2,2-diethoxyethoxy)benzene (12a). This compound was obtained in 80% yield as a faintly brown oil. Characterization agrees with that previously reported [96]. ^1H NMR (400 MHz, CDCl_3) δ 1.26 (t, 6H, 2 $-\text{CH}_3$, $J=7.0\text{Hz}$), 3.68-3.83 (m, 4H, 2 $-\text{CH}_2$), 4.05 (d, 2H, $-\text{CH}_2$, $J=5.2\text{Hz}$), 4.88 (t, 1H, $-\text{CH}$, $J=5.2\text{Hz}$), 6.88 (m, 2H, 2 $-\text{CH}$), 7.24 (m, 1H, $-\text{CH}$), 7.53 (m, 1H, $-\text{CH}$).

4-Bromo-2-(2,2-diethoxy)toluene (12b). This compound was obtained in 83% yield. ^1H NMR (400 MHz, CDCl_3) δ 6.95-6.99 (m, 3H), 4.83-4.86 (t, $J = 5.2$ Hz, 1H), 3.97-3.99 (d, $J = 5.2\text{Hz}$, 2H), 3.63-3.80 (m, 4H), 2.17 (s, 3H), 1.24-1.27 (t, $J = 7.0$ Hz, 6H). ^{13}C NMR (100 MHz, CDCl_3) δ 157.4, 131.6, 125.9, 123.6, 119.4, 114.7, 100.5, 69.0, 62.8, 15.9, 15.4. *High resolution ms*: (ESI, positive ion mode): calc'd for $\text{C}_{13}\text{H}_{19}\text{O}_3^{79}\text{Br}$, ($\text{M}^+ + \text{Na}$), 325.0415; found 325.0429.

3-Bromo-4-(2,2-diethoxy)toluene (12e). This compound was obtained in 97% yield as a light brown oil. Characterization agrees with that previously reported [96]. ^1H NMR (400 MHz, CDCl_3) δ 1.25 (t, 6H, 2 $-\text{CH}_3$, $J=7.0$ Hz), 2.26 (s, 3H, $-\text{CH}_3$), 3.65-3.84 (m, 4H, 2 $-\text{CH}_2$), 4.02 (d, 2H, $-\text{CH}_2$, $J=5.2$ Hz), 4.86 (t, 1H, $-\text{CH}$, $J=5.2$ Hz), 6.80 (d, 1H, $-\text{CH}$, $J=8.2$ Hz), 7.03 (dd, 1H, $-\text{CH}$, $J=1.8, 8.2$ Hz), 7.35 (dd, 1H, $-\text{CH}$, $J=1.8$ Hz). ^{13}C NMR (100 MHz, CDCl_3) δ 15.37, 20.18, 63.33, 70.39, 100.76, 111.96, 113.56, 128.84, 131.91, 133.74, 152.98.

4-Bromo-7-methylbenzofuran (13b). This compound was obtained in 23% yield as a white solid: mp 34 $^\circ\text{C}$. ^1H NMR (400 MHz, CDCl_3) δ 7.64 (d, $J = 2.0$ Hz, 1H), 7.26-7.28 (d, $J = 7.8$ Hz, 1H), 6.94-6.96 (d, $J = 7.8$ Hz, 1H), 6.78 (d, $J = 2.0$ Hz, 1H), 2.47 (s, 3H). ^{13}C NMR (100 MHz, CDCl_3) δ 153.8, 145.1, 128.2, 126.1, 125.7, 121.0, 111.1, 107.0, 14.8.

5-Bromobenzofuran (13c). This compound was obtained in 28% yield as a clear oil. Characterization agrees with that previously reported [140]. ^1H NMR (400 MHz, CDCl_3) δ 6.72 (d, 1H, -CH, $J=2.0\text{Hz}$), 7.38 (s, 1H, -CH), 7.62 (d, 1H, -CH, $J=2.0\text{ Hz}$), 7.73 (s, 1H, -CH).

7-Bromobenzofuran (13d). This compound was obtained in 31% yield as a colorless oil. Characterization agrees with that previously reported [96]. ^1H NMR (400 MHz, CDCl_3) δ 6.85 (m, 1H, -CH), 7.13 (m, 1H, -CH), 7.48 (m, 1H, -CH), 7.55, (m, 1H, -CH), 7.69, (m, 1H, -CH).

7-Bromo-5-methylbenzofuran (13e). This compound was obtained in 25% yield as a clear oil. Characterization agrees with that previously reported [141]. ^1H NMR (400 MHz, CDCl_3) δ 2.42 (s, 3H, - CH_3), 6.75 (s, 1H, -CH), 7.29 (s, 1H, -CH), 7.31 (s, 1H, -CH), 7.64 (s, 1H, -CH). ^{13}C NMR (100 MHz, CDCl_3) δ 21.03, 103.54, 107.14, 120.32, 128.40, 128.66, 133.98, 145.68, 150.51.

General procedure for compounds 14a-g. The published procedure for Buchwald-Hartwig amination was followed [15]. All substituted piperazines were commercially available. Briefly, in dry conditions a solution of the appropriate aryl halide **13** (1.0 mmol) in toluene (5 mL) was treated with a 4-substituted piperazine (1.2 mmol) in the presence of *tert*-butoxide (2.0 mmol) catalysts tris(dibenzylideneacetone)dipalladium(0) (0.01 mmol), and racemic 2,2'-bis(diphenylphosphino)-1,1'-binaphthyl (0.01 mmol). The mixture was heated at reflux for 1 day before quenching with H_2O . After cooling, the product was extracted into diethyl ether (3 X 10 mL). The organic layer was dried over MgSO_4 , filtered and concentrated under reduced pressure before purification (dichloromethane:methanol, 10:1) yielded substituted arylpiperazines **14**.

6-(4-Methylpiperazino)benzofuran hydrobromide (14a). This compound was obtained through a modification of the general procedure listed above. As **13a** was not able to be isolated from its constitutional isomer, the reaction was performed using a crude mixture of its isomers. Workup and purification by flash chromatography using a mobile phase of dichloromethane:methanol (10:1) gave a

mixture of constitutional isomers. This mixture was resolved by enrichment through crystallization. To the isomeric mixture was added one drop of MeOH and diethyl ether (3 mL), followed by HBr (48%, 1 drop). To the solution was then added 5 mL ether and after several hours at room temperature, **14a** precipitated as a white solid. This procedure was repeated until the salt was isolated as determined by ^1H NMR in 38% yield: mp 206 °C. ^1H NMR (400 MHz, DMSO) δ 9.6 (broad s, 1H), 7.84 (d, $J = 2.0\text{Hz}$, 1H), 7.52 (d, $J = 8.5\text{Hz}$, 1H), 7.22 (s, 1H), 7.02 (dd, $J = 2.0\text{Hz}$, 8.5Hz, 1H), 6.83 (d, $J = 1.4\text{Hz}$, 1H), 3.4-3.6 (broad m, 2H), 3.8-4.0 (broad m, 2H), 3.1-3.3 (broad m, 2H), 2.9-3.1 (broad m, 2H), 2.87 (s, 3H). *Anal.* Calcd for $\text{C}_{13}\text{H}_{16}\text{N}_2\text{O} \cdot \text{HBr}$: C, 52.54; H, 5.77; N, 9.43. Found: C, 53.07; H, 5.92; N, 9.71.

7-Methyl-4-(N-methylpiperazino)benzofuran dihydrobromide (14b). The free base was obtained in 38% yield as a white crystalline solid: mp 62-64 °C. ^1H NMR for the free base (400 MHz, CDCl_3) δ 7.58 (d, $J = 2.0\text{ Hz}$, 1H), 6.99-7.01 (d, $J = 7.8\text{ Hz}$, 1H), 6.77 (d, $J = 2.0\text{ Hz}$, 1H), 6.62-6.64 (d, $J = 7.8\text{ Hz}$, 1H), 3.19-3.22 (m, 4H), 2.64-2.67 (m, 4H), 2.46 (s, 3H), 2.39 (s, 3H). ^{13}C NMR for the free base (100 MHz, CDCl_3) δ 154.9, 144.3, 143.3, 125.3, 119.9, 115.7, 109.8, 105.5, 55.4, 51.4, 46.2, 14.6. *High resolution ms* (ESI, positive ion mode): calcd for $\text{C}_{14}\text{H}_{18}\text{N}_2\text{O}$, ($\text{M}^+ + \text{H}$), m/z 231.1497; found m/z 231.1490. A hydrobromide salt: mp 263 - 265 °C. *Anal.* Calcd for $\text{C}_{14}\text{H}_{18}\text{N}_2\text{O} \cdot 2\text{HBr}$: C, 42.88; H, 5.14; N, 7.14. Found: C, 42.76; H, 5.20; N, 7.14.

5-(4-Methylpiperazino)benzofuran hydrobromide (14c). The free base was obtained in 34% yield. ^1H NMR for the free base (400 MHz, CDCl_3) δ 7.56 (s, 1H), 7.39 (d, $J = 9.0\text{ Hz}$, 1H), 7.11 (s, 1H), 7.00 (d, $J = 9.0\text{ Hz}$, 1H), 6.68 (s, 1H), 3.19 (m, 4H), 2.64 (m, 4H), 2.38 (s, 3H). A hydrobromide salt. *Anal.* Calcd for $\text{C}_{13}\text{H}_{16}\text{N}_2\text{O} \cdot \text{HBr}, \frac{1}{2}\text{H}_2\text{O}$: C, 50.99; H, 5.93; N, 9.15. Found: C, 51.19; H, 5.93; N, 9.32.

7-(N-Methylpiperazino)benzofuran dihydrobromide (14d). The free base was obtained in 39% yield and characterization matched that previously reported [98]. ^1H NMR for the free base (400 MHz, CDCl_3) δ , 7.60 (s, 1H), 7.12-7.22 (m, 2H), 6.74-6.79 (m, 2H), 3.38 (m, 4H), 2.68 (m, 4H), 2.39 (s, 3H). *High*

resolution ms (ESI, positive ion mode): calcd for $C_{13}H_{16}N_2O$, ($M^+ + 1$), m/z 231.1497; found m/z 231.1490.

A hydrobromide salt: mp 242 °C. *Anal.* Calcd for $C_{13}H_{16}N_2O \cdot 2 HBr$, H_2O : C, 39.42; H, 5.09; N, 7.07.

Found: C, 39.62; H, 5.21; N, 6.79.

1-Methyl-4-(5-methyl-7-benzofuryl)piperazine hydrobromide (14e). The free base was obtained in 46% yield as a colorless oil. 1H NMR (400 MHz, $CDCl_3$) δ 2.39 (s, 3H, $-CH_3$), 2.46 (s, 3H, $-CH_3$), 2.64-2.67 (m, 4H, 2 $-CH_2$), 3.19-3.22 (m, 4H, 2 $-CH_2$), 6.62-6.64 (d, 1H, $-CH$, $J=7.8$ Hz), 6.77 (d, 1H, $-CH$, $J=2.0$ Hz), 6.99-7.01 (d, 1H, $-CH$, $J=7.8$ Hz), 7.58 (d, 1H, $-CH$, $J=2.0$ Hz). ^{13}C NMR (100 MHz, $CDCl_3$) δ 14.63, 46.20, 51.36, 55.37, 105.48, 109.78, 115.71, 119.94, 125.30, 143.25, 144.32, 154.89. *High resolution ms* (ESI, positive ion mode): calcd for $C_{13}H_{16}N_2O$, ($M^+ + 1$), m/z 231.1497; found m/z 231.1490 A hydrobromide salt: mp 212 - 213 °C (dec.). EA (CHN) Calcd for $C_{14}H_{18}N_2O \cdot 2 HBr$: C, 42.88; H, 5.14; N, 7.14. Found: C, 42.76; H, 5.20; N, 7.14.

tert-Butyl 4-(5-methyl-7-benzofuranyl)piperazine-1-carboxylate (14f). The free base was obtained in 51% yield as a light yellow glass. 1H NMR (400 MHz, $CDCl_3$) δ 7.56 (d, 1H, $-CH$, $J=1.6$ Hz), 7.01 (s, 1H, $-CH$), 6.67 (d, 1H, $-CH$, $J=1.6$ Hz), 6.57 (s, 1H, $-CH$), 3.66 (m, 4H, 2 $-CH_2$) 3.26 (m, 4H, 2 $-CH_2$), 2.40 (s, 3H, $-CH_3$), 1.50 (s, 9H, 3 $-CH_3$). ^{13}C NMR (100 MHz, $CDCl_3$) δ 154.7, 145.3, 144.1, 136.7, 133.0, 128.7, 114.3, 112.8, 106.7, 79.8, 49.8, 43.5, 28.4, 21.6.

5-Methyl-(7-piperazino)benzofuran (14g). This compound was prepared according to the published procedure. In summary, to a solution of **14f** (1.3g, 4.1 mmol) in dichloromethane (5 mL) was added TFA (2.0 mL). The mixture was stirred for several hours until the presence of starting material was no longer detected by TLC. Purification by chromatography (dichloromethane:methanol, 10:1) gave **17** (0.78g, 3.6 mmol, 88%) as a light yellow glass. Characterization matched that previously reported. 1H NMR (400 MHz, $CDCl_3$) δ 2.41 (s, 3H, $-CH_3$), 3.43 (m, 4H, 2 $-CH_2$), 3.57 (m, 4H, 2 $-CH_2$), 6.58 (s, 1H, $-CH$), 6.69 (d, 1H, $-CH$, $J=2.0$ Hz), 7.07 (s, 1H, $-CH$), 7.57 (d, 1H, $-CH$).

(4-Bromo-1,1-dimethylbutyl)sulfonylbenzene (15). This compound was prepared according to the literature. Briefly, a solution of isopropyl phenyl sulfide (0.50 g, 3.3 mmol) in dichloromethane (30 mL) was treated dropwise with a solution of *m*-chloroperoxybenzoic acid (2.4 g, 50% by wt, 7 mmol). The mixture was stirred under mild heating (38 °C) and resulted in steady bubbling and a white precipitate. After complete addition, the reaction was quenched and washed with water. Preparatory chromatography yielded [(1-methylethyl)sulfonyl]benzene in quantitative yield. To a dry flask containing (1-methylethyl)sulfonylbenzene was added 5 mL anhydrous THF. After cooling to -78 °C, *n*-butyllithium (1.3 mL, 3.3 mmol) was added dropwise and stirred for 30 min before the addition of an excess of 1,3 dibromopropane (2.0 g, 10 mmol). The mixture was then stirred and allowed to reach 0 °C before quenching with aqueous ammonium chloride. The product was extracted into diethyl ether (2 X 20 mL) and the extract was dried over magnesium sulfate and concentrated. Purification on a chromatotron (hexanes:dichloromethane, 9:1) yielded **19** in 35% yield as a white solid: mp 69 - 70 °C. Characterization agrees with that previously reported. [83] ¹H NMR (400 MHz, CDCl₃) δ 1.31 (s, 6H, 2 - CH₃), 1.83-1.87 (m, 2H, -CH₂), 1.95-2.00 (m, 2H, -CH₂), 3.40 (t, 2H, -CH₂, *J*=6.6 Hz), 7.57 (t, 2H, 2 -CH, *J*=7.6 Hz), 7.67 (t, 1H, -CH, *J*=7.6 Hz), 7.88 (d, 2H, 2 -CH₂, *J*=7.6 Hz).

6-Bromo-*N*-(4-cyanophenyl)methylhexanamide (16). The published procedure was followed [84]. Briefly, a solution of 4-(aminomethyl)benzotrile (2.64 g, 20 mmol) in aqueous sodium hydroxide (0.5 M, 50 mL) was stirred vigorously and treated dropwise with 6-bromohexanoyl chloride (5.0 g, 23.4 mmol). The pH of the reaction was maintained near 9 with aqueous sodium hydroxide (0.5 M, 100 mL). After 30 min, the resulting white precipitant was extracted with dichloromethane. The resulting residue was recrystallized from diethyl ether to yield **16** as a white semisolid. Characterization agrees with that previously reported. ¹H NMR (400 MHz, CDCl₃) δ 7.62 (d, *J* = 8.0 Hz, 2H), 7.38 (d, *J* = 8.0 Hz, 2H), 5.89 (broad s, 1H), 4.50 (d, *J* = 6.0 Hz, 2H), 3.42 (t, *J* = 6.6 Hz, 2H), 2.27 (t, *J* = 7.4 Hz, 2H), 1.88 (m, 2H), 1.71 (m, 2H), 1.50 (m, 2H).

General procedure for compounds 17a-b. A solution of the appropriate bromide (0.25 mmol) in acetonitrile (5 mL) was treated with the appropriate amine (0.25 mmol). To this mixture was added K_2CO_3 (0.50 mmol). The mixture was heated under reflux for 1-3 days, until the starting materials were no longer detected by TLC. Water (10 mL) was added to the mixture and the products were extracted into diethyl ether. The extract was dried over magnesium sulfate, filtered and concentrated under reduced pressure. Purification on a chromatotron (dichloromethane:methanol, 10:1) yielded **17a-b**. Characterization of these compounds follows.

1-[4-(Benzenesulfonyl)-4-methylpentyl]-4-(5-methyl-7-benzofuranyl)piperazine (17a). The free base was obtained in 30% yield as a faintly yellow oil. 1H NMR (400 MHz, $CDCl_3$) δ 1.32 (s, 6H), 1.64 (m, 2H), 1.76 (m, 2H), 2.41 (m, 5H), 2.68 (m, 4H), 3.33 (m, 4H), 6.56 (m, 1H), 6.66 (m, 1H), 6.99 (m, 1H), 7.56 (m, 3H), 7.66 (t, $J = 7.4$ Hz, 1H), 7.89 (d, $J = 7.4$ Hz, 2H). ^{13}C NMR (100 MHz, $CDCl_3$) δ 145.3, 144.0, 136.9, 135.6, 133.5, 133.0, 130.6, 128.7, 128.6, 113.9, 112.6, 106.6, 62.9, 58.7, 53.4, 49.8, 32.8, 21.7, 21.5, 20.9.

N-(4-Cyanobenzyl)-6-(4-(5-methyl-7-benzofuranyl)piperazino)hexanamide (17b). The free base was obtained in 28% yield. 1H NMR (400 MHz, $CDCl_3$) δ 7.60 (d, $J = 7.8$ Hz, 2H), 7.56 (s, 1H), 7.38 (d, $J = 7.8$ Hz, 2H), 7.00 (s, 1H), 6.67 (m, 1H), 6.56 (m, 1H), 6.16 (broad s, 1H), 4.49 (d, $J = 5.8$ Hz, 2H), 3.38 (m, 4H), 2.75 (m, 4H), 2.49 (t, $J = 7.6$ Hz), 2.40 (s, 3H), 2.28 (t, $J = 7.4$ Hz), 1.72 (m, 2H), 1.62 (m, 2H), 1.40 (m, 2H). ^{13}C NMR (100 MHz, $CDCl_3$) δ 173.1, 145.2, 144.1 (2 signals), 136.6, 133.1, 132.4, 128.6, 128.2, 118.7, 114.1, 112.6, 111.2, 106.7, 58.3, 53.2, 49.4, 43.0, 36.3, 26.9, 26.1, 25.4, 21.7. *High resolution ms:* (ESI, positive ion mode): calcd for $C_{27}H_{32}N_4O_2$, ($M^+ + 1$), m/z 445.2604; found m/z 445.2591.

REFERENCES

- [1] Harden DB; Mokrosz MJ; Strekowski L., M. J. Mokrosz, and L. Strekowski, "Addition and Substitution Reactions of Chloropyrimidines with Lithium Reagents," *J Org Chem*, vol. 53, pp. 4137-4140, 1988.
- [2] L. Strekowski, D. B. Harden, W. B. Grubb III, S. E. Patterson, "Synthesis of 2-Chloro-4,6-di(heteroaryl)pyrimidines," *Journal of Heterocyclic Chemistry*, vol. 27, pp. 1393-1400, 1990.
- [3] M. N. M. P. A. B. M Kolaczowski, "Receptor-Based Pharmacophores for Serotonin 5-HT7R Antagonists," *J Med Chem*, vol. 49, pp. 6732-6741, 2006.
- [4] M. L. Lopez-Rodriguez, et al., "Optimization of the Pharmacophore Model for 5-HT7R Antagonism. Design and Synthesis of New Naphtholactam and Naphthosultam Derivatives," *Journal of Medicinal Chemistry*, vol. 46, pp. 5638-5650, 2003.
- [5] E. A. Raux, J. D. Klenc, A. Blake, J. Saczewski, and L. Strekowski, "Conjugate addition of nucleophiles to the vinyl function of 2-chloro-4-vinylpyrimidine derivatives," *Molecules*, vol. 15, no. 3, pp. 1973-1984, 2010.
- [6] P. Whitaker-Azmitia, "The discovery of serotonin and its role in neuroscience," *Neuropsychopharmacology*, vol. 21, no. 2S, pp. 2S-8S, 1999.
- [7] V. M. Erspamer V, "Ricerche sul secreto delle cellule enterocromaffini.," *Boll d Soc Med-chir Pavia*, vol. 51, pp. 357-363, 1937.
- [8] A. B. Erspamer V, "Identification of enteramine, specific hormone of enterochromaffin cells, as 5-hydroxytryptamine," *Nature*, vol. 169, pp. 800-801, 1952.
- [9] G. A. P. I. Rapport MM, "Partial purification of the vasoconstrictor in beef serum.," *J Biol Chem*, vol. 174, pp. 735-738, 1948.
- [10] G. A. P. I. Rapport MM, "Crystalline Serotonin," *Science*, vol. 108, pp. 329-330, 1948.
- [11] M. Rapport, "Serum vasoconstrictor (serotonin). V. The presence of creatine in the complex: A proposed structure of the vasoconstrictor principle.," *J Biol Chem*, vol. 180, pp. 961-969, 1949.
- [12] P. I. Twarog BM, "Serotonin content of some mammalian tissues and urine and a model for its

- determination," *Am J Physiol*, vol. 175, pp. 157-161, 1953.
- [13] P. A. S. P. Brodie BB, "Evidence that serotonin has a role in brain functions," *Science*, vol. 122, p. 968, 1955.
- [14] J. T. MD Gershon, "The Serotonin Signaling System: From Basic Understanding to Drug Development for Functional GI Disorders," *Gastroenterology*, vol. 132, pp. 397-414, 2007.
- [15] H. Jin and e. al., "Substituted 3-(4-(1,3,5-triazin-2-yl)-phenyl)-2-aminopropanoic acids as novel tryptophan hydroxylase inhibitors.," *Bioorganic and Medicinal Chemistry Letters*, vol. 19, no. 17, pp. 5229-5232, 2009.
- [16] A. T. Sands, "Pharmaceutical compositions containing multicyclic amino acid derivative tryptophan hydroxylase inhibitors and methods of using them in treatment, prevention and combination therapy of pulmonary hypertension and related diseases," Patent 2009:55673, Jan. 15, 2009.
- [17] Z.-C. Shi and e. al., "Modulation of Peripheral Serotonin Levels by Novel Tryptophan Hydroxylase Inhibitors for the Potential Treatment of Functional Gastrointestinal Disorders," *J Med Chem*, vol. 51, no. 13, p. 3684, 2008.
- [18] C. Tanaka, Y.-J. Yoh, and S. Takori, "Relation between brain monoamine tryptophan hydroxylase inhibitors.," *Brain Research*, vol. 45, no. 1, pp. 153-164, 1972.
- [19] L. Quinyun and e. al., "Discovery and characterization of novel tryptophan hydroxylase inhibitors that selectively inhibit serotonin synthesis in the gastrointestinal tract," *The Journal of Pharmacology and Experimental Therapeutics*, vol. 325, no. 1, pp. 47-55, 2008.
- [20] L. McGoey, "Profitable failure: antidepressant drugs and the triumph of flawed experiments," *Hist Human Sci*, vol. 23, no. 1, pp. 58-78, 2010.
- [21] B. B.-A. EK Moltzen, "Serotonin Reuptake Inhibitors: The Corner Stone in Treatment of Depression for Half a Century - A Medicinal Chemistry Survey," *Current Topics in Medicinal Chemistry*, vol. 6, pp. 1801-1823, 2006.
- [22] M. Zhou, K. Engel, and J. Wang, "Evidence for significant contribution of a newly identified monoamine transporter (PMAT) to serotonin uptake in the human brain," *Biochem Pharmacol*, vol. 73, no. 1, pp. 147-154, 2007.
- [23] C. G. H Volz, "Monoamine Oxidase Inhibitors: A Perspective on their Use in the Elderly," *Drugs and Aging*, vol. 13, no. 5, pp. 341-355, 1998.
- [24] R. Glennon, "Serotonin Receptors: Clinical Implications," *Neuroscience and Biobehavioral Reviews*, vol. 14, pp. 35-47, 1990.

- [25] J. Hornung, "The human raphe nuclei and the serotonergic system," *Journal of Chemical Neuroanatomy*, vol. 26, pp. 331-343, 2003.
- [26] M. Gershon, "Review article: serotonin receptors and transporters - roles in normal and abnormal gastrointestinal motility.," *Aliment Pharmacol Ther*, vol. 20, no. (Suppl 7), pp. 3-14, 2004.
- [27] V. J. W. M. C. A. O. B. de Jong TR, "Serotonin and the neurobiology of the ejaculatory threshold," *Neuroscience and Biobehavioral Reviews*, vol. 30, pp. 893-907, 2006.
- [28] J. Hensler, "Serotonergic modulation of the limbic system," *Neuroscience and Biobehavioral Reviews*, vol. 30, pp. 203-214, 2006.
- [29] G. G. J. AC Gallup, "Yawning and thermoregulation," *Physiology and Behavior*, vol. 95, pp. 10-16, 2008.
- [30] G. Richerson, "Serotonergic neurons as carbon dioxide sensors that maintain pH homeostasis," *Nature Reviews*, vol. 5, pp. 449-461, 2004.
- [31] C. V. AG Ramage, "5-Hydroxytryptamine and cardiovascular regulation," *Trends in Pharmacological Sciences*, vol. 29, no. 9, pp. 472-483, 2008.
- [32] J. H. E. B. C. L. J. B. JCG Halford, "Serotonergic Drugs: Effects on Appetite Expression and Use for the Treatment of Obesity," *Drugs*, vol. 67, no. 1, pp. 27-55, 2007.
- [33] G. Molodtsova, "Serotonergic mechanisms of memory trace retrieval," *Behavioral Brain Research*, vol. 195, pp. 7-16, 2008.
- [34] S. J. Beattie DT, "Serotonin pharmacology in the gastrointestinal tract: a review," *Naunyn-Schmiedeberg's Arch Pharmacol*, vol. 377, pp. 181-203, 2008.
- [35] H. F. M Yoshimura, "Mechanisms for the Anti-noceptive Actions of the Descending Noradrenergic and Serotonergic Systems in the Spinal Cord," *Journal of Pharmacological Sciences*, vol. 101, pp. 107-117, 2006.
- [36] S. H. A. B. BL Roth, "Serotonin receptors represent highly favorable molecular targets for cognitive enhancement in schizophrenia and other disorders," *Psychopharmacology*, vol. 174, pp. 17-24, 2004.
- [37] F. V. H. S. A. L. B Scholtissen, "Serotonergic mechanisms in Parkinson's disease: opposing results from preclinical and clinical data," *Journal of Neural Transmission*, vol. 113, pp. 59-73, 2005.
- [38] V. K. P. R. R. J. G Bagdy, "Serotonin and epilepsy," *Journal of Neurochemistry*, vol. 100, pp. 857-873, 2007.

- [39] T. S. HY Meltzer, "Does stimulation of 5-HT_{1a} receptors improve cognition in schizophrenia?," *Behavioural Brain Research*, vol. 195, pp. 98-102, 2008.
- [40] L. D. J. H. LE Schechter, "The Potential Utility of 5-HT_{1a} Receptor Antagonists in the Treatment of Cognitive Dysfunction Associated with Alzheimer's Disease," *Current Pharmaceutical Design*, vol. 8, pp. 139-145, 2002.
- [41] F. C. A.-N. W. G. F. Del-Ben CM, "Serotonergic modulation of face emotion recognition," *Brazilian Journal of Medical and Biological Research*, vol. 41, pp. 263-269, 2008.
- [42] P. J. A. H.-S. J. M. A. S. CA Lowry, "Modulation of anxiety circuits by serotonergic systems," *Stress*, vol. 8, no. 4, pp. 233-246, 2005.
- [43] J. S. J. J. Carver CS, "Serotonergic Function, Two-Mode Models of Self-Regulation, and Vulnerability to Depression: What Depression Has in Common With Impulsive Aggression," *Psychological Bulletin*, vol. 134, no. 6, pp. 912-943, 2008.
- [44] H. M. M Mays, "The serotonin hypothesis of major depression," in *Psychopharmacology: The Fourth Generation of Progress*. New York, NY: Raven Press, 1995, pp. 933-944.
- [45] L. Tecott, "Serotonin and the Orchestration of Energy Balance," *Cell Metabolism*, vol. 6, pp. 352-361, 2007.
- [46] E. Szabadi, "Drugs for sleep disorders: mechanisms and therapeutic prospects," *British Journal of Clinical Pharmacology*, vol. 61, no. 6, pp. 761-766, 2006.
- [47] A. Panconesi, "Serotonin and migraine: a reconsideration of the central theory.," *J Headache Pain*, pp. 267-276, 2008.
- [48] E. Hamel, "Serotonin and migraine: biology and clinical implications," *Cephalagia*, vol. 27, no. 11, pp. 1293-1300, 2007.
- [49] T. D. P. K. A. C. S O'Mahony, "Central serotonergic and noradrenergic receptors in functional dyspepsia," *World J Gastroenterol*, vol. 12, no. 17, pp. 2681-2687, 2006.
- [50] A. Spinelli, "Irritable Bowel Syndrome," *Clin Drug Invest*, vol. 27, no. 1, pp. 15-33, 2007.
- [51] G. T. R Fass, "Functional heartburn: the stimulus, the pain, and the brain," *Gut*, vol. 51, no. 6, pp. 885-892, 2002.
- [52] W. H. U Ladabaum, "Novel Approaches to the treatment of nausea and vomiting," *Digestive Diseases*, vol. 17, no. 3, pp. 125-132, 1999.

- [53] C. K. Dhonchadha BAC, "Serotonergic mechanisms in addiction-related memories," *Behavioral Brain Research*, vol. 195, pp. 39-53, 2009.
- [54] M. Leopoldo, "Serotonin₇ Receptors (5-HT₇R) and their Ligands," *Current Medicinal Chemistry*, vol. 11, pp. 629-661, 2004.
- [55] D. E. Nichols and C. D. Nichols, "Serotonin Receptors," *Chem Rev*, vol. 108, pp. 1614-1641, 2008.
- [56] B. Kobilka and G. F. Schertler, "New G-protein-coupled receptor crystal structures: insights and limitations," *Trends in Pharmacological Sciences*, vol. 29, no. 2, pp. 79-83, 2008.
- [57] K. Palczewski, et al., "Crystal structure of rhodopsin: a G protein-coupled receptor," *Science*, vol. 289, pp. 739-745, 2000.
- [58] C. N. DE Nichols, "Serotonin Receptors," *Chem Rev*, vol. 106, pp. 1614-1641, 2008.
- [59] P. Bonaventure, et al., "Radioligand binding analysis of knockout mice reveals 5-hydroxytryptamine₇ receptor distribution and uncovers 8-hydroxy-2-(di-n-propylamino)tetralin," *Neuroscience*, vol. 124, no. 4, pp. 901-911, 2004.
- [60] T. Kvernmo, J. Houben, and I. Sylte, "Receptor-Binding and Pharmacokinetic Properties of Dopaminergic Agonists," *Current Topics in Medicinal Chemistry*, vol. 8, no. 12, pp. 1049-1067, 2008.
- [61] A. Brenchat, et al., "5-HT₇ receptor activation inhibits mechanical hypersensitivity secondary to capsaicin sensitization in mice," *Pain*, vol. 141, no. 3, pp. 239-247, 2009.
- [62] J. A. Bard, et al., "Cloning of a novel human serotonin receptor (5-HT₇) positively linked to adenylate cyclase," *J Biol Chem*, vol. 268, pp. 23422-23426, 1993.
- [63] P. R. Saxena, "Serotonin receptors: subtypes, functional responses and therapeutic relevance," *Pharmac Ther*, vol. 66, pp. 339-368, 1995.
- [64] K. A. Krobert, T. Bach, T. Syversveen, A. M. Kvingedal, and F. O. Levy, "The cloned human 5-HT₇ receptor splice variants: a comparative characterization of their pharmacology, function and distribution," *Naunyn-Schmiedeberg's Arch Pharmacol*, vol. 363, pp. 620-632, 2001.
- [65] D. E. Heidmann, P. Szot, R. Kohen, and M. W. Hamblin, "Four 5-hydroxytryptamine₇ (5-HT₇) receptor isoforms in human and rat produced by alternative splicing: species differences due to altered intron-exon organization," *J Neurochem*, vol. 68, pp. 1372-1381, 1997.
- [66] M. Leopoldo, "Serotonin₇ Receptors (5-HT₇R) and their Ligands," *Curr Med Chem*, vol. 11, pp. 629-661, 2004.

- [67] P. B. Hedlund and J. G. Sutcliffe, "Functional, molecular and pharmacological advances in 5-HT₇ receptor research," *Trends in Pharmacological Sciences*, vol. 25, no. 9, 2004.
- [68] P. R. Saxena, C. M. Villalon, D. Centurion, L. F. Valdivia, and P. de Vries, "Migraine: pathophysiology, pharmacology, treatment and future trends," *Curr Vasc Pharmacol*, vol. 1, no. 1, pp. 71-84, 2003.
- [69] B. C. Zou, L. Dong, Y. Wang, S. H. Wang, and M. B. Cao, "Expression and role of 5-HT₇ receptor in brain and intestine in rats with irritable bowel syndrome," *Chin Med J*, vol. 120, no. 23, pp. 2069-2074, 2007.
- [70] T. Adayev, B. Ranasinghe, and P. Banerjee, "Transmembrane Signaling in the Brain by Serotonin, A Key Regulator of Physiology and Emotion," *Bioscience Reports*, vol. 25, no. 5/6, pp. 363-385, 2005.
- [71] M. Errico, R. A. Crozier, M. R. Plummer, and D. S. Cowen, "5-HT₇ receptors activate the mitogen activated protein kinase extracellular signal related kinase in cultured rat hippocampal neurons," *Neuroscience*, vol. 102, pp. 361-367, 2001.
- [72] T. Kenakin, "Agonist-receptor efficacy II: agonist trafficking of receptor signals," *Trends in Pharmacological Sciences*, vol. 16, no. 7, pp. 232-238, 1995.
- [73] H. Zheng, H. Loh, and P.-Y. Law, "Agonist-Selective Signaling of G Protein-Coupled Receptor: Mechanisms and Implications," *Life*, vol. 62, no. 2, pp. 112-119, 2010.
- [74] J. Gonzalez-Maeso and S. C. Sealton, "Agonist-trafficking and hallucinogens," *Curr Med Chem*, vol. 16, no. 8, pp. 1017-1027, 2009.
- [75] J. R. Shah, P. D. Mosier, B. L. Roth, G. E. Kellog, and R. B. Westkaemper, "Synthesis, structure-affinity relationships, and modeling of AMDA analogs at 5HT_{2A} and H₁ receptors: structural factors contributing to selectivity.," *Bioorg Med Chem*, vol. 17, no. 18, pp. 6496-6504, 2009.
- [76] C. Dezi, et al., "Multistructure 3D-QSAR studies on a series of conformationally constrained butyrophenones docked into a new homology model of the 5-HT_{2A} receptor," *J Med Chem*, vol. 50, no. 14, pp. 3242-3255, 2007.
- [77] M. Kolaczowski, M. Nowak, M. Pawlowski, and A. J. Bojarski, "Receptor-Based Pharmacophores for Serotonin 5-HT_{7R} Antagonists-Implications to Selectivity," *Journal of Medicinal Chemistry*, vol. 49, pp. 6732-6741, 2006.
- [78] C. Kikuchi, H. Nagaso, T. Hiranuma, and M. Koyama, "Tetrahydrobenzindoles: Selective Antagonists of the 5-HT₇ Receptor," *Journal of Medicinal Chemistry*, vol. 42, no. 4, pp. 533-535, 1999.

- [79] M. L. Lopez-Rodriguez, et al., "First Pharmacophoric Hypothesis for 5-HT₇ Antagonism," *Bioorganic & Medicinal Chemistry Letters*, vol. 10, pp. 1097-1100, 2000.
- [80] R. E. Wilcox, et al., "High-affinity interactions of ligands at recombinant Guinea pig 5HT₇ receptors," *Journal of Computer-Aided Molecular Design*, vol. 15, pp. 883-909, 2001.
- [81] E. S. Vermeulen, A. W. Schmidt, J. S. Sprouse, H. V. Wikstrom, and C. J. Grol, "Characterization of the 5-HT₇ Receptor. Determination of the Pharmacophore for 5-HT₇ Receptor Agonism and CoMFA-Based Modeling of the Agonist Binding Site," *Journal of Medicinal Chemistry*, vol. 46, pp. 5365-5374, 2003.
- [82] R. Perrone, F. Berardi, E. L. Colabufo, M. Leopoldo, and V. Tortorella, "Structure-affinity relationship study on N-(1,2,3,4-tetrahydronaphthalen-1-yl)-4-aryl-1-piperazinealkylamides, a new class of 5-hydroxytryptamine receptor agents," *J Med Chem*, vol. 47, no. 26, pp. 6616-6624, 2003.
- [83] P. Raubo, et al., "Aminoalkyl phenyl sulfones - a novel series of 5-HT₇ receptor ligands," *Bioorganic & Medicinal Chemistry Letters*, vol. 16, pp. 1255-1258, 2006.
- [84] M. Leopoldo, et al., "Structural Modifications of N-(1,2,3,4-Tetrahydronaphthalen-1-yl)-4-Aryl-1-piperazinehexanamides: Influence on Lipophilicity and 5-HT₇ Receptor Activity. Part III," *J Med Chem*, vol. 51, no. 18, pp. 5813-5822, 2008.
- [85] R. A. Medina, et al., "Synthesis of New Serotonin 5-HT₇ Receptor Ligands. Determinants of 5-HT₇/5-HT_{1A} Receptor Selectivity," *J Med Chem*, vol. 52, pp. 2384-2392, 2009.
- [86] A. Sanin, et al., "5-Aryl substituted (S)-2-(dimethylamino)-tetralins novel serotonin 5HT₇ receptor ligands," in *Proceedings of the 14th Camerino-Noord Symposium. Ongoing Progress in the Receptor Chemistry.*, Italy, 2003, p. 27.
- [87] T. Nilsson, et al., *Eur J Pharmacol*, vol. 372, p. 49, 1999.
- [88] M. D. Tricklebank, C. Forler, and J. R. Fozard, "The involvement of subtypes of the 5-HT₁ receptor and of catecholaminergic systems in the behavioural response to 8-hydroxy-2-(di-N-propylamino)tetralin in the rat," *Eur J Pharmacol*, vol. 106, no. 2, pp. 271-282, 1984.
- [89] C. Faure, O. Mnie-Filali, H. Scarna, G. Debonnel, and N. Haddjeri, "Effects of the 5-HT₇ receptor antagonist SB-269970 on rat hormonal and temperature responses to the 5-HT₇/1a receptor antagonist 8-OH-DPAT," *Neuroscience Lett*, vol. 404, no. 1-2, pp. 122-126, 2006.
- [90] D. J. Cushing, J. M. Zgombick, D. L. Nelson, and M. L. Cohen, *J Pharmacol Exp Ther*, vol. 277, p. 1560, 1996.
- [91] R. Rezaie, et al., *J Pharm Pharmacol*, vol. 53, p. 959, 2001.

- [92] P. J. Lovell, PCT Int. Appl. WO 0056712 133:252456, 2000.
- [93] D. Denhart, et al., "Diaminopyrimidine and diaminopyridine 5-HT7 ligands," *Bioorganic and Medicinal Chemistry Letters*, vol. 14, no. 16, pp. 4249-4252, 2004.
- [94] B. Wakefield, *Organolithium Methods*. San Diego, CA: Academic Press Inc., 1988.
- [95] A. Demir and O. Sesenoglu, "Novel enantioselective synthesis of both enantiomers of furan-2-yl amines and amino acids," *helvetica chimica acta*, vol. 86, pp. 91-105, 2003.
- [96] J. J. Baldwin, et al., "Preparation of diaminoalkanes, particularly N-(2-aminopropan-2-yl)piperidine-1-carboxamides, as aspartic protease inhibitors.," USA Application WO 2005-US36230, 2006.
- [97] J. P. Wolfe and S. L. Buchwald, "Palladium-catalyzed amination of aryl halides and aryl triflates: N-hexyl-2-methyl-4-methoxyaniline and N-methyl-N-(4-chlorophenyl)aniline," *Organic Syntheses*, vol. 78, p. 23, 2002.
- [98] F. Kerrigan, C. Martin, and G. H. Thomas, "Synthesis of arylpiperazines via palladium-catalyzed aromatic amination reactions of bromoarenes with N-tert-butoxycarbonylpiperazine," *Tetrahedron Letters*, vol. 39, no. 15, pp. 2219-2222, 1998.
- [99] Y. C. Martin, "3D QSAR: Current State, Scope, and Limitations," *Perspectives in Drug Discovery and Design*, vol. 12, pp. 3-23, 1998.
- [100] Tripos International, *SYBYL Manual*. St. Louis, USA.
- [101] M. R. Doddareddy, Y. S. Cho, H. Y. Koh, and A. N. Pae, "CoMFA and CoMSIA 3D QSAR analysis on N1-arylsulfonylindole compounds as 5-HT6 antagonists," *Bioorganic & Medicinal Chemistry*, vol. 12, no. 15, pp. 3977-3985, 2004.
- [102] G. Klebe, U. Abraham, and T. Mietzner, "Molecular Similarity Indices in a Comparative Analysis (CoMSIA) of Drug Molecules to Correlate and Predict Their Biological Activity," *Journal of Medicinal Chemistry*, vol. 37, no. 24, pp. 4130-4146, 1994.
- [103] R. D. Cramer III, D. E. Patterson, and J. D. Bunce, "Comparative molecular field analysis (CoMFA). 1. Effect of shape on binding of steroids to carrier proteins," *Journal of the American Chemical Society*, vol. 110, no. 18, pp. 5959-5967, 1988.
- [104] U. Norinder, "Recent Progress in CoMFA Methodology and Related Techniques," *Perspectives in Drug Discovery and Design*, vol. 12, pp. 25-39, 1998.
- [105] H. Y. Park, S. M. Ju, D. Y. Lee, H. Zhang, and C. K. Kim, "3D-QSAR studies on DATAs and DAPYs for HIV-RT inhibitors using CoMFA and CoMSIA approaches," *QSAR and Comb Sci*, vol. 28, no. 2, pp.

218-225, 2009.

- [106] G. B. De Freitas, L. L. da Silva, N. C. Romeiro, and C. A. Fraga, "Development of CoMFA and CoMSIA models of affinity and selectivity for indole ligands of cannabinoid CB1 and CB2 receptors," *European Journal of Medicinal Chemistry*, vol. 44, no. 6, pp. 2482-2496, 2009.
- [107] P. R. Murukmar, S. D. Gupta, V. P. Zambre, R. Giridhar, and M. R. Yadav, "Development of Predictive 3D-QSAR CoMFA and CoMSIA Models for β -aminohydroxamic Acid-Derived Tumor Necrosis Factor- α Converting Enzyme Inhibitors," *Chemical Biology and Drug Design*, vol. 73, no. 1, pp. 97-107, Jan. 2009.
- [108] M. Boehm, J. Sturzebecher, and G. Klebe, "3D QSAR Analyses Using Comparative Molecular Field Analysis and Comparative Molecular Similarity Indices Analysis To Elucidate Selectivity Differences of Inhibitors Binding to Trypsin, Thrombin, and Factor Xa," *Journal of Medicinal Chemistry*, vol. 42, no. 3, pp. 458-477, 1999.
- [109] P. L. Jackson, K. R. Scott, W. M. Southerland, and Y.-Y. Fang, "Enaminones 8: CoMFA and CoMSIA studies on some anticonvulsant enaminones," *Bioorganic & Medicinal Chemistry*, vol. 17, no. 1, pp. 133-140, 2009.
- [110] Y. C. Martin, "3D QSAR: current state, scope, and limitations," *Perspectives in Drug Discovery and Design*, vol. 12, pp. 3-23, 1998.
- [111] L. Stahle and S. Wold, "Multivariate Data Analysis and Experimental Design in Biomedical Research," *Progress in Medicinal Chemistry*, vol. 25, pp. 291-338, 1988.
- [112] P. Geladi and B. R. Kowalski, "Partial least squares regression: a tutorial," *Analytica Chimica Acta*, vol. 185, pp. 1-17, 1986.
- [113] K. Roy, "On some aspects of validation of predictive quantitative structure-activity relationship models," *Expert Opinion on Drug Discovery*, vol. 2, no. 12, pp. 1567-1577, 2007.
- [114] P. Geladi and B. R. Kowalski, "An example of 2-block predictive partial least-squares regression with simulated data.," *Analytica Chimica Acta*, vol. 185, pp. 19-32, 1986.
- [115] A. Golbraikh and A. Tropsha, "Beware of q^2 !," *J Mol Graph Model*, vol. 20, no. 4, pp. 269-276, 2002.
- [116] A. J. Bojarski, et al., "Structure-activity relationship studies of CNS agents. Part 9: 5-HT_{1A} and 5-HT₂ receptor affinity of some 2- and 3-substituted 1,2,3,4-tetrahydro-betacarbolines.," *Pharmazie*, vol. 48, no. 4, pp. 289-294, 1993.
- [117] E. A. Amin and W. J. Welsh, "Highly predictive CoMFA and CoMSIA models for two series of

- Stromelysin-1 (MMP-3) inhibitors elucidate S1' and S1-S2' binding modes," *Journal of Chemical Information and Modeling*, vol. 46, no. 4, pp. 1775-1783, 2006.
- [118] J. Y. Shim, et al., "Three-dimensional quantitative structure-activity relationship study of the cannabimimetic (aminoalkyl)indoles using comparative molecular field analysis," *Journal of Medicinal Chemistry*, vol. 41, no. 23, pp. 4521-4532, 1998.
- [119] S. Paula, M. R. Tabet, S. M. Keenan, W. J. Welsh, and W. J. Ball, "Three-dimensional quantitative structure-activity relationship modeling of cocaine binding to two monoclonal antibodies by comparative molecular field analysis," *Journal of Molecular Biology*, vol. 325, no. 3, p. 515, 2003.
- [120] W. Tong, et al., "Evaluation of quantitative structure-activity relationship methods for large-scale prediction of chemicals binding to the estrogen receptor," *Journal of Chemical Information and Computer Sciences*, vol. 38, no. 4, pp. 669-677, 1998.
- [121] F. Boeckler, et al., "CoMFA and CoMSIA investigations revealing novel insights into the binding modes of dopamine D3 receptor agonists," *Journal of Medicinal Chemistry*, vol. 48, no. 7, pp. 2493-2508, 2005.
- [122] J. E. Schachtner, H. Stachel, S. S. Chatterjee, H. Hauer, and K. Polborn, "Synthesis and anticonvulsive activity of thiolosigamone," *Journal of Medicinal Chemistry*, vol. 33, no. 7-8, pp. 665-669, 1998.
- [123] G. Yang and X. Huang, "Development of quantitative structure-activity relationships and its application in rational drug design," *Current Pharmaceutical Design*, vol. 12, no. 35, pp. 4601-4611, 2006.
- [124] M. Olah, C. Bologa, and T. I. Oprea, "An automated PLS search for biologically relevant QSAR descriptors," *Journal of Computer-Aided Molecular Design*, vol. 18, no. 7-9, pp. 437-449, 2004.
- [125] H. Kubinyi, G. Folkers, and Y. C. Martin, Eds., *3D QSAR in Drug Design*. New York, USA: Kluwer Academic Publishers, 2002, pp. 443-485.
- [126] L. Shen, G. Liu, and Y. Tang, "Molecular docking and 3D-QSAR studies of 2-substituted 1-indanone derivatives as acetylcholinesterase inhibitors," *Acta Pharmacologica Sinica*, vol. 28, no. 12, pp. 2053-2063, 2007.
- [127] V. P. Zambre, P. R. Murumkar, R. Giridhar, and M. R. Yadav, "Structural investigations of acridine derivatives by CoMFA and CoMSIA reveal novel insight into their structures toward DNA G-quadruplex mediated telomerase inhibition and offer a highly predictive model for substituted acridines," *Journal of Chemical Information and Modeling*, vol. 49, no. 5, pp. 1298-1311, 2009.

- [128] D. B. Harden, L. Strekowski, J. L. Mokrosz, and A. J. Bojarski, "Conformational analysis of 4-(2-furyl)-2-(methylamino)pyrimidine," *Journal of Heterocyclic Chemistry*, vol. 33, no. 4, pp. 1207-1210, 1996.
- [129] L. Strekowski, F. A. Tanious, S. Chandrasekaran, R. Watson, and W. D. Wilson, "New approach to conformational analysis of heterobiaryls in solution," *Tetrahedron Letters*, vol. 27, no. 50, pp. 6045-6048, 1986.
- [130] R. A. Medina, et al., "Synthesis of New Serotonin 5-HT₇ Receptor Ligands. Determinants of 5-HT₇/5-HT_{1A} Receptor Selectivity," *Journal of Medicinal Chemistry*, vol. 52, pp. 2384-2392, 2009.
- [131] E. S. Vermeulen, et al., "Novel 5-HT₇ Receptor Inverse Agonists. Synthesis and Molecular Modeling of Arylpiperazine- and 1,2,3,4-Tetrahydroisoquinoline-Based Arylsulfonamides," *Journal of Medicinal Chemistry*, vol. 47, pp. 5451-5466, 2004.
- [132] Y. Cheng and W. H. Prusoff, "Relationship between the inhibition constant (K_i) and the concentration of inhibitor which causes 50 percent inhibition (I₅₀) of an enzymatic reaction," *Biochemical Pharmacology*, vol. 22, no. 23, pp. 3099-3108, 1973.
- [133] A. J. Bojarski, et al., "1-aryl-4-(4-succinimidobutyl)piperazines and their conformationally constrained analogues: synthesis, binding to serotonin (5-HT_{1A}, 5-HT_{2A}, 5-HT₇), alpha₁-adrenergic, and dopaminergic D₂ receptors, and in vivo 5-HT_{1A} functional characteristics," vol. 13, no. 6, pp. 2293-2303, 2005.
- [134] J. Mokrosz, et al., "Structure-activity relationship studies of CNS agents. Part 29. N-Methylpiperazino-substituted derivatives of quinazoline, phthalazine and quinoline as novel alpha₁, 5-HT_{1A}, 5-HT_{2A} receptor ligands," *European Journal of Medicinal Chemistry*, pp. 973-980(8), 1996.
- [135] D. R. Thomas, et al., "Functional characterisation of the human cloned 5-HT₇ receptor (long form); antagonist profile of SB-258719," *British Journal of Pharmacology*, vol. 124, no. 6, pp. 1300-1306, 1998.
- [136] D. H. M. M. L. Strekowski, "Addition and Substitution Reactions of Chloropyrimidines with Lithium Reagents," *JOC*, vol. 53, no. 17, pp. 4137-4140, 1988.
- [137] J. Soderquist and G. Hsu, "Pure, Unsolvated (alpha-Methoxyvinyl)lithium and Related Acyl Anion Equivalents via the Transmetalation of Organotin Compounds," *Organometallics*, vol. 1, pp. 830-833, 1982.
- [138] J. G. Saczewski, et al., "Synthesis of 4-substituted 2-(4-methylpiperazino)pyrimidines and quinazolin analogs as serotonin 5-HT_{2A} receptor ligands," vol. 46, no. 6, pp. 1259-1265, 2009.

- [139] H. Gilman, R. G. Jones, and L. A. Woods, "The preparation of methylcopper and some observations on the decomposition of organocopper compounds," *Journal of Organic Chemistry*, vol. 17, no. 12, pp. 1630-1634, 1952.
- [140] B. Zhang, F. Wang, and J. Yue, "A new efficient method for the total synthesis of linear furocoumarins," vol. 4, pp. 567-570, 2006.
- [141] R. E. Mewshaw and S. T. Cohn, "Preparation of (hydroxyphenyl)arylcarbaldehyde oximes as estrogenic agents.," Canada Patent 1037051, Dec. 2, 2004.
- [142] P. W.-A. EC Azmitia, "Awakening the sleeping giant: anatomy and plasticity of the brain serotonergic system," *Journal of Clinical Psychiatry*, pp. S4-S16, 1991.
- [143] S. J. J. CS Carver, "Serotonergic Function, Two-Mode Models of Self-Regulation, and Vulnerability to Depression: What Depression Has in Common With Impulsive Aggression," *Psychological Bulletin*, vol. 134, no. 6, pp. 912-943, 2008.
- [144] M. M. F. F. RM Moresco, "PET and SPET Molecular Imaging: Focus on Serotonin System," *Current Topics in Medicinal Chemistry*, vol. 6, pp. 2027-2034, 2006.
- [145] J. H. G. M. D Hoyer, "Molecular, pharmacological and functional diversity of 5-HT receptors," *Pharmacology, Biochemistry and Behavior*, vol. 71, pp. 533-554, 2002.
- [146] T. S. NM Barnes, "A review of central 5-HT receptors and their function," *Neuropharmacology*, vol. 38, pp. 1083-1152, 1999.
- [147] A. A. PL Yeagle, "G-protein coupled receptor structure," *Biochemica et Biophysica Acta*, pp. 808-824, 2007.
- [148] A. S. Kalgutkar, et al., "Biochemical basis for differences in metabolism dependent genotoxicity by two diazinylpiperazine-based 5-HT_{2c} receptor agonists," *Bioorganic & Medicinal Chemistry Letters*, vol. 19, pp. 1559-1563, 2009.
- [149] M. Jalali-Heravi and M. Asadollahi-Baboli, "Quantitative structure-activity relationship study of serotonin (5-HT₇) receptor inhibitors using modified and colony algorithm and adaptive neuro-fuzzy interference systems (ANFIS)," *European Journal of Medicinal Chemistry*, vol. 44, pp. 1463-1470, 2009.
- [150] S. Rault, et al., "Molecular Design Based on 3D Pharmacophores. Applications to 5-HT₇ Receptors," *Journal of Chemical Informatics and Computer Science*, vol. 44, pp. 1148-1152, 2004.
- [151] E. Nordling and E. Homan, "Generalization of a Targeted Library Design Protocol: Application to 5-HT₇ Receptor Ligands," *Journal of Chemical Informatics and Computer Science*, vol. 44, pp. 2207-

2215, 2004.

- [152] P. Raubo, et al., "Sulfone derivatives as 5-HT7 receptor ligands," Application US2004229864, Nov. 18, 2004.
- [153] P. Raubo, et al., "Aminoalkyl phenyl sulfones - a novel series of 5-HT7 receptor ligands," *Bioorganic and Medicinal Chemistry Letters*, vol. 16, 206.
- [154] C. Hansch and A. Leo, *Substituent Constants for Correlation Analysis in Chemistry and Biology*. New York, USA: John Wiley & Sons, 1979.
- [155] R. D. Cramer and B. Wendt, "Pushing the boundaries of 3D-QSAR," *Journal of Computer-Aided Design*, vol. 21, no. 1-3, pp. 23-32, 2007.
- [156] J. M. Blaney and J. S. Dixon, "Distance Geometry in Molecular Modeling," in *Reviews in Computational Chemistry, Volume 5*, K. B. Lipkowitz and D. B. Boyd, Eds. VCH Publishers, Inc, 2007, pp. 299-355.
- [157] M. Baroni, et al., "Generating optimal linear PLS estimations (GOLPE): An advanced chemometric tool for handling 3D-QSAR problems," vol. 12, no. 1, pp. 9-20, *Quantitative Structure-Activity Relationships*.
- [158] F. M. McRobb, B. Capuano, I. T. Crosby, D. K. Chalmers, and E. Yuriev, "Homology modeling and docking evaluation of aminergic G protein coupled receptors," *Journal of Chemical Information and Modeling*, vol. 50, no. 4, pp. 626-637, 2010.

APPENDICES

A. List of abbreviations

5-HT	-	5-hydroxytryptamine
ADD	-	attention deficit disorder
AR	-	aromatic
cAMP	-	cyclic adenosine monophosphate
cDNA	-	circular DNA
CNS	-	central nervous system
CoMFA	-	comparative molecular field analysis
CoMSIA	-	comparative molecular similarity indices analysis
DDQ	-	2,3-dichloro-5,6-dicyanoquinone
EDTA	-	ethylenediaminetetraacetic acid
ERK	-	extracellularly regulated kinase
GABA	-	gamma-aminobutyric acid
GPCR	-	G-protein coupled receptor
GI	-	gastrointestinal
HBA	-	hydrogen bond acceptor
HEK	-	human embryonic kidney
HTS	-	high throughput screening
HYD	-	hydrophobic
IL	-	intracellular loop
LOO	-	leave-one-out
LSD	-	lysergic acid diethylamide
MAO	-	monoamine oxidase
MAOI	-	monoamine oxidase inhibitor

mRNA	-	messenger RNA
N	-	number of principal components
OCD	-	obsessive compulsive disorder
PA	-	protonated amine
PLS	-	partial least squares
PMAT	-	plasma membrane monoamine transporter
PRESS	-	predicted residual sum of squares
QSAR	-	quantitative structure-activity relationship
RMS	-	root mean square
SEM	-	standard error of measurement
SERT	-	serotonin transporter
SSRI	-	selective serotonin reuptake inhibitor
THF	-	tetrahydrofuran
TLC	-	thin layer chromatography
TM	-	transmembrane
TPH	-	tryptophan hydroxylase

B. Glossary

agonist - A compound which upon binding to a receptor causes activity identical to when the receptor is bound with the natural ligand

antagonist - A compound which upon binding to a receptor blocks activity identical to when the receptor is bound with the natural ligand

bioavailability - A measure of the percentage of a dosage which enters systemic circulation. Considerations relating to bioavailability include metabolism and absorption into the bloodstream.

- central nervous system** - Encompasses all of the brain and spinal cord
- circadian pacemaker** - Refers to the structures which maintain daily rhythms such as feeding and sleeping
- docking** - In this case, docking refers to molecular modeling methods which can be used to predict the binding mode of ligands. Docking studies find the best fit for known ligands within a binding site, according to their minimized interactions with the receptor.
- dyspepsia** - A loosely defined stomach ailment similar to an upset stomach or indigestion.
- enteric** - Pertaining to the intestines.
- enzyme** - A protein which catalyzes a chemical reaction.
- forebrain structures** - refers to structures implicated in higher order thought processes
- gastrointestinal** - Pertaining to the entire system which is used to extract nutrients from ingested food.
- G-protein** - Guanine binding proteins. These proteins are most commonly seen with G-protein coupled receptors and use the altering phosphorylation states of GTP as a step in signal transduction.
- higher order (protein) structure** - The complex three-dimensional folding patterns of proteins which form common structures, such as alpha helices.
- inhibitor** - A compound which blocks the activity of a specific protein upon binding.

- kinase** - An enzyme which transfers a phosphate group to a specific compound.
- neuronal** - Pertaining to the cells (neurons) which regulate the release and reuptake of neurotransmitters for the purpose of signal transmission between nerve cells.
- pharmacological** - Relating to the actions of biological systems on a specific compound.
- pharmacophore** - A map of regions which are necessary for a compound to bind to a receptor. A complete pharmacophore will include all necessary regions for binding and describe the nature of those interactions.
- physiological** - Referring to the biological purpose of a receptor as it relates to the processes it affects within the body.
- primary sequence** - The order of amino acid residues in a protein.
- principal component** - An algebraic matrix which represents compiled information about ligand structure for QSAR analysis.
- raphe nuclei** - Portion of the brain, near the brainstem, which houses the majority of serotonergic neurons.
- selectivity** - The ability of a ligand to bind only one (or few) 5-HT receptor subtypes and other monoamine receptors.
- sequence homology** - A measure of the similarity between the sequence of residues in two different proteins.

signal transduction - Describes the event of intracellular changes being effected by an extracellular signal, such as the presence of a neurotransmitter.

splice variants - Refers to proteins which are encoded from the same DNA sequence, yet have different sequences. In the case of the 5-HT₇ receptor, splice variants exist in which the protein sequence is truncated.

synapse - The space between neurons where signaling takes place. The presence of neurotransmitters in this gap is essential to cell signaling.

ternary complex model - This model assumes a direct relationship between the the differences in dissociation constants of two ligands with respect to a receptor. This is one way to determine the affinity of novel compounds to a receptor site.

vasoconstrictor - A compound which causes the blood vessels to become more narrow, due to constriction.

C. Spectra

